MORPHOLOGICAL AND STEREOLOGICAL STUDIES OF THE OLFACTORY BULBS AND CEREBRUM OF AFRICAN GIANT RATS (*Cricetomys gambianus*, Waterhouse -1840)

BY

Sunday Abraham MUSA

DEPARTMENT OF HUMAN ANATOMY
FACULTY OF MEDICINE
AHMADU BELLO UNIVERSITY, ZARIA, NIGERIA

JUNE, 2015

MORPHOLOGICAL AND STEREOLOGICAL STUDIES OF THE OLFACTORY BULBS AND CEREBRUM OF AFRICAN GIANT RATS (*Cricetomys gambianus*, Waterhouse -1840)

BY

Sunday Abraham MUSA, (BSc, 2001; MSc, 2007, ABU)
PhD/MED/10519/2007-2008

A Ph.D. DISSERTATION SUBMITTED TO THE SCHOOL OF POSTGRADUATE STUDIES, AHMADU BELLO UNIVERSITY, ZARIA

IN PARTIAL FULFILLMENT OF THE REQUIREMENTS FOR THE AWARD OF THE DEGREE OF DOCTOR OF PHILOSOPHY IN HUMAN ANATOMY

DEPARTMENT OF HUMAN ANATOMY
FACULTY OF MEDICINE
AHMADU BELLO UNIVERSITY, ZARIA, NIGERIA

JUNE 2015

DECLARATION

I declare that the work in this dissertation entitled 'Morphological and Stereological Studies of the Olfactory Bulbs and Cerebrum of African Giant Rats (*Cricetomys gambianus*, Waterhouse -1840)' has been carried out by me in the Department of Human Anatomy, Faculty of Medicine, Ahmadu Bello University, Zaria, Nigeria. The information derived from the literature has been dully acknowledged in the text and a list of references provided. No part of this dissertation was previously presented for another degree or diploma at this or any other Institution.

Sunday Abraham MUSA _____ _____

Signature Date

CERTIFICATION

This dissertation entitled "MORPHOLOGICAL AND STEREOLOGICAL STUDIES OF THE OLFACTORY BULBS AND CEREBRUM OF AFRICAN GIANT RATS (*Cricetomys gambianus*, Waterhouse -1840)" by Sunday Abraham MUSA, meets the regulations governing the award of the degree of Doctor of Philosophy in Human Anatomy of the Ahmadu Bello University, and is approved for its contribution to knowledge and literary presentation.

Prof. J. O. Hambolu (DVM, MSc, PhD, FCVSN) _____
Chairman, Supervisory Committee Signature and Date

Prof. S. A. Ojo (DVM, MSc, PhD, Mbiol, FCVSN) _____
Member, Supervisory Committee Signature and Date

Prof. S. S. Adebisi (BSc, MSc, PhD, MASN) _____
Member, Supervisory Committee Signature and Date

Prof. J. O. Ayo (DVM, MSc, PhD, FCVSN) _____
Member, Supervisory Committee Signature and Date

Prof. S. S. Adebisi (BSc, MSc, PhD, MASN) _____
Head of Department Signature and Date

Prof. Hassan A. Zoaka (DVM, MSc, PhD FCVSN) _____
Dean, School of Postgraduate Studies Signature and Date

DEDICATION

To

God Almighty for giving me the grace and enablement to embark on this study and for helping me to have good success

To

The loving memory of my late grandmother, Prophetess Veronica Aina Owoniyi, for being the angel God used to nurture me from the tender age of six month old. She passed on to eternity while I was serving as a Youth Corps member.

And to

Lovely wife, adorable children and gracious parents.

ACKNOWLEDGEMENT

I want to sincerely thank Almighty God for giving me the grace to embark on this journey of academic excellence, for seeing me through, and for providing for me all that I needed to bring it to a very successful end.

My very sincere appreciations and profound gratitude go to my supervisory committee for their academic and fatherly guidance. Thank you for your advice, positive criticism, help, encouragement, patience and mentoring.

Professor J.O. Hambolu, my major supervisor and chairman of my supervisory committee, is appreciated for being a father, a role model, a mentor, and a supervisor. Professor S.A. Ojo, you are a father indeed and an example of academic excellence. Your sincerity and frankness are well appreciated and worthy of emulation. Prof. S.S. Adebisi, thank you sir for being a teacher and a supervisor. To Professor J.O. Ayo, I say thank you sir for your encouragement and patient guidance.

I would like to specially thank my loving and supportive best friend, wife and mother of our lovely children, Oladunni Sarah Musa, you are a blessing and favour to my life from God. You always tell me not to give up, that I am a scientist with a difference.

To our lovely covenant children Oluwaferanmi, Oluwaseunfunmi and Oluwatoyin, thank you for your love, patience, endurance, encouragement, support and understanding throughout the period of this study.

I thank my parents Elder Bode Thomas Musa and Mrs. D.G. Akinwande, for putting me in the right track. You have always been source of inspiration. To my siblings, uncles, aunties and in-laws Special Apostle and Chief (Mrs.) S.K. Fagbemi (JP), I say thank you for your encouragement, support and prayers.

My special thanks to the management of Ahmadu Bello University, Zaria, Nigeria, for providing the enabling environment and full sponsorship for my PhD programme. To all my teachers, lecturers, instructors and mentors right from my primary school days, I say thank you for the good seed of academic excellence sowed into my life.

I want to thank Educational Trust Fund, now Tetfund for the sponsorship of my bench work in Stereology and Electron Microscopy Research Laboratory at Danish Neuroscience Centre, Aarhus University, Aarhus, Denmark.

I say thank you to Professor Jens Randel Nyengaard and his family, for his mentorship, encouragement, guidance, friendship role during the study. My sincere appreciation to Mrs. Vicki Elizabeth Vallund for her secretariat and administrative assistance while I was in Aarhus, Denmark and to Maj-Britt Ludorf for her skillful and technical assistance during the research work. Anette Larsen, thank you for your useful advice. My sincere gratitude go to Professor Dorph-Petersen, Dr. Nicoletta Navea,, Dr. Simon, Dr. Ali Rafatti, Dr. Maryam Rafatti, Professor Mark West, Miss Emilia, Miss Patrycja, Dr. Chen, for their encouragement during the research work while in the Stereology and Electron Microscopy Research Laboratory, Danish Neuroscience Centre, Aarhus, Denmark. Jens, you are a true mentor, a motivator and a trusted friend. You made it possible for me to learn stereology and exposed to all the wonders of stereology. To all the PhD students and postdoctoral fellows in the Stereology and Electron Microscopy Research Laboratory, Danish Neuroscience Centre, Aarhus, Denmark, I say thank you for your support and encouragement during the study. A big thank you to Dr. John Basgen, Director of the Morphometry and Stereology laboratory, Charles Drew University, USA, for your friendship and your useful comments and advice on the stereology aspect of this study. My sincere appreciation to the MIND Centre, Danish Neuroscience Centre, Aarhus University, Aarhus, Denmark, for sponsoring my PhD stereology course.

I thank my lecturers and senior colleagues in the Department of Human Anatomy, A.B.U. Zaria. Nigeria, Dr. B. Danborno, Dr. W. O. Hamman, Dr. A.O. Ibegbu, Dr. U.E. Umana, Dr. (Mrs.) J.N. Alawa, Dr. D.T. Ikyembe, and their families, for your academic and moral inputs in my life. And all my colleagues and friends in the department, Dr. N.A. Abdullahi, Dr. A.U. Dahiru, Dr. A.A. Lawal, Dr. A.A. Buraimoh, Dr. J.A. Timbuak, Mr. T. Murdakai (JP), Mr. I.A. Iliya, Hajia Z.M. Bauchi, Hajia Hadiza Rilwan, Mallam Kona, Mr. Abel N. Agbon, Mr. Danladi Jibrin, Dr. Musa, Dr. Mustapha, Dr. Tasiu, Dr. Ismail, thank you for your encouragement and prayers. And to all the laboratory, technical and secretariat staff of the Department of Human Anatomy, Faculty of Medicine, Ahmadu Bello University, Zaria, Nigeria, Bro. Peter S. Akpulu, Mr. Bamidele Adetiba, Mrs. Litini. Anche, Mrs. Ladi Musa, Barrister (Mrs.) Charity Otache, Mrs. P. Omebije, Mallama Nana Saidu, Mallam Ahmed (JJ Golf) for your encouragement and prayers during the course of the study. To my students in the Department of Human Anatomy, Faculty of Medicine, Ahmadu Bello University, Zaria, Nigeria, I say big thank you to all of you, for your good wishes and prayers.

I want to specially thank Dr. Dzenda of Department of Veterinary Physiology and Pharmacology, Faculty of Veterinary Medicine, A.B.U. Zaria, Nigeria, for providing the animals cages used for the research. Also, Dr. and Mrs. Victor Sinkalu, Dr. Christopher Yakubu Karago, Dr. Olusegun Adeyinka, Dr. Gabriel Daniel, Dr. and Mrs. Gabriel Adekunle Okunade, for your brotherly love, prayer and support.

I thank all the members of the English Chapel, and the entire members of Cherubim and Seraphim Movement Church, 47, Sokoto Road, Samaru, for your prayers and encouragement.

And to my beloved brethren in the International Harvest Christian Center, Aarhus, Denmark, Mr. John Afolabi and family, Pastor Frank and family, Mr. Tunde Ogundeku, Professor and Mrs. Conni Paldam and Family, and all the Yoruba Community in Aarhus, Denmark, for making my sojourning in Europe memorable and pleasant.

I am grateful to Professor Charles Okuofu, Professor J.O. Otun, Dr. Donatus Adie, Dr. Samaila Abubakar, Dr. Sunday Igboro, Dr. Babatunde Adeogun, all of Department of Water Resources and Environmental Engineering, Ahmadu Bello University, Zaria, Nigeria, for your interest in my progress and encouragement.

To all my students and friends, Mr. A.A. Sadeeq, Mr. Isa Jibril, Mr. Richards, Bro. Samson Ehindero, Mr. Iliyasu O. Musa, Mallam Amir Jafar and all my students past and present thank you all for being part of this study and my academic life. Mallam Shehu of Samaru Zaria, thank you for providing live African Giant rats used for the study.

I thank Professor Jean King, Professor Keith Trujullo, Professor Sharon Juliano, Professor Janis Weeks, Professor Eds Kravitz, Professor Edward Castennor, Professor Alfredo Quinones-Hinojosa, and all my lecturers and mentors in the Marine Biological Laboratory, Woods Holes, Boston, Masachussett, USA, for your mentorship, support, encouragement, for this study. I thank Professor Rae Nishi of the Department of Neurological Science, the University of Vermont, USA, for her mentorship and the offer to use her laboratory to learn immunohistochenistry, cell and tissue culture and confocal miceroscopy in order to further my research on African Giant rats.

At this junction I wish to thank you all so very much and may God bless, guide and protect you all in all your life undertakings (Amen).

ABSTRACT

Literature on the anatomy of the African Giant rats (AGR) is gradually building; there is paucity of information on the detailed morphometric, histologic analysis of the cerebrum and olfactory bulbs of the AGR. No stereologically study has been done on the olfactory bulb and cerebrum of the AGR. The quantification of cerebral layers and olfactory bulbs, their neuronal population and volume in AGRs, may shed light on neuroanatomical basis of their highly developed olfactory ability of the rodent and some of its behaviour. The general aim of the study was to investigate the cerebrum and olfactory bulbs of the AGR in order to elucidate the neuroanatomical basis for their special olfactory functions. Ten adult AGR *(Cricetomys gambianus,* Waterhouse-1840), consisting of five male and five females were used for this study and following standard procedures, the animals were captured alive around Zaria, using locally made rat traps, without any injury on them. The animals were anaesthetized with chloroform, sacrificed and transcardially perfused with a phosphate buffered solution of (pH 7.2, M = 0.12) 4% formaldehyde and 1% glutaraldehyde. The brain were removed and placed in the same fixative. The morphologic characteristics of the cerebrum and olfactory bulbs were observed with the naked eyes and electronic magnifying lens, and morphological features were recorded. Morphometric parameters of the cerebrum andolfactory bulb were taken, recorded and analyzed statistically using descriptive statistics and student's *t*- test. Histological sections were prepared after fixation and routine tissue processing, embedded in a low-gelling temperature agarose (6% agar), tissue sections of 60 um cut, perpendicular to the long axis (coronal section), were serially obtained with a calibrated vibratome and staining in thionin stain, stained tissues were viewed under the microscope and photomicrographs were taken. Designed-based stereological methods (optical fractionation and Cavalieri principle) were employed to estimate the neuronal number in olfactory bulb and volumes

of the different layers in the olfactory bulb and cerebral cortex stained in 0.2% Thionin solution. The results showed that the adult AGR have lissencephalics cerebrum, a mean absolute cerebral weight of 3.44 ± 0.07g, relative cerebral weight of 0.29 ± 0.23, a globular shaped olfactory bulb, the olfactory bulb accounts for 8 % the total body weight in the AGR, cyto-architectural arrangement was similar to that of the olfactory bulb of dog, and other rodents, a mean neuronal number in the different layers of the olfactory bulbs irrespective of sex for the periglomerular cells, tufted cells, mitral cells, periglomerular cells and the granule cells account for 20.72%, 6.44%, 4.61%, 3.27% and 63.68% of the neurons in the five layers of the olfactory bulb in AGR respectively. Results of the mean volumes of the glomerular cell layers and the granule cell layer of the AGR, showed that Layers I, 11, 111, IV, V and VI accounted for 19.7%, 18.5%, 18.6%, 21% and 23.7% of the volume of the cerebral cortex of the AGR, respectively. This study for the first time reports on the volume of the different layers of the olfactory bulbs and cerebral cortex in the African giant rat *(Cricetomys gambianus).* The results obtained from this study can be used in comparative anatomy of rodents of similar species, comparative neurology of rodents and other mammals, and in elucidating the mechanism of olfaction and other brain functions in this macrosomatic rodent. The number and of neurons and the volumes of the individual layers in olfactory bulb and the cerebrum, may represent a more accurate indicator of the neural machinery and synaptic microcircuitry in these brain regions in rodents and other mammals.

TABLE OF CONTENTS

Cover Page - - - - - - - - - i

Title Page - - - - - - - - - ii

Dedication - - - - - - - - - iii

Declaration - - - - - - - - - iv

Certification - - - - - - - - - v

Acknowledgement - - - - - - - - - vi

Abstract - - - - - - - - - x

Table of Contents - - - - - - - - - xii

List of Tables - - - - - - - - - xvii

List of Figures - - - - - - - - - xviii

List of Plates - - - - - - - - - xix

List of Appendices - - - - - - - - - xxi

CHAPTER ONE

1.0 Introduction - - - - - - - - - 1

1.1 Morphology - - - - - - - - - 2

1.2 Morphometry - - - - - - - - - 2

1.3 Stereology - - - - - - - - - 3

1.4 Statement of the Problem - - - - - - - - 6

1.5 Justification of the Study - - - - - - - - 6

1.6 General Aim of the Study - - - - - - - - 7

1.7 Specific Objectives of the Study - - - - - - - 7

CHAPTER TWO

2.0 Literature Review - - - - - - - - - 8

2.1 Geographic Range of African Giant Rats - - - - - - 8

2.2 Habitat of African Giant Rats - - - - - - 8

2.3 Physical Features of African Giant Rats - - - - - 8

2.4 Reproduction in African Giant Rats - - - - - 9

2.5 Brain Morphometry of African Giant Rats - - - - 11

2.6 Anatomy of the Olfactory Bulb - - - - - - 12

2.6.1 Development of the Olfactory Bulb - - - - - 13

2.6.2 Malformation of the Olfactory System - - - - - 16

2.6.3 Odour perception - - - - - - - 16

2.6.4 Main Olfactory Bulb - - - - - - - 19

2.6.5 Accessory Olfactory Bulb - - - - - - 21

2.6.6 Evolution of the Olfactory Bulb - - - - - 21

2.6.7 Olfactory Nerve Layer - - - - - - - 22

2.6.8 Olfactory Glomerular Layer - - - - - - 23

2.6.9 External Plexiform Layer - - - - - - 24

2.6.10 Mitral Cell Layer - - - - - - - 24

2.6.11 Granule Cell Layer - - - - - - - 26

2.7 Cerebral Cortex - - - - - - - - 29

2.8 Training of African Giant Rats for Mine Detection - - - 30

2.9 Use of African Giant Rats in Scent Detection of Tuberculosis - - 31

2.10 Cerebral Cortex - - - - - - - - 33

2.10.1 Embryology of the Cerebral Cortex - - - - - 34

2.10.2 Evolution of the Cerebral Cortex - - - - - 35

2.10.3 Layers of the Cerebral Cortex - - - - - - 36

2.10.4 Connections of the Cerebral Cortex - - - - - 40

2.10.5 Cortical Thickness - - - - - - - 41

2.10.6 Comparative Anatomy of the Cerebral Cortex in Rodents and Primates- 41

CHAPTER THREE

3.0 Materials and Methods - - - - - - - 46

3.1 Experimental Design - - - - - - - 46

3.1.1 Capturing of Animal - - - - - - - 46

3.1.2 Housing and Feeding of Animals - - - - - 46

3.1.3 Sacrificing of Animals - - - - - - - 46

3.2 Extraction and Preparation of the Brain - - - - - 46

3.2.1 Extraction of the Brain - - - - - - - 46

3.2.2 Separation of the Olfactory Bulbs, Cerebrum and Cerebellum - - 47

3.3 Anatomical Study of the Olfactory Bulbs and Cerebrum of African Giant Rats 47

3.3.1 Morphologic (Gross Anatomical) Study - - - - 47

3.3.2 Morphometric Study - - - - - - - 48

3.3.3 Light Microscopy Study of the Olfactory Bulbs and Cerebrum of African Giant Rats - - - - - - - - 48

3.3.3.1 Fixation - - - - - - - - 48

3.3.3.2 Embedding - - - - - - - - 49

3.3.3.3 Mounting on metal block - - - - - - 49

3.3.3.4 Tissue Sectioning and staining - - - - - 49

3.3.3.5 Mounting on Chrome-Gelatine Slides - - - - 50

3.3.3.6 Dehydration and Thionin Staining - - - - - 50

3.3.3.7 Light Microscopy Study and Photomicrography of Slides - - 50

3.4 Stereological Study of the Olfactory Bulbs and Cerebrum of African Giant Rats - - - - - - - - - 50

3.4.1 Estimation of Neuronal Number in Olfactory Bulbs of African Giant Rats Using Optical Fractionator - - - - - - 51

3.4.2 Estimation of Volume of Layer of Olfactory Bulbs in African Giant Rats Using the Cavalieri Principle - - - - - - 52

3.4.3 Point Counting - - - - - - - - - 52

3.4.4 Z- Axis Analysis - - - - - - - - 53

3.4.5 Counting Procedure for Neuronal Estimation of Olfactory Bulb Cells - 53

3.4.5.1 Counting Criteria for Cells of the Olfactory Bulb of African Giant Rats 54

3.4.5.2 Counting Criteria for Periglomerular Cells of olfactory bulb of African Giant Rats - - - - - - - - - 54

3.4.5.3 Counting Criteria for Mitral Cells - - - - - 54

3.4.5.4 Counting Criteria for Granule Cells - - - - - 55

3.5 Sampling Fraction - - - - - - - - - 55

3.6 Estimation of the Coefficient of Error - - - - - 56

3.7 Statistical Analysis - - - - - - - - 56

CHAPTER FOUR

4.0 Results - - - - - - - - - - 58

4.1. Physical Features of the Adult African Giant Rats - - - 58

4.2. Descriptive Statistics of the Morphometric Parameters of Adult African Giant Rats- - - - - - - - - - 60

4.3. Sexual Dimorphism in the Body Morphometric Parameters in the Adult African Giant Rats - - - - - - - - 62

4.4. Morphologic parameters of the Olfactory bulbs of Adult African Giant Rats 64

4.5. Morphological features of the cerebrum of adult African Giant Rats - 66

4.6. Morphometric Parameters of the Olfactory Bulbs of Adult African Giant Rats 73

4.7. Morphometric Parameters of the Olfactory Bulb in Male and Female Adult AGRs - - - - - - - - - - 75

4.8. Morphometric Parameters of the Cerebrum of Adult African Giant Rats 77

4.9. Sexual dimorphism in the Morphometric Parameters in the Cerebrum of Adult African Giant Rats - - - - - - - - 79

4.10. Cytoarchitecture of the Olfactory Bulb in the Adult African Giant Rats 81

4.11. Cytoarchitecture of Adult African Giant Rat Cerebral Cortex - - 88

4.12. Designed-based estimation of neuronal number in Olfactory Bulbs of the Adult African giant rats - - - - - - - 95

4.13. Descriptive Statistics (Optical fractionator) Olfactory Bulbs of the male and female adult AGR - - - - - - - 97

4.14. Descriptive Statistics (Cavalieri Principle) Olfactory Bulbs of adult African Giant Rat - - - - - - - 99

4.15. Descriptive Statistics of Designed-Based (Cavalieri Principle) Estimation of Volume of the Layers of the Olfactory Bulb in Adult African Giant Rat 101

4.16. Volume (mm^3) of the cerebral cortex layers of adult African Giant Rat, according to Cavalieri Principle- - - - - - 103

4.17. Descriptive Statistics of Designed-Based Stereological Estimation of Volume of Layers of Cerebral Cortex of Adult African Giant Rats by Cavalieri Principle - - - - - - - 105

CHAPTER FIVE

5.0 Discussion - - - - - - - - - 107

CHAPTER SIX

6.0 Summary, Conclusions and Recommendation - - - - 117

6.1 Summary - - - - - - - - - 117

6.2 Conclusion - - - - - - - - 118

6.3 Recommendation - - - - - - - - 119

References - - - - - - - - - 120

LIST OF TABLES

Table 1: Comparative cortical volumes in rodents - - - - 43

Table 2: The body weight and nose-rump length of adult African Giant Rats 61

Table 3: Sexual Dimorphism in the Body Morphometry in the African Giant Rats - - - - - - - - 63

Table 4: Body weight, olfactory bulb weight, width and thickness of the African Giant Rat - - - - - - - 74

Table 5: Sexual Dimorphism in the Morphometry of the Olfactory bulb of adult African Giant Rats - - - - - - 76

Table 6: Cerebral weight, width and thickness in the African giant rats - 78

Table 7: Sexual Dimorphism in the Cerebral Morphometric Parameters in the African Giant Rat - - - - - - - 80

Table 8: Designed-based estimation of neuronal numbers in Olfactory Bulbs of the Adult African Giant Rat - - - - - 96

Table 9: Design-based estimation of neuronal numbers in the olfactory bulbs of adult male and female African Giant Rats - - - 98

Table 10: Volume (mm^3) of the different layers of the Olfactory Bulbs of adult African Giant Rats according to Cavalieri Principle - - 100

Table 11: Descriptive Statistics (Cavalieri Principle) of the Olfactory Bulb's layer in adult male and female African Giant Rats - - 102

Table 12: Volume (mm^3) of the Cerebral Cortex Layers of adult African Giant Rats - - - - - - - - 104

Table 13: Volume (mm^3) of the Cerebral Cortex Layers of adult male and female African Giant Rats - - - - - 106

LIST OF FIGURES

Figure 1: Development of the Olfactory Bulb - - - - 15

Figure 2: Olfactory bulb and its contents - - - - - 18

Figure 3: Layers of the cerebral cortex (histological structure of the cerebral cortex) - - - - - - 39

LIST OF PLATES

Plate I: African Giant rat (*Cricetomys gambianus*, Waterhouse - 1840) - 59

Plate II: The dorsal view of the brain of adult African Giant rat showing the left olfactory bulb, LOB and right olfactory bulb, ROB - - 65

Plate III: Dissected whole brain (in situ) of African giant rat (*Cricetomys gambianus*, Waterhouse-1840), showing longitudinal fissure, Lf. 67

Plate IV: The dorsal view of the cerebrum of adult African Giant rat, showing the left cerebral, LC; and right cerebral, RC, cerebral hemispheres; cerebellum, (Cb); longitudinal fissure, Lf and horizontal fissure, Hf. 68

Plate V: The dorsal view of the cerebrum of adult African Giant rat, showing the parietal region, Pr; frontal region, Fr; temporal region, Tr and Occipital region, Or. - - - - - - 69

Plate VI: The dorsal view of the cerebrum of adult African Giant Rat, showing the Dorsal surface, Dor. S of the cerebrum - - - 70

Plate VII: The cerebrum of adult African Giant Rat, showing the medial surface, Med. S of the cerebrum - - - - - 71

Plate VIII: The ventral view of the cerebrum of adult African Giant Rat, showing the ventral surface, Ven. S of the cerebrum - - 72

Plate IX: Transverse section of the cytoarchitecture of the olfactory bulb of adult African giant rat. Glomerular layer, GL; external plexiform layer, EPL; mitral cell layer, MCL; internal plexiform layer, IPL; granule cell layer, GCL; medulla, M - - - - - 82

Plate X: Transverse section of the cytoarchitecture of the olfactory bulb of adult African giant rat showing the periglomerular cells, PC and glomerulus, Glo of glomerular layer - - - - 83

Plate XI**:** Transverse section of the cytoarchitecture of the olfactory bulb of adult African giant rat showing the tufted cells, TC of external plexiform layer - - - - - - - 84

Plate XII: Transverse section of the cytoarchitecture of the olfactory bulb of African giant rat showing the mitral cells, MC of mitral cell layer 85

Plate XIII**:** Transverse section of the cytoarchitecture of the olfactory bulb of African Giant rat showing the granule cells, GC of granular layer 86

Plate XIV: Transverse section of the cytoarchitecture of the olfactory bulb of adult African Giant rat. Showing the medulla - - - 87

Plate XV: Transverse section of the cytoarchitecture of cerebral cortex of adult Africa Giant Rat. Layer I, molecular layer; layer II/III, external granular/pyramidal layer; layer IV, internal granular layer; layer V, internal pyramidal layer and layer VI, multiform or polymorphic layer 89

Plate XVI: Transverse section of the cytoarchitecture of cerebral cortex layer I (molecular layer) of adult African Giant rat. Dendrites of pyramidal neurone (DPN) - - - - - - - 90

Plate XVII: Transverse section of the cytoarchitecture of Cerebral Cortex layer II/III, external granular/pyramidal layer of the adult African Giant rat 91

Plate XVIII: Transverse section of the cytoarchitecture of the Cerebral cortex layer IV, internal granular layer of the African Giant rat - 92

Plate XIX: Transverse section of the cytoarchitecture of the Cerebral Cortex layer V, internal pyramidal layer, of the African Giant rat - 93

Plate XX: Transverse section of the cytoarchitecture of the Cerebral Cortex layer VI, multiform (polymorphic) layer of the African Giant Rat 94

LIST OF APPENDICES

Appendix I: Preparation of 1% glutaraldehyde and 4% formaldehyde fixatives 135

Appendix II: Composition and preparation of Thionin stain for fixed tissues (rat) 136

Appendix III: Preparation of agarose gel for embedding - - - 138

Appendix IV: Formulas - - - - - - - 139

Appendix IV: Glossary - - - - - - - 141

CHAPTER ONE

1.0. INTRODUCTION

The African Giant rat (AGR) (*Cricetomys gambianus,* Waterhouse-1840), also known as the Gambian pouched rat, is a wild rodent that belongs to the order *Rodentia*, and is quite common in Nigeria. The rats are well distributed but more dominant in the Savannah areas of the country. The AGR has potentials as a laboratory animal, but it is better sought after as meat delicacy by the local people (Onyeanusi *et al*., 2007), the male AGR is called "Burgu" and the female 'gafiya' in Hausa language, "Okete" in Yoruba language, "Ewi" in Igbo and "African rat geant" in French. An increasing amount of interest is presently being expressed on the biology of the AGR. The rats have already been successfully used to detect land mines in Mozambique because of their high acuity of odour perception (Magi, 2003). In Europe, AGR's imported from sub-Sahara Africa are trained to sniff out tuberculosis in humans. Attempts have been made to classify AGR as laboratory model (Ajayi, 1978; Olayemi and Adeshina, 2002). In United Kingdom, the AGR is increasingly becoming a popular pet (Copper, 2008).

The brain, the organ of thought and cognizance perception, is composed of the cerebrum, cerebellum and brainstem (Moore *et al*., 2014; Nolte, 2007; Sinnatamby, 2011). The cerebrum is the largest part of the brain. In humans, it is the part of the brain, where activities, including reasoning, learning, sensory perception and emotional responses, take place (Moore *et al*., 2014; Singh, 2014). It consists of two partially connected cerebral hemispheres. The cerebral hemisphere has three different poles, namely: (i) the frontal pole, which lies anteriorly; (ii) the occipital pole, which is posteriorly placed; and (iii) the temporal pole, which lies between the frontal and occipital poles and points forward and same whole downwards (Drake *et al*., 2012; Sinnatamby, 2011; Moore *et al*., 2014).

The olfactory bulb (*Bulbus olfactorious*) is a structure of the vertebrate forebrain involved in olfaction, the perception of odours (Nolte, 2007). In most vertebrates, the olfactory bulb is the most rostral (forward) part of the brain; while in humans, the olfactory bulb is on the inferior (bottom) side of the brain. The olfactory bulb is supported and protected by the cribriform plate of the ethmoid bone, which in mammals separates it from the olfactory epithelium, and which is perforated by olfactory nerve axons (Sinnatamby, 2011). The olfactory bulb is a highly organized structure, composed of several distinct layers and synaptic specializations. The layers (from outside toward the centre of the bulb) are differentiated into the following: glomerular layer, external plexiform layer, mitral cell layer, internal plexiform layer, granule cell layer (Mori *et al*., 2006; Wei *et al*., 2008).

1.1. Morphology

Morphology is the study of the form and structure of organisms and their specific structural features. This includes aspects of the outward appearance (shape, structure, colour, and pattern) (Hongtu *et al*., 2007). Shape descriptors offer a more informative representation of morphology, adding additional information over volumetric measurements (Wachinger *et al*., 2014). Morphology offers advantages for studying the shape variability within and across populations because additional information is available for the statistical analysis.

1.2. Morphometry

Morphometry as the measurement of morphology, in three dimension (3D), such measurements can be done directly; for example through determination of the height of a person using a measuring tape. However in biomedical research, morphometry is most frequently performed on thin sections using microscopy. These sections can often be

regarded as nearly two dimensions and, what is seen is not the whole three dimensions objects themselves, but only a fraction of their two dimensions representation. The goal of morphometry is the estimation of quantitative parameters such as volume, surface area, length or number of the 3D objects, and it has to take into account the loss of one dimension during the cutting process (Singleton *et al.*, 2011; Serag *et al.*, 2012). Brain morphometric is a subfield of both morphometry and the brain sciences, concerned with the measurement of brain structures and changes there of during development aging, learning, disease and evolution. Since autopsy-like dissection is generally impossible on living brains, brain morphometry starts with noninvasive neuroimaging data, typically obtained from magnetic resonance imaging (MRI). These data are born digital, which allows researchers to analyze the brain images further by using advanced mathematical and statistical methods such as shape quantification or multivariate analysis. This allows researchers to quantify anatomical features of the brain in terms of shape, mass, volume (e.g. of the cerebellum, or of the primary versus secondary visual cortex), and to derive more specific information, such as the encephalization quotient, grey matter density and white matter connectivity, gyrification, cortical thickness, or the amount of cerebrospinal fluid. These variables can then be mapped within the brain volume or on the brain surface, providing a convenient way to assess their pattern and extent over time, across individuals or even between different biological species (Fred, 2001).

1.3. Stereology

Stereology provides efficient tools for estimation of geometric quantities such as volume, surface area, length, or number of objects for 3-D tissue structures, contained within an organ from measurements made on a set of 2-D sections (West, 1993; Gundersen, 1999). Stereological analyses involve a two-step process (West, 2002). Statistical sampling principles are used to obtain statistically valid histological sections from an organ to

reduce the amount of tissue for analysis without reducing the precision of the estimate (Gundersen, 1999; Nyengaard, 1999). Design-based stereology provides estimates of total volume, surface area, length, or cell number in an organ, making no assumptions about the structures in an organ. Strict adherence to the principles of stereology guarantees accuracy; that is, the mean of the estimates comes closer and closer to the true value with replication. Accurate estimation of particle numbers from tissue sections became possible only in 1984 with the invention of the physical dissector (Sterio, 1984; Boyce, 2010). Unbiased stereology has been considered by modern neuroscientists as the most preferred method to measure or quantify morphological properties of the central nervous system (CNS) (Grady *et al*., 2003). This is particularly important in identification of subtle, yet important alterations in the morphology of the brains, based on disturbances during development or in neuropsychiatric and neurodegenerative diseases (Boyce *et al*., 2010).

Some of the probes employed in unbiased stereology include optical fractionator and Cavalieri principle (Glaser *et al*., 2007). The optical fractionator is a designed-based stereological method using a two-stage systematic sampling method to estimate the number of objects in a specified region of an organ (West, 2002). This method combines the optical disector methods with fractionator sampling method. It is the most commonly used stereological probe in the life sciences. It can be used to estimate the total number of objects in any three-dimensional volume regardless of that volume's shape (Glaser *et al*., 2007). The optical fractionator is appropriate for the quantification of such objects as cells, synapses, glomeruli, and any discrete objects within biological tissues (Gundersen *et al*., 1999; Hosseini-Sharifabad and Nyengaard, 2007). The optical fractionator uses thick sections and estimates the total number of cells from the number of cells sampled with a systematic uniform, randomly sampled set of unbiased virtual counting spaces, covering the entire region of interest with uniform distance between unbiased virtual

counting spaces in directions X, Y, and Z (Nyengaard, 1999; Schmitz and Hof, 2005; Glaser *et al*., 2007). The optical fractionator is immune to tissue shrinkage due to histological processing (Dorph-Petersen *et al*., 2004; Boyce *et al*., 2010). Additionally, it is easier to estimate the precision of the number of estimate; that is, the coefficient of error (CE) generated using the optical fractionator, making it the method of choice (Gundersen *et al*., 1999; Nyengaard, 1999; Schmitz and Hof. 2005).

The Cavalieri is used to estimate volume (Grady *et al*., 2003). This instrument/method is often used in conjunction with other estimators that approximate density such as number density, length density, or surface density. The sections for Cavalieri principle are sampled using the fractionator principle. A rule of thumb is to use 10 to 15 sections. Suppose that the tissue is sectioned into 80 sections; If every 6^{th} section is used, then around 13 sections are used. This is usually an adequate number of sections. The fractions are used in the sampling fraction (ssf). The Cavalieri estimator is usually performed using a point grid. The points need to be appropriately spaced. The points are usually spaced equally both across and down. A rule of thumb is to count 200 to 250 points. Some experimentation is usually required to determine an adequate spacing of the point grid. Regions that have complicated profiles or profiles that are thin require closer points than simple shapes. The distance between the points can be used to compute the intensity of the probe (Nielsen *et al*., 2001). The number of points that hit each section is counted and it is used to compute the volume and CE (Gundersen *et al*., 1986a). The formula for calculating volume in the Cavalieri Principle is given as:

$$V= t^* a/p *\sum P$$

Formula for volume

Where V is the volume, t is the thickness of the tissue section, a/p is the area of points and ∑P is the sum of points (Gundersen *et al*., 1986b).

1.4. Statement of the Problem

The National Wildlife Conservation Committee has encouraged the domestication of the African Giant rats because of its numerous usefulness (Ikede and Ajayi, 1976, NRC, 1991). Therefore, there is a need to understand the biology of this rodent in order to elucidate the neuroanatomical basis of the olfactory behaviour of AGR. It is because of this need that the study of the cerebrum and olfactory bulbs of the AGR was carried out. Although literature on the anatomy of the AGR is gradually building up (Ogwuegbu *et al*, 1983; Oke and Aire, 1989, 1990; Oke *et al*., 1996; Nzalak *et al.,* 2005; Ibe *et al*, 2012), there is paucity of information on the detailed morphometric, histologic analysis of the olfactory bulbs and cerebrum of the AGR. There is also no information on the stereologic study of the olfactory bulb and cerebrum of the AGR. Quantitative morphology is important in neurobiology, developmental and clinical human biology. The quantification of cerebral layers and olfactory bulbs, their neuronal population and volume in AGRs, may shed light on the neuroanatomical basis of the highly-developed olfactory ability of the rodent and some of its behaviour.

1.5. Justification of the Study

There is need to study the olfactory bulb cerebrum and of this rodent. This may serve as a fulcrum for future clinical and research applications, involving this macrosomatic animal. The findings from the anatomical studies of structures of the cerebrum and olfactory bulbs in the rodent may contribute to our current understanding of some of its unique behaviour, such as the ability to detect explosives in mines and tuberculosis bacteria in saliva. A detailed stereological study of the neuronal assortment of olfactory bulbs of the

AGR may also provide information on the behavioural trait, especially the strong olfactory ability of the AGR.

1.6. General Aim of the Study

The general aim of the study was to investigate the olfactory bulbs and cerebrum of the AGR in order to elucidate the neuroanatomical basis for their special olfactory acquity and visual attention.

1.7. Specific Objectives of the Study

The specific objectives of the study were to:

i. Determine the gross morphology of the olfactory bulbs cerebrum and of the African Giant rat.
ii. Evaluate the morphometric features of the olfactory bulbs cerebrum and of the African Giant rat.
iii. Investigate the histological structures of the olfactory bulbs cerebrum and of the African Giant rat.
iv. Describe some stereological parameters such as the Optical fractionation and Cavalieri principle of the olfactory bulbs cerebrum and of the African Giant rat.

CHAPTER TWO

2.0. LITERATURE REVIEW

Two remarkable domestication programme have been initiated in Africa: the grasscutter in West Africa and the African Giant rat in Ghana and Nigeria. Both animals provide popular "bushmeat" and researchers are now studying how to raise them in captivity (Ikede and Ajayi, 1976; Baptist and Mensah, 1986; Mensah, 1991).

2.1. Geographic Range of African Giant Rats

African Giant rats are found in West, Central and East Africa, in regions south of the Sahara desert as far south of Zululand. These include countries such as Nigeria, Mozambique, in regions south of the Sahara desert as far south as Zululand (Ajayi *et al*., 1978; Kingdon, 1989).

2.2. Habitat of African Giant Rats

African Giant rats (AGRs) live in varieties of habitats, ranging from arid areas to temperate areas, but need some form of shelter to survive. They are not usually found in completely open areas, but in areas with cover, including hollow trees, rock out-cropping, or burrows made by other animals. They are occasionally known to venture into urban areas and can become pest animals. Their terrestrial biomes include the Savanna, grassland, forest and mountains. They also live in urban and agricultural settlements (Ajayi, 1978; Kingdon, 1989).

2.3. Physical Features of African Giant Rats

The AGRs are similar in size to the other species of giant pouched rat, African giant pouched rats, but are often confused with this species. AGRs have coarse, brown fur and a dark ring around the eyes, in contrast to African giant pouched rats, which have soft, grey coats with white fur on the belly. Their long tails are scaly and they have narrow

heads with small eyes. The main physical characteristic of AGRs, and all Cricetomys in general, are their large cheek pouches. These pouches can expand to a great size, allowing AGRs to transport massive quantities of food, if necessary. Cheek pouches also exist in other families of *Rodentia*, such as the African hamster and members of the sub-family *Cricetinae*. Males and females are usually the same size, with little sexual dimorphism. African giant rats can reach sizes up to 910 mm and beyond, including the tail. These rats also have very low-fat content, which may be the cause of their susceptibility to cold (Ajayi, 1978; Kingdon, 1989; Ryan, 1989; Nowak, 1999). They are endothermic, and use metabolically-generated heat to regulate body temperature independently of ambient temperature. AGRs have bilateral symmetry; that is, they have body symmetry such that the animal can be divided in one plane into two mirror-image halves. Animals with bilateral symmetry have dorsal and ventral sides, as well as anterior and posterior ends. They exhibit sexual dimorphism. They weigh between 1 to 1.47 kg, with an average range length of 645 to 910 mm (25.39 to 35.83 in), and have an average basal metabolic rate of 71 cm^3.O2/g/h (Kingdon, 1989; Ryan, 1989; Nowak, 1999).

2.4. Reproduction in African Giant Rats

Mating in AGRs involves the formation of a social pair-bond between one male and one female. The male usually sniffs or licks the urogenital areas of the female before attempting to mount the female. Gambian rats also display peculiar courtship behaviours (Knight, 1988). The male and female often stand upright and scratch one another, then chase each other until the female is ready for copulation. If the female is not receptive or rejects the male, she bites the male on the tail and back among other areas before courtship behaviors begin (Ajayi *et al*., 1978; Kingdon, 1989; Amador, 2003). The mating system in AGRs is monogamous, having one mate at a time. They are seasonal breeders, usually breeding in the summer. The estrous cycle lasts between 3 and 15 days,

while the length of estrus ranges from about 1.4 to 7.8 days. Interestingly, the estrous cycle is often irregular and seems dependent upon many external factors, especially the environmental factors: Other factors include the presence of males and captivity. Females reach sexual maturity at about 6 months and will typically have about 9 litters annually. The gestation period is approximately 30 to 32 days. Female AGRs are also very aggressive, when giving birth to a litter. Breeding usually occurs in the summer and number of offspring ranges from 1 to 5, with an average of 3.5 offspring (Ajayi *et al*., 1978; Kingdon, 1989; Nowak, 1999; Malekani, *et al*., 2002).

The gestational period in AGR is 30 to 32 days. An average birth mass is 25.7 g. Average weaning age is 28 days and average time to independence is 30 days. Average age at sexual or reproductive maturity (female) is 6 months. The AGRs are iteroparous, offsprings are produced in more than one group (litters, clutches,) and across multiple seasons (or other periods hospitable to reproduction). The young of the AGR's are born hairless, with eyes and ears closed. The characteristic long-tail does not show substantial growth until about 30 to 35 days. The eyes do not open until about 21 days into development, although the young are completely covered with fur and have open ears at about 14 days. The female AGR provides the most parental care, both as a source of warmth for the naked young and as a source of milk. The female also changes her food preference before the young are weaned, choosing softer foods. The male, on the other hand, shows almost no care to the young. It shows tolerance at best, and will sometimes kill its young and eat them. This is not seen as often in females. An interesting form of altruism exists amongst females, where a female with a separate litter may take care of a motherless litter (Ajayi *et al*., 1978).

2.5. Brain Morphology of African Giant Rats

Nzalak *et al.* (2008) reported the morphometric parameters of the cerebellum and forebrain of the AGR, and obtained the following values: the mean weights and lengths taking the measurements from the tip of the olfactory bulb to the caudal border of the cerebellum, were reported to be 4.88 ± 0.183 and 4.40 ± 0.193g respectively, while the mean weights length of the cerebellum and forebrain are 0.642 ± 0.61g and 3.317 ± 0.119 g for cerebellum and 1.138 ± 0.656 cm and 2.75 ± 0.1087cm for the forebrain. The cerebellum account for 13% and the forebrain account for 68.4% of the total brain weight. The study reported that the olfactory bulb accounted for 19.01% of the total brain target of AGRs, which indicated that the 0.13 is grossly large and, therefore, can facilitate experimental procedures for the study of olfaction.

In another study by Olude *et al.* (2009) on neuro-cranial measurements of the skulls of the AGR, the mean neuro-cranial volume, length and height were reported to be 5.06 ± 0.05 mL, 3.38 ± 0.8 cm and 1.39 ± 0.4 cm, respectively. The study also reported the neuro-cranial index to be 41.74%, while the mean skull length and height were 6.32 ± 0.86 cm and 2.98 ± 0.05 cm, respectively. The above measurements were taken with mandible, while without mandible, the skull height was 1.83 ± 0.02 cm and the index was 28.41 ± 0.58. The finding indicates that the height of the skull of the hair was approximately 47% of the skull length. The study established the possibility of estimation of brain density and the use of the rodent for cranial pressure experiments. The study which used 16 AGRs, consisting of 8 male and 8 female rats, did not indicate whether the animals were adult or young rodents, but gave a good insight into the study of the neuro-cranial parameters of the AGR.

Another study by Ibe *et al.* (2010) reported sexual dimorphism in the whole brain and brainstem in the morphometry of the AGR cerebral cortex. The study reported significant difference in the absolute brain weight of male and female AGR. The male AGRs have higher absolute brain weight than the female; while the female had higher relative brain weight than the males, although the difference was not significant. There was also no significant difference in the length of the brain and myelencephalon, but there was a significant difference in the length of width of the pyramid, with the male having a higher value for the female. The study demonstrated the role of sex in morphometric values of the brainstem in the AGR.

The olfactory bulb transmits smell information from the nose to the brain; and is thus necessary for a proper sense of smell (*Mori et al*., 2006). Although from an evolutionary stand-point, olfaction is one of the most ancient senses, its investigation lags far behind that on vision and hearing, apparently because it is harder to study the olfactory system (Mori *et al*., 2006). In 1991, Linda and Richard discovered the family of transmembrane proteins that were believed to be the odor receptors and some of the genes that encode them. They cloned and characterized 18 different members of an extremely large multigene family that encodes the seven transmembrane proteins, whose expression was restricted to the olfactory epithelium. This was a break-through in the potential understanding of the olfactory system. Since then, many studies on the olfactory system have been conducted (Wei *et al*., 2008).

2.6. Anatomy of the Olfactory Bulb

The olfactory bulb is a structure found in the brains of vertebrates. It is involved in processing information about odours, and is a key part of the neural system responsible for the sense of smell (Moore and Persaud, 2003; Hamilton *et al*., 2005). Cells located in

the nose that process odour input send signals directly to the olfactory bulb, which then serves as a pathway for that input to travel to different locations in the rest of the brain. It is a part of the limbic system. Within the brain, the bulb is located in the forebrain, though in humans it sits at the bottom. In other vertebrates, the bulb sits at the very front of a bony structure, called the cribriform plate cradles, which protects and separates it from the nasal cavity. It is divided into two sections, the main olfactory bulb and the accessory olfactory bulb (Halpern and Martínez-Marcos, 2003; Drake *et al*., 2012; Spors *et al*., 2012).

2.6.1. Development of the Olfactory Bulb

The primordia of the olfactory system consist of two placodes on the right and left of the antero-inferior portion of the frontal prominence, situated above the stomodeum, and below and lateral to the forebrain (Moore and Persaud, 2003; Sadler, 2005). The primordia appear about day 30, after those of the optic and otic placodes. At this time, too, the neural tube is completely closed. The placodes are primarily induced by the adjacent mesoderm and secondarily by the ventral surface of the prosencephalon. Each placode invaginates, in the direction of the adjacent brain, to form the olfactory pits. The stratified placodal base of the invagination forms the olfactory epithelium. The lateral walls around the invaginating pits form the surface ectodermal covering of the nasal cavities (Moore and Persaud, 2003; Sadler, 2005). The placodal cells of the olfactory epithelium differentiate into neurosensory cells within the thickness of the epithelium and eventually give origin to olfactory nerve fibres. At about five months, the deep pole of the superficial cells gives rise to an axon that crosses the epithelium and the mesenchyme and contacts the olfactory area of the cerebral hemisphere (telencephalon) (Moore and Persaud, 2003; Sadler, 2005). The arrival of these fibres at the telencephalon induces formation of the olfactory bulb. The axons then connect with the specialized structures of

the central nervous system, corresponding to the olfactory system; namely, the bulbs (Moore and Persaud, 2003; Sadler, 2005). Near the end of third month, the mesenchyme between the sensory epithelium and the bulb gives rise to a cartilaginous structure, the *lamina cribrosa* of the ethmoid bone, which is eventually organized around the olfactory nerve networks and separates them into a number of bundles. The cartilage ossifies here to form the cribriform plate of the ethmoid bone through which the nerves pass to enter the olfactory bulbs. The olfactory bulb elongates and eventually the extension of the ventricular cavity into it becomes obliterated (Halpern and Martínez-Marcos, 2003; Moore and Persaud, 2003; Sadler, 2005; Treloar *et al*., 2010).

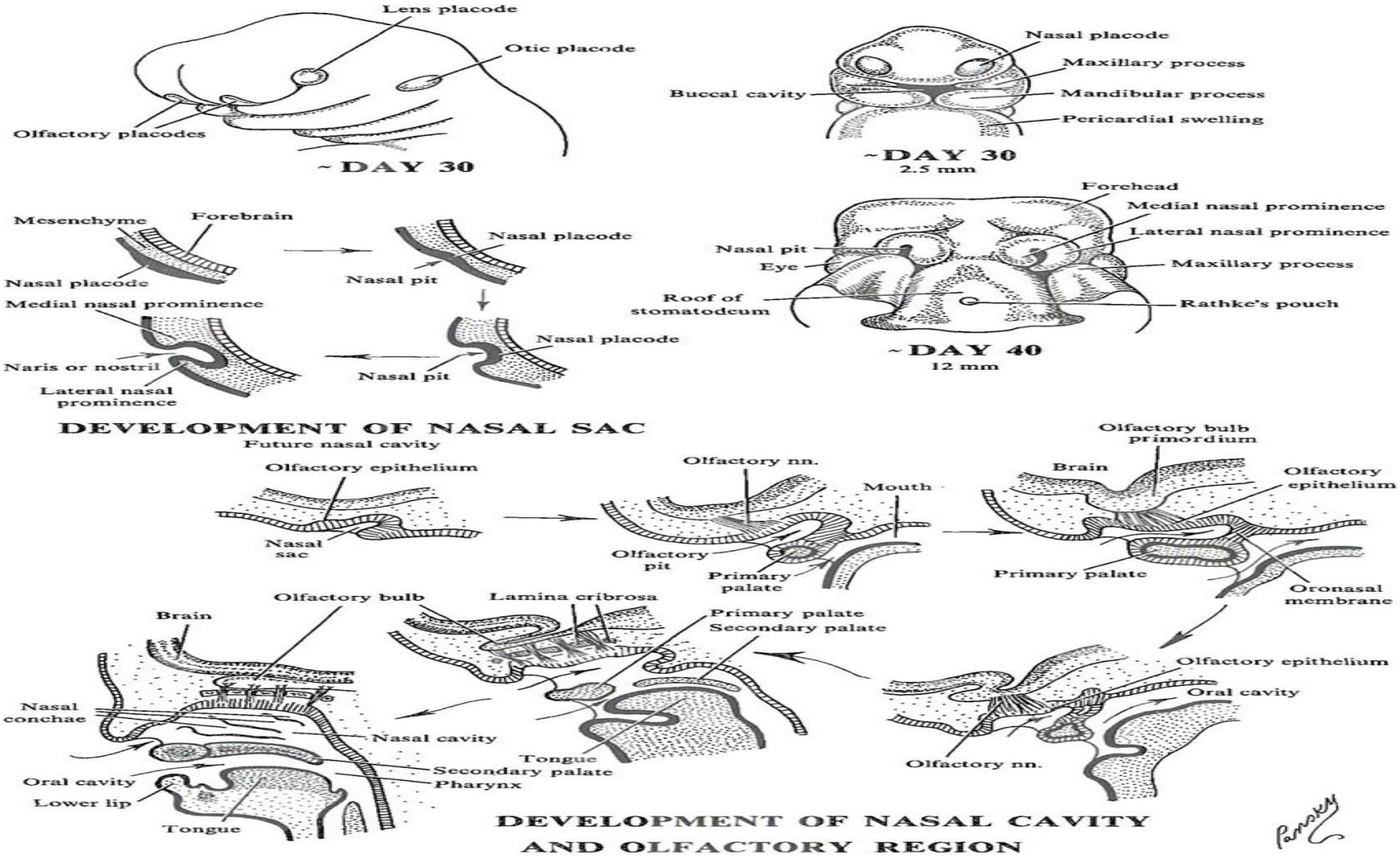


Figure 1: Development of the Olfactory Bulb (Courtesy of LifeMap Sciences Inc., 2002)

Cells in the bulb, around which the olfactory nerve fibres terminate and synapse, give origin to secondary olfactory fibres, which grow centrally and form the olfactory tract (Moore and Persaud, 2003). The olfactory tract terminates in the region of the piriform cortex. Fibres of the olfactory nerves are entirely of placodal origin and their cell bodies remain in the olfactory epithelium. In lower mammals, a special part of the olfactory nerve is distributed to Jacobson's organ as the vomeronasal nerve. The organ is found in the lower part of the nasal septum (Sadler, 2005; Treloar *et al*., 2010).

2.6.2. Malformations of the Olfactory System

Malformations are usually quite serious because they are always accompanied by anomalies of the central nervous system and the face. They are classified in the category of the more general malformations, examples include ethmocephalus, arrhinencephaly. In these malformations, the nose is replaced by a proboscis with a single canal, as a result of convergence of both nasal primordia on the mid-line (Levy *et al*., 2000). The sensory epithelium is much reduced or even totally absent (Leopold *et al*., 2002; Moore and Persaud, 2003). The olfactory bulbs also may be absent. In some cases, there may be two proboscise or even trunks. There are also minor types of this malformation, in which the nose is more or less cylindrical and the nasal fossae are totally closed (Sadler, 2005; Treloar *et al*., 2010). In humans, many of the causes of these malformations are apparently genetic in origin (Sadler, 2005; Treloar *et al*., 2010; Basile *et al*., 2012).

2.6.3. Odour Perception

When an odour enters the nasal cavity, it interacts with the millions of olfactory receptors located there. The receptors send signals along their axons, which are the parts of the cells that carry information away from them. The axons extend through the cribiform plate and directly into the main olfactory bulb, and actually make up a portion of the structure.

They form spherical clusters known as glomeruli, which in turn interact with neurones known as mitral cells. The mitral cells take the signals the rest of the way to the olfactory cortex; this is where awareness and identification of specific odours takes place (figure 2). In animals with a strong sense of smell (macrosomatics), the olfactory bulb is relatively large. Animals with less olfactory capacity, including humans (microsomatics), tend to have a smaller bulb in proportion to their brain. Research has shown that the olfactory bulb changes in size over the course of human adulthood. There is also a direct correlation between the amount of input being processed by the bulb and its size. For example, individuals who have lost the sense of smell due to injury or disease may have smaller olfactory bulb than average (Halpern and Martínez-Marcos, 2003).

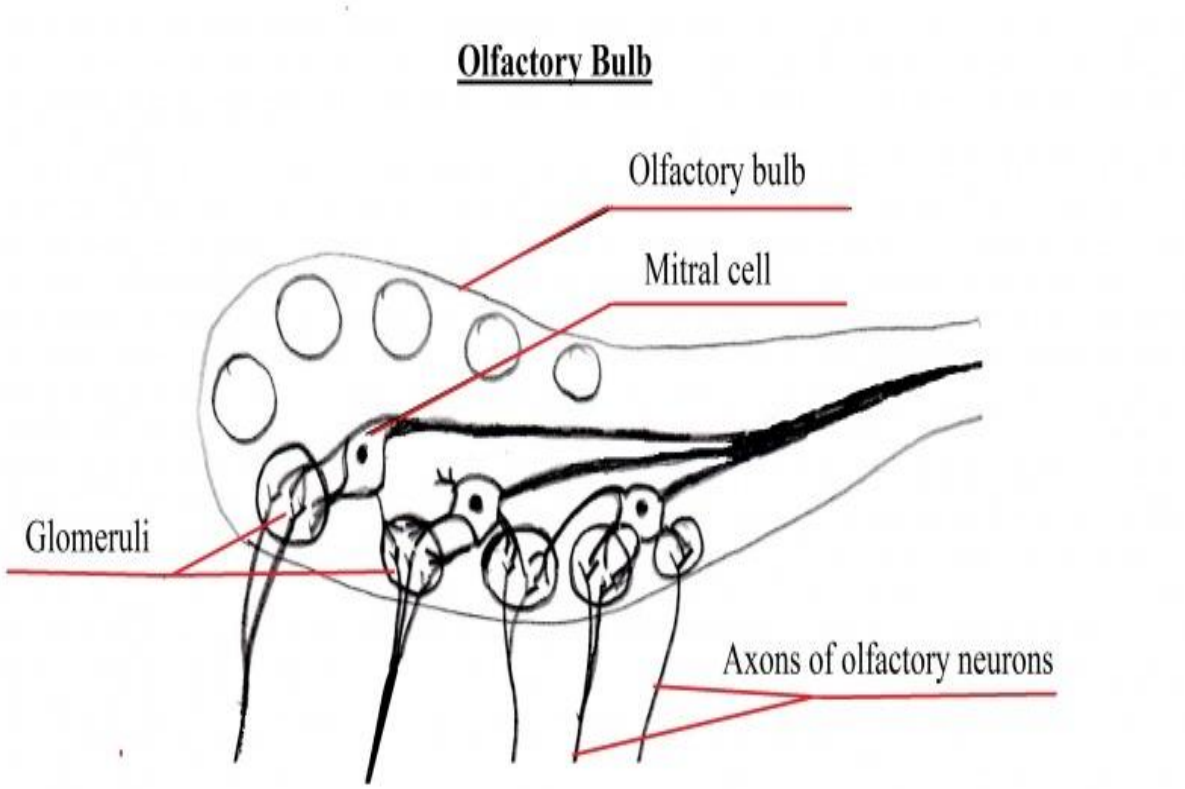


Figure 2: Olfactory bulb and its contents (Treloar *et al*., 2010)

In most vertebrates, the olfactory bulb is the most rostral (forward) part of the brain (Treloar *et al*., 2010). In humans, however, the olfactory bulb is on the inferior (bottom) side of the brain (Moore and Persaud, 2003; Sadler, 2005).

2.6.4. Main Olfactory Bulb

The main olfactory bulb has a multi-layer cellular architecture. In order from surface to the centre, the layers are glomerular layer, external plexiform layer, mitral cell layer, internal plexiform layer, granule cell layer (Halpern and Martínez-Marcos, 2003; Nolte, 2007; Wei *et al.*, 2008; Treloar *et al*., 2010). The olfactory bulb transmits smell information from the nose to the brain, and is, thus, necessary for a proper sense of smell. As a neural circuit, the glomerular layer receives direct input from olfactory nerves, made up of the axons from approximately ten million olfactory receptor neurones in the olfactory mucosa, a region of the nasal cavity (Wei *et al.*, 2008; Treloar *et al*., 2010). The ends of the axons cluster in spherical structures known as glomeruli such that each glomerulus receives input primarily from olfactory receptor neurons that express the same olfactory receptor. Glomeruli are also permeated by dendrites from neurones called mitral cells, which in turn output to the olfactory cortex. Numerous interneurone types exist in the olfactory bulb, including periglomerular cells which synapse within and between glomeruli, and granule cells which synapse with mitral cells (Ache and Young, 2005; Wei *et al.*, 2008; Treloar *et al*., 2010).

As a neural circuit, the olfactory bulb has one source of sensory input (axons from olfactory receptor neurones of the olfactory epithelium), and one output (mitral cell axons) (Wei *et al*., 2008). As a result, it is generally assumed that it functions as a filter, as opposed to an associative circuit that has many inputs and many outputs (Halpern and Martínez-Marcos, 2003). However, the olfactory bulb also receives "top-down"

information from such brain areas as the amygdala, neocortex, hippocampus, *locus coeruleus*, and *substantia nigra*. Thus, the potential functions of the olfactory bulb can be placed into four non-exclusive categories:

i. Discrimination among odours;
ii. Enhancement sensitivity of odour detection;
iii. Filtering out of many background odors to enhance the transmission of a few selected odours, and
iv. Permission of higher brain areas, involved in arousal and attention to modify the detection or the discrimination of odours.

Although all the functions could theoretically arise from the olfactory bulb's circuit layout, it is unclear which, if any, of the functions are performed exclusively by the olfactory bulb (Halpern and Martínez-Marcos, 2003). By analogy to similar parts of the brain such as the retina, many researchers have focused on how the olfactory bulb filters incoming information from receptor neurones in space, or how it filters incoming information in time. At the core of the proposed filters are the two classes of interneurones; the periglomerular cells, and the granule cells (Halpern and Martínez-Marcos, 2003; Wei *et al*., 2008). The basal dendrites of mitral cells are connected to interneurones known as granule cells, which by some theories produce lateral inhibition between mitral cells. It is not clear what the functional role of lateral inhibition would be, though it may be involved in boosting the signal-to-noise ratio of odour signals by silencing the basal firing rate of surrounding non-activated neurones. The synapse between mitral and granule cells is of a rare class of synapses that are "dendro-dendritic," which means that both sides of the synapse are dendrites that release neurotransmitters (Halpern and Martínez-Marcos, 2003; Wei *et al*., 2008). In this specific case, mitral cells release the excitatory neurotransmitter, glutamate, and granule cells release the inhibitory

neurotransmitter gamma-aminobutyric acid (GABA). As a result of its bi-directionality, the dendro-dendritic synapse can cause mitral cells to inhibit themselves (auto-inhibition), as well as neighbouring mitral cells (lateral inhibition). Olfaction is distinct from the other sensory systems, where peripheral sensory receptors have a relay in the diencephalon. Therefore, the olfactory bulb plays this role for the olfactory system (Halpern and Martínez-Marcos, 2003).

2.6.5. Accessory Olfactory Bulb

The accessory olfactory bulb, which resides on the dorsal-posterior region of the main olfactory bulb, forms a parallel pathway independent from the main olfactory bulb. It is the second processing stage of the accessory olfactory system. It receives axonal input from the vomero-nasal organ, a distinct sensory epithelium from the main olfactory epithelium that detects pheromones among other chemical stimuli (Peter and Frank, 2006). As in the main olfactory bulb, axonal input to the accessory olfactory bulb forms synapses with mitral cells within glomeruli. However, mitral cells in the accessory olfactory bulb project their axons to targets in the amygdala and hypothalamus, where they may influence aggressive and mating behaviour. The olfactory bulbs in humans also sense an impending danger. There is evidence against the presence of a functional accessory olfactory bulb in humans and other higher primates (Peter and Frank, 2006; Treloar *et al*., 2010).

2.6.6. Evolution of the Olfactory Bulb

Comparing the structure of the olfactory bulb among vertebrate species, such as the leopard, the frog and the lab mouse, reveals that they all share the same fundamental lay-out (five layers containing the nuclei of three major cell types), despite being dissimilar in shape and size. Of note, a similar structure is shared by the analogous olfactory centre in the fruit fly, *Drosophila melanogaster*, the antennal lobe (Ache, 2010;

Wang, 2012). One possibility is that vertebrate olfactory bulb and insect antennal lobe structure may be similar because they contain an optimal solution to a computational problem, experienced by all olfactory systems. Thus, the two structures may have evolved independently in different phyla - a phenomenon generally known as convergent evolution (Bastir *et al*., 2011).

The increase in brain size relative to body size – encephalization - is intimately linked with human evolution. However, two genetically different evolutionary lineages, Neanderthals and modern humans have produced similarly large-brain human species. Thus, understanding human brain evolution should include research into specific cerebral reorganisation, possibly reflected by brain shape changes. Three-dimensional geometric morphometric analyses of endo-basi-cranial shape reveal previously undocumented details of evolutionary changes in *Homo sapiens* (Bastir *et al*., 2011). Larger olfactory bulbs, relatively wider orbito-frontal cortex, relatively increased and forward-projecting temporal lobe poles appear unique to modern humans (Zhu, 2002). Such brain reorganisation, beside physical consequences for overall skull shape, might have contributed to the evolution of *Homo sapien*s' learning and social capacities, in which higher olfactory functions and its cognitive, neurological behavioural implications could have been hitherto under-estimated factors (Zhu, 2002; Bastir, 2011).

2.6.7. Olfactory Nerve Layer

The olfactory nerve layer, at the margin of the olfactory bulb, is mainly consisted of axons that were bundled in groups of 10－100 by olfactory receptor neurones. The olfactory neurones contact with odours in the atmosphere, and conduct this signal to a certain quantity (2－3) and certain type of olfactory glomerular by its axons through nerve impulses (Nolte, 2007). It achieves the goal of spatial encoding of olfactory

information during this course of conduction. Many bundles of fibres formed by olfactory neuronal axons reach the glomerular. Wei *et al*. (2008) reported that the width of the olfactory nerve layer in male juvenile dogs was 236.09 µm on average and about 220.81µm for female juveniles. There was no significant ($P > 0.05$) difference in the width of olfactory nerve layer between adult female and male dogs. The width of the olfactory nerve layer in adult male dogs was 469.45 µm and 454.55 µm in adult female animals. However, the difference in the width of the olfactory nerve layer and density of cells in this layer between adult and juvenile dogs reached the significant level ($P < 0.01$). The width of the olfactory nerve layer is distributed unevenly in the olfactory bulb, and the widest position is at the apex of the bulb. The widest part of olfactory nerve layer in juvenile dogs is about 750 µm and about 1200 µm in adult animals (Wei *et al*., 2008). The olfactory neurones in certain areas of the olfactory epithelium accept odorant information and conduct it to certain areas of the olfactory nerve layer according to the principal of space - to - space projection (Wei *et al*., 2008).

2.6.8. Olfactory Glomerular Layer

The olfactory glomerular layer, at which the mitral cell dendrites are in synaptic contact with the olfactory nerves, and also with the periglomerular cells, consists of glomerulars, comprising the synapses described above. Oval olfactory glomerulars are arranged regularly in the olfactory bulb, and are surrounded by glial cells. Periglomerular cells which are distributed around the glomerulars are interspace neurones, and they connect closely with glomerulars. The olfactory information can be converged at this layer. The impulse generated by olfactory neurones is conducted to mitral cells, tufted cells and periglomerulars in this layer, through which the impulses could be modified. There is no significant difference in the width of the olfactory glomerular layer between male and female juvenile dogs (Wei *et al*., 2008). The average width of this layer in male juvenile

dogs was 155.8 µm, and 162.21 µm for female animals. There is also no significant difference in the width of olfactory glomerular layer between adult male and female dogs, but the width increased significantly with age. The average width of this layer in adult male dogs is 282.93 µm and 297.06 µm in female animals. On the other hand, the density of cells in this layer decreased significantly with age and there was also obvious difference in the quantity of cells in this layer between male and female juvenile dogs (Wei *et al.*, 2008).

2.6.9. External Plexiform Layer

The external plexiform layer is mainly made up of the primary dendrites of mitral cells and tufted cells, and nerve fibres. The tufted cells are distributed unevenly, and they increased in size closer to the mitral cell layer. The average width of the external plexiform layer was 262.13 µm for male juvenile dogs and 263.64µm for female juvenile dogs. The difference of the external plexiform layer's width between juvenile dogs of different sexes is not significant ($P>0.05$). The average width of the external plexiform layer is 398.35 µm in adult male dogs and 351.07 µm in adult female dogs. Although there is no significant difference between the values, the width increased significantly with age, cells' density in this layer between adults and juveniles does not differ (Wei *et al*., 2008).

2.6.10. Mitral Cell Layer

The mitral cell layer mainly includes mitral cell bodies and their dendrites, tufted cells and a small quantity of granule cells. The pyramidal mitral cells are the largest cells in the olfactory bulb. The primary dendrites, which are somewhat larger than the secondary dendrites, extend more or less rapidly across the plexiform layer, and enter the glomerular formations in the superficial layer of the olfactory bulb (Ache *et al*., 2005). Mitral cells

excite granule cells, while granules inhibit mitral cells. This layer can unite the olfactory information during the course of signal efference. Mitral cells are the secondary olfactory neurones, and their axons project to the cortex of the central nervous system. The olfactory nerve axons are in synaptic contact with the mitral cell dendrites within the glomerular, and the impulses are conducted to the mitral cells in this area. It has long been demonstrated that it is a kind of stimulant synapse, modulated by γ-aminobutyrate (GABA). The most important feature of mitral cells is that it is only in synaptic contact with olfactory nerves, belonging to the same groups. Since the olfactory glomerular are arranged regularly in the olfactory bulb, the same kind of olfactory nerves project to a certain area of the olfactory bulb, and this engenders the second spatial encoding. Every mitral cell accepts a number of (25－100) olfactory tracts (Wei *et al*., 2008), an axon belonging to the same kind of neurones; therefore, as long as one of these olfactory neurones is excited, it will excite the corresponding mitral cell. This feature enhances smell sensitivity (Segev, 1999).

The mitral cell layer is a thin layer in the olfactory bulb, consisting of 1－2 layers of cells. There are also many tufted cells and granule cells in this layer. The average width of the mitral cell layer was found to be 107.27 μm in male juvenile dogs and 110.32 μm in female juvenile dogs (Wei *et al*., 2008). There was no significant ($P > 0.05$) difference in the width of mitral cell layer's between dogs of different sexes. The average width of the mitral cell layer was 154.34 μm in adult male dogs and 157.06 μm in adult female dogs. There was also no significant ($P > 0.05$) difference between the values The width of the mitral cell layer increased significantly during the course of a dog's growth from juvenile to adult and the density of the cells decreased obviously during this course. Mitral cells are the main efferent cells in the olfactory bulb, and there was no significant ($P > 0.05$) difference in size and quantity between females and males in juvenile animals.

The colour of nucleoli of mitral cells is light and its brim is blurry in juvenile dogs. According to the results obtained by Wei *et al.* (2008), there was a significant difference in the morphology of mitral cells between male and female adult dogs. Like its name, the morphology of mitral cells in females is mitral, and it also has obvious prominency and heavy colour in nucleoli. The colour of oval mitral cells in males is light. The quantity of mitral cells between males and females differs significantly ($P < 0.01$). There are 51.5 cells on average in each visual field in males and 66.6 cells in females. This difference might be the reason for the difference in smell sensitivity between males and females as a result of the importance of mitral cells in the olfactory system (Zhu, 2002).

2.6.11. Granule Cell Layer

The granule cell layer takes up a large part of the olfactory bulb and is mainly made up of granule cells and their prominency. There are also some short axon cells in this layer. Round granule cells are the interspace neurones, and they are in synaptic contact with the mitral cells, tufted cells and short axons cells and branches, among which the synapses with mitral cells are reciprocal synapses (Zhu, 2002; Wei *et al*., 2008). The dendrites of granule cells are the key position that modulates the output of odour signal by the brain. The granule cells lie inside the olfactory bulb, and there are more of them than mitral cells. There are 11.8 cells per 1000 μm^2 on the average in male juvenile dogs and about 12.7 cells in females, but the difference in the quantity of cells between males and females is insignificant ($P > 0.05$). The density of granule cells is 9.08 cells per 1000 μm^2 on the average in adult male dogs and 9.57 cells in females. The difference in the quantity of cells between males and females is also not significant ($P > 0.05$), although the difference in cells density in this layer between adults and juveniles is insignificant ($P > 0.05$). The width of the granular cell layer is 604.08 µm in male juvenile dogs, 602.83 µm in female juvenile dogs, 673.52 µm in adult males, and 662.59 µm in adult females. The

difference between males and females is not significant ($P > 0.05$). From juvenile to adult, the width of the granule cell layer increases considerably, while the quantity of cells decreases and the volume increases. This change may affect the development of the olfactory system (Zhu, 2002; Wei *et al*., 2008).

All of these layers are arranged very clearly and regularly in the olfactory bulb. These features of the olfactory bulb's structure make it easier for information processing, and they also provide a structural foundation for the spatial encoding of olfactory information. According to classical research, the olfactory bulb includes four kinds of cells: mitral cell, granule cell, tufted cell and short axon cell (Mori *et al*., 2006). Of these neurones, the granule cell has long been known to be morphologically unusual for having no typical axon, and electron-microscopic studies have shown that it participates in unusual reciprocal synaptic connections with the mitral cells (Hirata, 1964; Andres, 1965; Rall *et al*., 1966; Mori *et al*., 2006). Mitral cells are the largest cells in the olfactory bulb, and they are also the major efferent neurones of the olfactory bulb as indicated by electron microscopy (Andres, 1965) and light microscopy (Wei *et al*., 2008) studies.

The dendrites of mitral cells can be classified into primary and secondary dendrites, and both smooth primary and secondary dendrites pass superficially into the external plexiform layer, but only the primary dendrites project down to the olfactory glomerulars (Orona *et al.*, 1984; Mori *et al.*, 2006). Within the glomerular the mitral cell dendrites are in synaptic contact with the olfactory nerves and also with the periglomerular cells, but elsewhere the only synapses on mitral cells are the "reciprocal synapses" with the granule cells (Rall *et al*., 1966; Jackowski *et al*., 1978; Spors, 2012). Anatomical research has suggested that there are inhibitive synapses on mitral cells (Crespo *et al*, 2001). Mitral cells, as the major efferent neurones of the olfactory bulb, also play an important role on the conduction and modification of the olfactory signal. And difference between different

sexes may supply reasons for explaining the sexual variance in smell sensitivity of dogs. The impulse is the result of the binding of odour and olfactory receptors, conducted to the dendrites of mitral cell through the axons of olfactory receptor neurones. From the mitral cells, the message is sent directly to the higher levels of the central nervous system in the cortico-medial amygdala portion of the brain (via the olfactory nerve tract), where the signal process is decoded and olfactory interpretation and response occur. The granule cell processes the impulse during the course of the conduction from mitral cells to the central nervous system (Wei *et al*., 2008). During the course of olfactory signal conduction, the olfactory receptor cells, which express the same receptors from axons, are bundled in groups of 10－100 to penetrate the ethmoidal cribriform plate of bone, reaching the olfactory bulb of the brain, where they converge to terminate with post-synaptic cells to form synaptic structures called glomerular (Wei *et al*., 2008).

The glomerular are connected in groups that converge into mitral cells. Physiologically, this convergence increases the sensitivity of the olfactory signal sent to the brain and achieves the goal of spatial encoding. Therefore, the olfactory bulb plays an important role in information modification and encoding during the conduction of the olfactory signal. Since the sexual variation is the main difference in animals. There are certain difference in smell sensitivity between males and females (Koelega and Koster, 1974: Royet and Plailly, 2004). Many studies on tissue and organ differences result from sexual variation have been conducted in recent years (Halpern and Martínez-Marcos, 2003; Ache and Young, 2005; Wei *et al*., 2008; Ibe *et al*., 2010; Tsai and Barnea, 2014). However, there are few studies on structure difference in olfactory system between males and females, especially in the AGR. There are studies on the olfactory system at the cellular and molecular level. African giant rats just like dogs have a powerful sense of smell,

belonging to macrosmatic animals. The histological structure of AGR olfactory bulb remains largely unknown.

2.7. Uses of African Giant Rats

Military and paramilitary forces have planted millions of land mines since 1900. Many of the mines still remain and do great harm by denying civilians access to their homes and land, as well as by causing bodily harm, death, and psychological duress. People in more than 70 countries are adversely affected by mined areas, and nearly 500,000 people live with injuries inflicted by mines (Land Mine Report, 2009). Victims often are usually severely handicapped and unable to afford the rehabilitation and other services that they need. Demining hazardous areas is important, but it is also costly and time-consuming. Demining is accomplished through the use of mechanical devices, such as armoured automotive tillers and flails or hand-held metal detectors, and with the help of animals, usually trained dogs (Geneva International Centre for Humanitarian Demining, 2007). In recent years, researchers have explored the possibility of using AGR as demining animals in Africa. The rats have an excellent sense of smell and are native to sub-Saharan Africa and, therefore, are resistant to local parasites and diseases. Moreover, they weigh too little to activate most mines and have long-working lives (up to 6 years). Ethologists and other researchers have long studied the operant behaviour of rats (Skinner, 1938, 1953), although not specifically in *Cricetomys gambianus*, and have developed excellent procedures for training the animals (Iversen and Lattal, 1991a, 1991b). Operant discrimination training has been shown to be successful in teaching AGR to search for land mines in a simulated minefield (Verhagen *et al*., 2003) and in limited tests on an actual minefield (Verhagen *et al*., 2006).

2.8. Training of African Giant Rats for Mine Detection

Trained AGRs were used in 2009 in demining operations in Gaza Province, Mozambique, where mines were placed during the civil war that ended in 1992. The rate at which AGRs detect mines was evaluated. Failures to find mines (misses) are a serious safety concern, and a zero miss rate is always desired, although sometimes unattainable (Guelle *et al*., 2003). Adult AGRs with body lengths of 25 to 45 cm and live weights 1 to 2 kg were used. The adult AGRs used were born and trained in Morogoro, Tanzania. From 4 to 6 weeks of age, pups were socialized by being extensively handled and exposed to a variety of stimuli. The training occurred over approximately 185 days (Poling *et al*., 2010a, 2010b). The training involved the use of Clicker, in which a sound was repeatedly presented just before food to establish it as a conditioned reinforcer as well as a discriminative stimulus for approaching handlers, occurring after the initial socialisation. Initial response training took place in a metal cage that contained a 2-cm hole in the floor, below which a positive training sample was presented. This sample, presented in a small pot, consisted of 2 g of sandy soil to which up to five drops of aqueous 2,4,6-trinitrotoluene (TNT; 100 ng per microliter) was added. TNT is the main explosive charge in the majority of land mines. The trainer sounded a click and presented a mouthful of mashed bananas mixed with crushed rat chow through a plastic syringe, if the rat placed its nose in the hole for 2, and later 5, consecutive seconds. Multiple daily trials occurred until the rat placed its nose in the hole within 5 second of being put in the cage and kept it there for the required number of seconds on 10 consecutive tests, after which discrimination training began. In all stages, correct and incorrect responses were recorded by each rat's trainer (Poling *et al*., 2011).

Discrimination training begins in a three-hole cage, which allowed positive and negative samples to be presented. Positive samples were as described above, whereas negative

samples consisted of 2 g of sandy soil spiked with water. During initial discrimination training, half of the pots contained TNT-contaminated soil and half contained plain soil. The trainer sounded a click and delivered food on each trial that a rat kept its nose in a hole above TNT for 5 s, but not at any other time. Training with 60 to 90 samples per day continued until a rat consistently emitted the indicator response on 100% of occasions when TNT was present and on no more than one occasion when TNT was absent (Poling *et al*., 2011). The ability of the AGR to detect mines is due to its very strong olfactory ability, which is a function of the olfactory bulbs. The present study, therefore attempts to study stereological, histological, morphometrical and histological features of the olfactory bulbs.

2.9. Use of African Giant Rats in Scent Detection of Tuberculosis

According to the World Health Organisation, about one-third of the world's population is currently infected with the *Mycobacterium tuberculosis*, which causes tuberculosis (TB), and an estimated 1.7 million people died from TB in 2009. The prevalence of TB is very high in East Africa compared to the rest of the world, and TB causes many deaths and much suffering in East Africa (World Health Organization, 2010). The most common method for identifying TB in East Africa is sputum smear microscopy. This technique, though relatively inexpensive, is time-consuming and fails to detect a substantial number of TB-positive cases, when large numbers of samples are analyzed (Steingart *et al*., 2006; Mase *et al*., 2007). Scent detection of TB using African pouched rats (*Cricetomys gambianus*) has been evaluated by researchers in Tanzania. An initial proof-of-principle study suggested that the rats can detect TB-positive sputum samples quickly and more accurately than microscopy (Weetjens *et al*., 2009). In 2009 researchers reported that scent detection rats increased new TB-positive patient findings by 31% over microscopy alone (Weetjens, *et al*., 2009). A recent study, involving 10,523 patients from Direct

Observation of Treatment Short-Course (DOTS) centres in Dar-es-Salaam, Tanzania showed that use of the rats in simulated second-line screening during 2009 increased case detections by 44%, from 1,403 to 2,023 (Poling *et al*., 2010). Each sputum sample was evaluated by 10 rats and considered positive, if at least two of them identified it as such. Mahoney *et al*. (2012) presented original data gathered during 2010 with an additional 12,329 patients. The importance of the study is that it expands to over 20,000 the number of patients evaluated by the rats in simulated second-line screening. The study evaluated whether the results were comparable to those previously reported by Poling *et al*. (2010) which can be replicated under conditions somewhat different from those of the original investigation. Specifically, some of the rats used in the original investigation were used in the study, but approximately 30% of the total animals were new and they were used in different configurations in the study. Thus, in the first study a sample was considered to be TB-positive, if 2 of 10 rats in a group identified as TB positive. Different groups were used in the new study and in some cases the groups comprised 8 or 9, rather than 10, rats. Using operant conditioning procedures, Giant African pouched rats were trained to detect TB from human sputum samples. Despite its poor sensitivity, microscopy is often used for TB detection in developing countries. Patients missed by microscopy are thought to spread the disease to 10-15 other people, and it is the primary cause of death in people with HIV (World Health Organization, 2010). Relative to smear microscopy, the rat sample-wise sensitivity was 89% and specificity was 76.3%. Patient-wise sensitivity was 95.6% and specificity was 73.6%. Detection rats identified 716 additional TB-positive patients, increasing new case detection by 42.8%. These previously unpublished results extend to over 20,000 the number of patients evaluated by pouched rats in simulated second-line screening and confirm prior reports that detection rats are a fast and cost-effective way to identify a substantial number of patents missed by microscopy (Mahoney

et al., 2012). Overall, the high olfactory sensitivity of the AGR has important special physiological and anatomical features of the rat, which are yet to be investigated. The practical significance of the high acuity of olfaction in the AGR is of great value in landmine detection and TB diagnosis.

2.10. Cerebral Cortex

The cerebral cortex is the outermost sheet of neural tissue of the cerebrum of the brain in some vertebrates (Nolte, 2007; Sinnatamby, 2011). It covers the cerebrum and is divided into left and right hemispheres. The cerebral cortex plays a key role in memory, attention, perceptual awareness, thought, language, and consciousness. The cerebral cortex is uniform. It is composed of many structurally and functionally-unique subunits that perform a wide range of sensory, motor, and mnemonic processes associated with cognition (Nolte, 2001; Sinnatamby, 2011). Like other parts of the central nervous system, the cerebral cortex does not function in isolation, rather it is part of an intricate plexus of overlapping circuits. The cerebral cortex can function only because of the diverse interconnections with other central nervous system structures. The intrinsic and extrinsic circuitries enable the principal functions of the cerebral cortex (Peter *et al*., 1994). It consists of up to six horizontal layers, each with a different composition in terms of neurones and connectivity. The human cerebral cortex is 2 to 4 mm thick (Kandel *et al.*, 2000).

In preserved brains, it has a grey colour, hence the name "grey matter". In contrast to grey matter that is formed from neurones and their unmyelinated fibres, the white matter below them is formed predominantly by myelinated axons, interconnecting neurones in different regions of the cerebral cortex with each other and neurones in other parts of the central nervous system (Michael and Wojciech, 2006; Gilbert and Sigma, 2007).

2.10.1. Embryology of the Cerebral Cortex

The cerebral cortex develops from the most anterior part of the neural plate, a specialized part of the embryonic ectoderm. The neural plate folds and closes to form the neural tube. From the cavity inside the neural tube develops the ventricular system, and, from the epithelial cells of its walls, the neurones and glia of the nervous system. The most anterior (frontal) part of the neural tube, the telencephalon, gives rise to the cerebral hemispheres and cortex (Moore and Persaud, 2003; Sadler, 2005).

The development of the neocortex arises in an inside-out manner as mitotically dividing progenitors migrate outward along radial glia. The first neurones to differentiate and migrate to what will become layer VI. As the G1 phase of mitosis is elongated, the newly-born neurones migrate to more superficial layers of the cortex (Calegari *et al*., 2005).

Cortical neurones are generated within the ventricular zone, next to the ventricles. At first, this zone contains "progenitor" cells, which divide to produce glial cells and neurones (Stephen *et al*., 2001). The glial fibres produced in the first divisions of progenitor cells are radially oriented, spanning the thickness of the cortex from the ventricular zone to the outer, pial surface, and provide scaffolding for the migration of neurones outwards from the ventricular zone. The first divisions of the progenitor cells are symmetric, which duplicates the total number of progenitor cells at each mitotic cycle. Then, some progenitor cells begin to divide asymmetrically, producing one post-mitotic cell that migrates along the radial glial fibres, leaving the ventricular zone and one progenitor cell; which continues to divide until the end of development, when it differentiates into a glial cell or an ependymal cell. The migrating daughter cells become the pyramidal cells of the cerebral cortex (Rakic, 1995).

The layered structure of the mature cerebral cortex is formed during development (Moore and Persaud, 2003; Sadler, 2005). The first pyramidal neurones generated migrate out of the ventricular zone and subventricular zone, together with Cajal–Retzius cells from the preplate. Next, a cohort of neurones migrating into the middle of the preplate divides this transient layer into the superficial marginal zone, which become layer 'I' of the mature neocortex, and the subplate, forming a middle layer called the cortical plate. These cells form the deep layers of the mature cortex, layers five and six. Later born neurones migrate radially into the cortical plate past the deep layer neurones, and become the upper layers (two to four). Thus, the layers of the cortex are created in an inside-out order. The only exception to this inside-out sequence of neurogenesis occurs in the layer I of primates, in which, in contrast to rodents, neurogenesis continues throughout the entire period of corticogenesis (Zecevic and Rakic, 2001).

2.10.2. Evolution of the Cerebral Cortex

The cerebral cortex is derived from the pallium, a layered structure found in the forebrain of all vertebrates. The basic form of the pallium is a cylindrical layer enclosing fluid-filled ventricles. Around the circumference of the cylinder are four zones, the dorsal pallium, medial pallium, ventral pallium, and lateral pallium, which are thought, to give rise to the neocortex, hippocampus, amygdala and olfactory cortex, respectively (Sadler, 2005; Moore *et al*., 2014).

Until recently, no counterpart to the cerebral cortex had been recognized in invertebrates. However, based on gene expression profiles, strong affinities have been reported between the cerebral cortex and the mushroom bodies of rag worms (Tomer, *et al.*, 2010). Mushroom bodies are structures in the brains of many types of worms and arthropods that are known to play important roles in learning and memory; the genetic evidence indicates

a common evolutionary origin, and, therefore, indicates that the origins of the earliest precursors of the cerebral cortex date back to the early Precambrian era (Tomer *et al.*, 2010).

2.10.3. Layers of the Cerebral Cortex

Cytoarchitecture refers to the typical pattern of cellular arrangement in the cerebral. The size and packing densities of neurones are not uniform in the cerebral cortex. The underlying tenet of this approach to neuroscience is that structural differences in the cerebral cortex are associated with functionally unique areas. The differentiation of cortical layers is largely based on the distinctive population of projection neurons in each layer. A neuron is considered to be in a layer according to its cell body. A pyramidal neuron with a cell body in layer V may be referred to as a layer V neuron, or a layer may be described as having pyramidal neurones (Peter and Jones, 1994; Conn, 1995).

The different cortical layers each contain a characteristic distribution of neuronal cell types and connections with other cortical and subcortical regions. One of the clearest examples of cortical layering is the Stria of Gennari in the primary visual cortex. This is a band of whiter tissue that can be observed with the naked eye in the fundus of the calcarine sulcus of the occipital lobe. The Stria of Gennari is composed of axons, bringing visual information from the thalamus into layer four of visual cortex. Staining cross-sections of the cortex to reveal the position of neuronal cell bodies and the intracortical axon tracts allowed neuroanatomists in the early 20th century to produce a detailed description of the laminar structure of the cortex in different species. After the work of Brodmann (1909), the neurones of the cerebral cortex are grouped into six main layers, from outside (pial surface) to inside (white matter) as follows:

a. **Layer I**, the molecular layer, contains few scattered neurones and consists mainly of extensions of apical dendritic tufts of pyramidal neurones and horizontally-oriented

axons, as well as glial cells (Shipp, 2007). Some Cajal-Retzius and spiny stellate cells can be found here. Inputs to the apical tufts are thought to be crucial for the "feedback" interactions in the cerebral cortex, involved in associative learning and attention (Gilbert and Sigman, 2007). While it was once thought that the input to layer I came from the cortex itself (Cauller, 1995), it is now realized that layer I across the cerebral cortex mantle receives substantial input from ''matrix'' or M-type thalamus cells (Rubio-Garrido *et al*., 2009). This is in contrast to ''core'' or C-type that go as to layer IV (Jones, 1998).

b. **Layer II**, the external granular layer, contains small pyramidal neurones and numerous stellate neurones.
c. **Layer III**, the external pyramidal layer, contains predominantly small and medium-size pyramidal neurones, as well as non-pyramidal neurones with vertically-oriented intracortical axons; layers I through III are the main target of interhemispheric cortico-cortical afferents, and layer III is the principal source of cortico-cortical efferents.
d. **Layer IV**, the internal granular layer, contains different types of stellate and pyramidal neurones, and is the main target of thalamo-cortical afferents from thalamus type C neurones (Jones, 1998), as well as intra-hemispheric cortico-cortical afferents.
e. **Layer V**, the internal pyramidal layer, contains large pyramidal neurones (such as the Betz cells in the primary motor cortex). There are large pyramidal cells, which give rise to axons, leaving the cortex and running down through the basal ganglia, the brain stem and the spinal cord.
f. **Layer VI**, the polymorphic or multiform layer, contains few large pyramidal neurones and many small spindle-like pyramidal and multiform neurones; layer VI sends efferent fibres to the thalamus, establishing a very precise reciprocal

interconnection between the cortex and the thalamus (Creutzfeldt, 1995). These connections are both excitatory and inhibitory. Neurones send excitatory fibres to neurones in the thalamus and also from collateral to them via the thalamic reticular nucleus that inhibits the thalamus neurones or those ones adjacent to them (Lam and Sherman, 2010). Since the inhibitory output is reduced by cholinergic input to the cerebral cortex, this provides the brainstem with adjustable "gain control for the relay of lemnsical inputs" (Lam and Sherman, 2010).

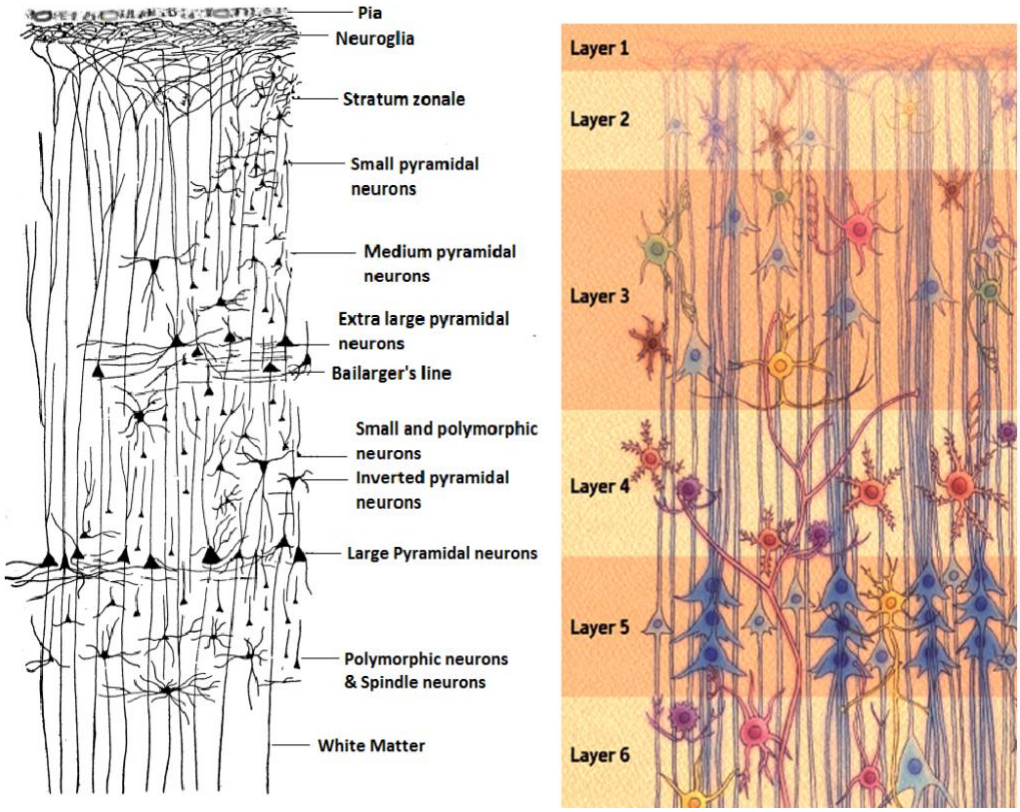


Figure 3: Layers of the cerebral cortex (histological structure of the cerebral cortex). http://chronopause.com/chronopause.com/index.php/2012/02/21/the-effects-of-cryopreservation-on-the-cat-part-3/index.html

It is important to note that the cortical layers are not simply stacked one over the other; there exist characteristic connections between different layers and neuronal types, which span all the thickness of the cortex. These cortical microcircuits are grouped into cortical columns and minicolumns, the latter of which have been proposed to be the basic functional units of the cortex. Mountcastle (1997) showed that the functional properties of the cortex change abruptly between laterally adjacent points; however, they are continuous in the direction perpendicular to the surface. Later works have provided evidence of the presence of functionally distinct cortical columns in the visual cortex (Hubel and Wiesel, 1959), auditory cortex and associative cortex (Rubio-Garrido *et al*., 2009) Cortical areas that lack a layer IV are called agranular. Cortical areas that have only a rudimentary layer IV are called dysgranular. Information processing within each layer is determined by different temporal dynamics with that in the layers II/III having a slow 2 Hz oscillation, while that in layer V has a fast 10–15 Hz (Sun and Dan, 2009).

2.10.4. Connections of the Cerebral Cortex

The cerebral cortex is connected to various subcortical structures such as the thalamus and the basal ganglia, sending information to them along efferent connections, and receiving information from them via afferent connections. Most sensory information is routed to the cerebral cortex via the thalamus. Olfactory information, however, passes through the olfactory bulb to the olfactory cortex (piriform cortex). The vast majority of connections are from one area of the cortex to another, rather than to subcortical areas; Braitenberg and Schüz (1991) put the figure as high as 99%. The cortex is commonly described as comprising three parts: sensory, motor, and association areas (Conn, 1995).

2.10.5. Cortical Thickness

For mammals, species with larger brains (in absolute terms, not just in relation to body size) tend to have thicker cortices (Nieuwenhuys *et al*., 1998). The range, however, is not very great, the only a factor of 7 between the thickest and thinnest cortices. The smallest mammals, such as shrews, have a neocortical thickness of about 0.5 mm; the ones with the largest brains, such as humans and fin whales, have thicknesses of 2.3—2.8 mm. There is an approximately logarithmic relationship between brain weight and cortical thickness; dolphins, however, have considerably thinner cortices than the overall relationship would predict (Nieuwenhuys *et al*., 1998).

With magnetic resonance brain scanners, it is possible to get a measure for the thickness of the human cerebral cortex and relate it to other measures. The thickness of different cortical areas varies. In general, sensory cortex is thinner and motor cortex is thicker (Kruggel *et al.,* 2003). One study has found some positive association between the cortical thickness and intelligence (Katherine, 2007). Another study has found that the somato-sensory cortex is thicker in migraine sufferers (Alexandre, 2007).

2.10.6. Comparative Anatomy of the Cerebral Cortex in Rodents and Primates

Rodents and primates both show considerable variation in the overall size, the radial and tangential dimensions, folding and subdivisions into distinct areas of their cerebral cortex. The current understanding of brain development is based on a handful of model systems. A detailed comparative analysis of the cellular and molecular mechanisms that regulate neural progenitor production, cell migration, and circuit assembly can provide much needed insights into the working of neocortical evolution. From the limited comparative data currently available, it is apparent that the emergence and variation of the neuronal progenitor cells have led to the production of increased neuronal populations and the

evolution of the cortex (Mashiko *et al*., 2012). Further diversification and compartmentalisation of the germinal zone together with changing proportions of radial glia in the ventricular zone and various intermediate progenitors in the subventricular zone may have been the driving force behind increased cell numbers in larger brains both in rodents and primates (Mashiko *et al*., 2012). Radial and tangential migratory patterns are both present in rodents and primates, but in different proportions. There are apparent differences between the mouse and in humans in the generation and elaboration of the interneuronal subtypes, and also in gene expression patterns associated with the appearance of distinct cortical areas. The increased cortical dimensions and the formation of a more elaborate cortical architecture in primates require a larger and more compartmentalised transient subplate zone during development (Molnár and Clowry, 2012). More comparative analysis in rodent and primate species with large, small, smooth and folded brains is needed to reveal the biological significance of the alterations in these cortical developmental programes (Molnár and Clowry, 2012).

Table 1: Comparative cortical volumes in rodents Butler and Hodos, (2005)

Species	V_G	V_W	A_G	A_W	T_G	N_{G+W}	O_W	F_E
Mus musculus	107.11 ± 44.40	8.78 ± 5.25	147.77 ± 35.91	81.80 ± 40.74	0.749 ± 0.115	6.845×10^6	3.696×10^6	1.02
Rattus norvegicus	430.82 ± 41.44	64.60 ± 8.27	355.54 ± 26.55	271.72 ± 70.58	1.248 ± 0.008	15.510×10^6	12.928×10^6	1.04
Cavia porcellus	812.43 ± 109.97	94.47 ± 20.30	571.18 ± 49.58	341.40 ± 42.24	1.584 ± 0.058	21.755×10^6	27.318×10^6	1.04
Dasyprocta primnolopha	2607.84	672.52	1412.67	1257.80	1.911	56.320×10^6	118.097×10^6	1.17
Hydrochoerus hydrochoeris	16896.51	4987.28	6004.54	4986.58	3.089	153.150×10^6	707.518×10^6	1.30
Tupaia glis	531.9	181.8	497.0	323.8	1.09	$21.95 \pm 1.60 \times 10^6$	16.22×10^6	1.04
Callithrix jacchus	2036.1	887.1	1534.0	1087.6	1.31	$120.33 \pm 43.30 \times 10^6$	74.63×10^6	1.18
Otolemur garnetii	2492.0	1060.3	1745.0	1235.4	1.46	$88.50 \pm 14.75 \times 10^6$	102.89×10^6	1.25
Aotus trivirgatus	3295.4	1265.2	2214.0	1588.0	1.50	200.32 ± 67.34	170.04×10^6	1.36
Callimico goeldii	3125.1	1413.4	1953.0	1470.1	1.60	178.77×10^6	157.13×10^6	1.26
Saimiri sciureus	7706.7	4452.5	5250.0	4377.8	1.47	$645.73 \pm 43.74 \times 10^6$	353.05×10^6	1.57
M. fascicularis	13234.4	11911.2	9381.0	7920.1	1.41	400.74×10^6	484.40×10^6	1.65
M. radiata	13220.4	9114.1	8441.0	7289.9	1.57	829.60×10^6	841.38×10^6	1.81
Cebus apella	13475.6	8220.5	7653.0	6025.0	1.77	$930.67 \pm 507.78 \times 10^6$	868.73×10^6	1.69
Papio cynocephalus	33910.3	17814.2	16689.0	13963.4	2.03	$1420.34 \pm 18.07 \times 10^6$	1860.00×10^6	1.92

All values are average ± standard deviation and refer to one cerebral cortical hemisphere only. V_G, volume of the cortical gray matter (mm^3); V_W, volume of the subcortical white matter (mm^3); A_G, surface area of the cortical gray matter (mm^2); A_W, surface area of the subcortical white matter (i.e., of the gray-white matter interface, in mm^2); T_G, thickness of the gray matter (mm); N_{G+W}, total number of neurons in the cerebral cortex (GM and occasional neurons found in the WM; O_W, number of other (non-neuronal) cells in the WM; F_G, folding index of the GM (total GM surface/exposed GM surface).

Nzalak *et al.* (2008), in comparative morphometric studies of the cerebellum and fore brain of the AGR (*Cricetomys gambianus*-Waterhouse) and that of the Grasscutter (*Thryonomys swinderianus*), reported that the mean live weight of AGR in grams to be 891.7 ± 100.3, and the brain weight, cerebellum and forebrain to be 4.94 ± 017.6, 0.62 ± 0.06, 3.32 ± 0.12 and 10.03 ± 0.32, 1.25 ± 0.05, 7.22 ± 0.18, respectively, which accounted for 14.0, 66.0, 12.5 and 67.5 % for the cerebellum and forebrain, respectively. In the same study they reported the mean brain weight and length of the AGR to be 4.94 ± 0.179, 4.33 ± 0.20 cm. Nzalak et al. (2008) also reported morphometric measurement for the olfactory bulb of the AGR and grasscutter to be 1.07 ± 0.16 and 0.56 ± 0.0 cm; with a significant difference in favour of the AGR, which accounted for 19.01 and 9.0%, respectively. By this report, Nzalak *et al.* (2008) postulated that AGR has better sense of smell compared to the grasscutter. However, in this report there was no stereological estimate for the volume of the layers of the cerebral cortex and no estimate of the numbers of the different neurones in the different layers of the cerebral cortex of the AGR.

Based on the afore-mentioned potentials of AGRs, this research was focused on the sexual dimorphism, morphological, morphometric and stereological differences in the structures of AGR olfactory bulb and cerebrum by histological and stereological methods. This was an attempt to provide base-line data on the morphologic, morphometric, histologic and stereological parameters of the rodent for a better understanding of the neurobiology and the unique olfactory ability of the rodent. The thickness of olfactory bulb layers and its main cells, such as mitral cells and granule cells, will be analyzed comparatively using Thionin-staining and statistical methods. The analysis will be used to

study the development of olfactory bulbs and the structural differences of AGR which may affect olfaction in both males and females.

CHAPTER THREE

3.0 MATERIALS AND METHODS

3.1 Experimental Animals and Management

3.1.1 Capturing of Animal

Ten adult AGR (*Cricetomys gambianus*, Waterhouse-1840), consisting of five male and five females were used for this study; the animals were captured alive around Zaria, using locally made rat traps for the rat, without inflicting any injury on them.

3.1.2 Housing and Feeding of Animals

The AGRs were maintained in the animal house of the Department of Anatomy, Faculty of Medicine, Ahmadu Bello University, Zaria, Nigeria in metal cages each of 16 x 10 x 12 cm dimension (length, breadth, height). The animals were fed with groundnut cake, ground nut, biscuits, maize, and drinking was given *ad libitum*. They were allowed to acclimatize for 2-3 weeks before the commencement of the study.

3.1.3 Sacrificing of Animals

The animals were anaesthetized with chloroform (ClFl, Merck, Germany), sacrificed and transcardially perfused with a phosphate-buffered solution of (pH 7.2, M = 0.12) 4% formaldehyde and 1% glutaraldehyde (Bie and Barnsten, Sandbaekvej, Denmark-2610 Rodovre, Batch No. 150306-009). The brains were removed and placed in the same fixative, and numbered according to the method of Hosseini-Sharifabad and Nyengaard, (2007).

3.2 Retrieval and Preparation of the Brain

3.2.1 Retrieval of the Brain

The live weight of each AGR was obtained using the Mettler balance P1210 (Mettler Instrument AG, Switzerland) with a sensitivity of 0.001 g. The AGRs were sacrificed by

the method of Adeyemo and Oke (1990). Each skull containing the brain was obtained after it had been skinned and stripped of all facial muscles immediately after sacrifice. Thereafter the skull was exposed by longitudinal sections along the mid-cranial line with a saw and the brain excised and weighed using an electronic digital balance ACCULAB ATILON (Sartorious group, ATL-2202, 24206050, Germany), with a sensitivity of 0.001g.

3.2.2 Separation of the Olfactory Bulbs and Cerebrum

To separate the cerebrum from the cerebellum, the floculli of the cerebellum were manually raised to expose the cerebellar peduncles. Thereafter, they were gently separated from the cerebrum, using a scalpel and a surgical blade. The olfactory bulbs and cerebrum were weighed using the electronic digital balance, ACCULAB ATILON (Sartorious group, ATL-2202, 24206050, Germany).

3.3 Anatomical Study of the Olfactory Bulbs and Cerebrum of African Giant Rat

3.3.1 Morphologic (Gross Anatomical) Study

The morphologic characteristics of the olfactory bulbs were observed with the naked eyes and electronic magnifying lens (LUXOL, LFM-101-104, Germany), after which each AGR was carefully dissected and the brain removed gently from the skull after fixation. The morphologic characteristics observed included shapes, sizes, surfaces, borders and angles. The presence and absence of sulci, fissures or prominences were also examined in the cerebrum and cerebellum. The olfactory bulbs were weighed using an electronic digital balance, ACCULAB ATILON. All the physically- and lens-observed features were recorded.

3.3.2. Morphometric Study of the Olfactory Bulb and the Cerebrum

The AGR were weighed using a weighing balance (ACCULAB ATILON) which has a sensitivity of 0.001g. The nose-rump length was measured using a tape rule in centimeter (cm). The whole brain, olfactory bulb and cerebrum were weighed using an electronic digital balance (ACCULAB ATILON). The length, width and thickness of the olfactory bulb and cerebrum were measures using a digital Vernier caliper which has a sensitivity of 0.001mm. Weights were measured in gram (g), lengths in centimeter (cm), width and thickness in millimetre (mm). sex differences were taken into consideration. All measured parameters were recorded and expressed as mean±standard error of mean (MEAN±SEM).

3.3.3. Light Microscopy Study of the Olfactory Bulbs and Cerebrum of African Giant Rat

Each AGR for light microscopy study was perfused with phosphate-buffered (0.12 M, pH 7.0) solution through the heart immediately after sacrifice using 10 Ml syringes and 19 gauge needle. The perfusion was done by flushing in order to free the brain of blood. This procedure was followed by perfusion of the brain with a phosphate-buffered solution of (pH 7.2, 0.12 M) 4% formaldehyde and 1% glutaraldehyde. The skull was opened and the brain removed by the method earlier described (Hosseini-Sharifabad and Nyengaard, 2007).

3.3.3.1 Fixation of the Olfactory Bulb and the Cerebrum of AGR

The brain was removed and placed in a phosphate-buffered solution (pH 7.2, 0.12 M) of 4% formaldehyde and 1% glutaraldehyde, the same fixative used for perfusion. Each brain, with intact olfactory bulbs, was numbered (Hosseini-Sharifabad and Nyengaard, 2007).

3.3.3.2 Embedding of the Olfactory Bulb and the Cerebrum of AGR

Each brain block was embedded in a low-gelling temperature agarose (6% agar), (BDBacto^{TM} Agar, Becton, Dickson and Company, Sparks, MD, USA, Ref. No. 214010). Agar is a solidifying agent in which extraneous matter, pigmented portions and salts have been reduced to a minimum (Hosseini-Sharifabad and Nyengaard, 2007).

3.3.3.3 Mounting on Metal Block of the Olfactory Bulb and the Cerebrum of AGR

The resulting agarose blocks containing the tissue pieces were then glued to a metal block and transferred to the vibratome for sectioning.

3.3.3.4 Tissue Sectioning and Staining

The vibration amplitude, speed, and angle of the blade were all controllable. Sectioning was carried out with the tissue submerged in the buffer bath. Tissue sections of 60 µm diameter cut perpendicular to the long axis (coronal section), were serially obtained with a calibrated Vibratome Series 3000 Plus-Tissue Sectioning System (Serial No. VO 25140305, manufactured by The Vibratome Company, 5918 Evergreen Blvd, St. Louis, MO, USA). The sectioning was done in the Stereology and Electron Microscopy Laboratory of Danish Neuroscience Centre, Aarhus University Hospital, Aarhus, Denmark. The sections were carried out along the entire extent of the brain.

One of the six series of sections was collected for staining, using systematic uniform random sampling. For example, the first section in each series was chosen at random from the first six sections and from then on every sixth section (with an interval of 360 µm) was sampled. Individual sections were then collected with a fine brush and transferred to multi-well plates, containing phosphate-buffered solution.

3.3.3.5 Mounting on Chrome-Gelatine Slides

The vibratome sections were mounted on chrome-gelatine coated slides, water was absorbed around the sections with tissue paper, and slides were laid vertically and air-dried at room for 20 minutes.

3.3.3.6 Dehydration and Thionin Staining

The staining was done serially as described by Bancroft *et al*. (2008). Briefly, dried sections were re-hydrated in demineralized water for 15 minutes, stained in 0.25% Thionin solution (stain for fixed tissue) for 1 minute; differentiated colour fixation in demineralized water with changes of the water; dehydrated in 50% ethanol (1x1 minute); 70% ethanol (1x1 minute); 96% ethanol (2x1 minute); 99% ethanol (3x1 minute); cleared in xylene (3x5 minute); and covered with a thin (100 µm) coverslip. Mild weight was placed upon the coverslips to remove excess Epon and to ensure that the sections were flat between the objective glass and the coverslip during polymerisation. The sections were allowed to dry at room temperature (24 ^{o}C). Thionin stain demonstrated the different cortical layers in the olfactory bulbs and cerebral cortex.

3.3.3.7 Light Microscopy Study and Photomicrography of the Olfactory Bulb and the Cerebrum of AGR Slides

The Thionin stained slides were examined using the Olympus system microscope (Heidenhain, Germany), with a motorized x-y specimen stage. Photomicrographs were taken with a digital camera (OLYMPUS DP73), mounted on the Olympus microscope. The sections were viewed using different magnifications.

3.4. Stereological Study of the Olfactory Bulbs and Cerebrum of African Giant Rats (Gundersen, 1999; Hosseini-Sharifabad and Nyengaard, 2007)

Two combined stereological principles were used: (1) the optical fractionator, and (2) the fractionator sampling design (Gundersen, 1999). The fractionator technique involved

counting particles with optical dissector in a systematic, uniform and random sample that constituted a known fraction of the structure to be analyzed (Gundersen, 1987; Nyengaard and Gundersen, 2006).

The unbiased Cavalieri principle of point counting was used to estimate the volumes of the different layers of the cerebral cortex and the different layers of the olfactory bulb (Gundersen, 1986; Nyengaard and Gundersen, 2006). Areas of the cut surfaces of the fixative-fixed sections (∑ area) were estimated using a point grid (West, 2002).

3.4.1 Estimation of Neuronal Number in Olfactory Bulbs of African Giant Rats using Optical Fractionator (Gundersen, 1999; Hosseini-Sharifabad and Nyengaard, 2007)

Each olfactory bulb block was embedded in 6 % agar. Sections of 60 µm thickness were cut serially, perpendicular to the long axis (coronal sections), with a calibrated Vibratome Series 3000 Plus-Tissue Sectioning System, and were collected along the entire extent of the olfactory bulb. One of the five series of sections was selected for staining using systematic uniformly random sampling (SURS). The first section in each series was chosen at random from the first five sections; and, thereafter, from every fifth section, with an interval of 360 µm was sampled. The sections were transferred onto chrome-gelatinised glass slides and covered with extra-thin (110 µm thick) cover slip. Mild weights were placed upon the coverslips to remove excess Epon and to ensure that the sections were flat between the objective lense and the coverslip.

An Olympus BH2 microscope equipped with a MT12 microcator and ND281 readout (Heidenhain, Germany), and a motorized x-y specimen stage (Merzhauser, Germany) were used. A video camera (JAI-2040, Protect, Japan) connected to a computer was mounted on top of the microscope. The computer, with a frame-grabber (FlasPoint, Integral Technologies, Indiana, IN USA), was connected to the monitor and equipped

with the newCAST^{TM} software, version 2.1 (Visiopharm, Hørsholm, Denmark). Delineation of the regions was performed using a 4 x objective lens (Olympus, Splan, Numerical Apparatus (NA) 0.16). The sections were analyzed using a 100 x oil immersion objective (Olympus, Splan, NA 1.40) at a final magnification of 2232.

3.4.2 Estimation of Volume of Layers of Olfactory Bulbs in African Giant Rats using the Cavalieri Principle (Gundersen, 1999; Hosseini-Sharifabad and Nyengaard, 2007)

The stereological measurements of volumes were performed using the Cavalieri principle according to the method of Hosseini-Sharifabad *et al.* (2007). The estimated volume, *V,* of the different layers in the cerebral cortex and olfactory bulb of the AGR was obtained, where *t* is the slab thickness, or intersectional distance (usually 2.0 mm as indicated above), P_i is the number of points that hit tissue on the slab *i*, and a/p is the area associated with each point.

3.4.3 Point Counting of the Layers of Olfactory Bulb and the Cerebrum of AGR (Gundersen, 1999; Garcia-Finana, 2003)

Point counting was done according to the recommendations described in Gundersen *et al*. (1999; Garcia-Finana, 2003), and was performed using the newCAST-grid stereology software (Olympus). The entire section, processed from tissue blocks were delineated (Meander sampling). The step length was fixed to 2000 × 1400 μm, enabling the evaluation of the total tissue area with a × 4 objective (a total of 125 times magnification on the computer monitor); that is, the sum of all fields of vision from a section equals the whole section. The Meander sampling gave rise to 70 to 130 fields to be evaluated on the sample of sections. The fields were superposed with a test system with regularly arranged points. Point counting was performed with areas per point (a/p), ranging from 4000 to 46,000 μm and depending on the individual layer, which provided a total number of hitting points ($\Sigma P_{i)}$ between 100 and 200.

3.4.4 Z-Axis Analysis (Dorph-Petersen *et al*., 2001; Gardella *et al*., 2003)

A z-axis distribution analysis was performed on each series of sections to verify complete stain penetration (Dorph-Petersen *et al*., 2001). The position of 200-300 particles was measured relative to the section thickness within the view field. For counting particles, centres of nuclei (rather than tops or bottoms of particles) were scored (Gardella *et al*., 2003), to avoid any over- or undercount in the bins, adjacent to the surface at the top or bottom of the tissue section.

3.4.5 Counting Procedure for Neuronal Estimation of Olfactory Bulb Cells of AGR (Gundersen, 1999; Hosseini-Sharifabad and Nyengaard, 2007)

This was achieved by counting cells on a known fraction of sections (ssf), under a known fraction of the sectional area of the region (asf) in a known fraction of the thickness of a section (hsf). The total cell numbers were obtained by multiplying the total number of counted particles (∑Q□) by the reciprocal sampling fractions, adding a multiplication of 2 for bilateral number:

$$N_{total} = (1/ssf. 1/asf .1/hsf \sum Q□)2$$

The optical disector, a 3D probe was placed randomly on the sections generated with the aid of a microscope and an oil immersion objective, in order to observe thin focal planes inside thick sections. The microscope was connected via a video camera to a colour monitor. A microcator, used to measure distances in the *z*-axis, is mounted on the microscope. A counting frame with exclusion and inclusion lines was superimposed on the magnified image of the tissue on a monitor (Gundersen *et al*., 1999; Solveig *et al*., 2010).

3.4.5.1. Counting Criteria for Cells of the Olfactory Bulbs of African Giant Rat (Gundersen, 1999; Hosseini-Sharifabad and Nyengaard, 2007)

The cells were first identified based on their location in the different layer of the olfactory bulb and their individual basic histologic features. Cells were identified as neurones if they had a clearly defined nucleus with a pale cytoplasm and a dark centrally-located nucleolus, including a relatively large size of the cell body. Glial cells were defined as much smaller than neurones, without a clear identifiable nucleolus and cytoplasm (Hosseini-Sharifabad and Nyengaard, 2007).

3.4.5.2. Counting Criteria for Periglomerular Cells of the Olfactory Bulbs of African Giant Rat (Gundersen, 1999; Hosseini-Sharifabad and Nyengaard, 2007)

The external plexiform layer is made up of dendrites of mitral cells and periglomerular cells and nerve fibres. The periglomerular cells were distributed unevenly, and the cells increased in size closer to the mitral cell layer. The nuclei were used as the counting item, and the cells were counted only, if the nucleoli were in focus inside the counting frame and the disector height. Cells were identified as neurones if they had a clearly defined nucleus with a pale cytoplasm and a dark centrally-located nucleolus, including a relatively large size of the cell body (Wei *et al*., 2008). Glial cells were defined as much smaller than neurones, without a clear identifiable nucleolus and cytoplasm (Hosseini-Sharifabad and Nyengaard, 2007).

3.5.5.3. Counting Criteria for Mitral Cells of the Olfactory Bulbs of African Giant Rat (Gundersen, 1999; Hosseini-Sharifabad and Nyengaard, 2007; Wei *et al*., 2008)

The mitral cell layer is a thin layer in the olfactory bulb, consisting of 1-2 layers of mitral cells. The mitral cells were pyramidal in shape and were the largest cells in the olfactory bulb. They had prominent nucleoli. The nucleoli were used as the counting item, and the cells were counted only if the nucleoli were in focus inside the counting frame and the

disector height (Wei *et al*., 2008). Cells were identified as neurones if they had a clearly-defined nucleus, with a pale cytoplasm and a dark centrally-located nucleolus, including a relatively large size of the cell body. Glial cells were defined as much smaller than the neurones, without a clear identifiable nucleolus and cytoplasm (Gundersen, 1999; Hosseini-Sharifabad and Nyengaard, 2007).

3.4.5.4. Counting Criteria for Granule Cells of the Olfactory Bulbs of African Giant Rat (Gundersen, 1999; Hosseini-Sharifabad and Nyengaard, 2007; Wei *et al*., 2008)

The granule cell layer takes up a large part of the olfactory bulb and is mainly made up of granule cells and their prominency. There are also some short axon cells in this layer. Round granule cells are the interspace neurones, and they are in synaptic contact with the mitral cells, tufted cells and short axon cells' axons and branches, among which the synapses with mitral cells are reciprocal synapses. The dendrites of granule cells are the key position that modulates the output of odour signal by the brain. The granule cells lie inside the olfactory bulb, and there are more of them than mitral cells (Wei *et al*., 2008).

3.6. Sampling Fractions (Korbo *et al.*, 1990; Pakkenberg and Gundersen, 1997)

To ensure that all parts of the olfactory bulb were uniformly sampled, the design was based on systemic uniform random sampling (SURS). System sampling fraction (ssf), area sampling fraction (asf) and height sampling fraction (hsf) were estimated and optimised for statistical reasons to obtain a count of approximately 150-200 neurones and 150-200 glial cells per sample (Korbo *et al.*, 1990; Pakkenberg and Gundersen, 1997).

(i) ***Section sampling fraction*** *(ssf)*: depending on the size of the brain, ssf was chosen to be between ⅟260th to ⅟290th to obtain 12-13 sections per brain.

(ii) ***Area sampling fraction*** *(asf)*: in each sample section, neuronal count was made with optical disector at regular predetermined x, y position in the olfactory bulb. The disector

was positioned randomly over olfactory bulb within the x, y step pattern by the newCAST^{TM}-GRID software (Visiopharm, Denmark).

$$Asf = a\,(frame) \diagup a(x,y\text{-}step)$$

(iii) ***Height sample fraction (****hsf)*: this is the height of the disector relative to the section thickness. *hsf=h/tQ-*

3.7 Estimation of the Coefficient of Error

The following formula was used in this investigation for estimating the average coefficient of error (CE) (Cruz-Orive, 2005; Glaser *et al*., 2007):

$$\mathbf{CE} = \frac{\sqrt{Var_{SURS} + Var_{Noise}}}{\frac{N}{\sum_{1=1} P1}}$$

Where CE is the coefficient of error, Var_{SURS} is the variance of systematic uniform random sampling, Var_{Noise} is the variance of noise, N is the number of points, P is the point, and $\sum P$ is the sum of points.

3.8. Statistical Analysis

All recorded weights, widths, lengths and volumes are expressed as mean. The precision by which the volume or number of neurones was estimated was determined by the CE. The CE provided information about whether the sampling was sufficiently precise at the various levels of the sampling scheme. The CE is a function of the noise effect, and the SURS variance for sums of areas (Gundersen *et al*., 1999; Walløe *et al*., 2010), calculated using the formula below in CE. The noise effect was the uncertainty that came from point counting, and VAR_{SURS} was the uncertainty of sampling between sections (Gundersen *et al*., 1999). The sampling was considered optimal when CE was close to half the coefficient of variation (CV = SD/mean), given that CV^2= biological CV^2+ estimated

CE^2. Student's t-test was applied to test for differences in total number and volume of cells in the olfactory bulb. SURS variance: sum of areas sampling between sections.

Student's *t*-test was used to determine the differences between sexes in olfactory bulbs and cerebrum cortex. Spearman's correlation coefficient was used to test for the relationship between sex and brain size, and between total body length and brain size. Values of $P < 0.05$ were considered significant (Eriksen and Pakkenberg, 2007).

CHAPTER FOUR

4.0 RESULTS

4.1. Physical Features of the Adult African Giant Rats

The African Giant rats have soft grey fur on it body and a whitish fur on the belly on the ventral surface. It have dark ring around the eyes. They have scaly long tails which makes up half their length. They have narrow heads with small eyes. They have large cheek pouches to transport massive quantities of food and the pouches are more visible with food material in their mouth. The males are heavier than the females AGRs (Plate I).



Plate I: African Giant rat (*Cricetomys gambianus*, Waterhouse - 1840)

4.2. Descriptive Statistics of the Morphometric Parameters of Adult African Giant Rats

The mean absolute body weight and mean nose-rump length of all the ten adult AGRs, irrespective of their sex, were 1215.0 ± 78.2 g and 72.80 ± 0.854 cm respectively (Table 2).

Table 2: The body weight and nose-rump length of adult African Giant Rats

Variable	**n**	**Mean ± SEM**	**SD**	**Minimum**	**Maximum**
Body Weight (g)	10	1215.0 ± 78.2	247.3	800.0	1500.0
Nose-rump length (cm)	10	72.80 ± 0.85	2.70	66.0	76.0

Standard error of mean, SEM; standard deviation, SD and n= sample size

4.3. Sexual Dimorphism in the Body Morphometric Parameters in the Adult African Giant Rats

With respect to sex, the mean body weight in the adult male AGRs was 1400.0 ± 31.6 g, and that in the adult females was 1030.0 ± 97.0 g. Mean body weight was higher ($P < 0.05$) in the adult male AGRs than in the adult female AGRs. The mean nose-rump length in the adult male AGRs was 71.80 ± 1.46 cm, (Table 3), while that of the adult female AGRs the nose-rump was 73.80 ± 0.80 cm. The mean nose-rump was slightly higher in the female AGRs, but the difference was not significant, (Table 3).

Table 3: Sexual Dimorphism in the Body Morphometry in the African Giant Rats (Mean ± SEM)

Variable	Sex	n	Mean ± SEM	Minimum	Maximum	P-value
Body Weight (g)	F	5	1030.0 ± 97.0	800.0	1300.0	0.02^{S}
	M	5	1400.0 ± 31.6	1300.0	1500.0	
Nose-rump length (cm)	F	5	73.80 ± 0.80	72.00	76.00	0.28^{NS}
	M	5	71.80 ± 1.46	66.00	74.00	

Female, F; male, M; significant difference, S; standard error of mean, SEM; non-significant, NS; n= sample size

4.4. Morphologic parameters of the Olfactory bulbs of Adult African Giant Rats

Morphologically, the olfactory bulb of the adult AGR rat had a milk colour in appearance, and was the most rostral (forward) part of the brain of the rodent (Plate II). The Olfactory bulb of the adult AGR was relatively large (0.95 ± 0.03cm) and located at the frontal lobe of the brain posterior to the nasal cavity. It is globular in shape and was in pairs, namely the left olfactory bulb, LOB and right olfactory bulb, ROB (Plate II).

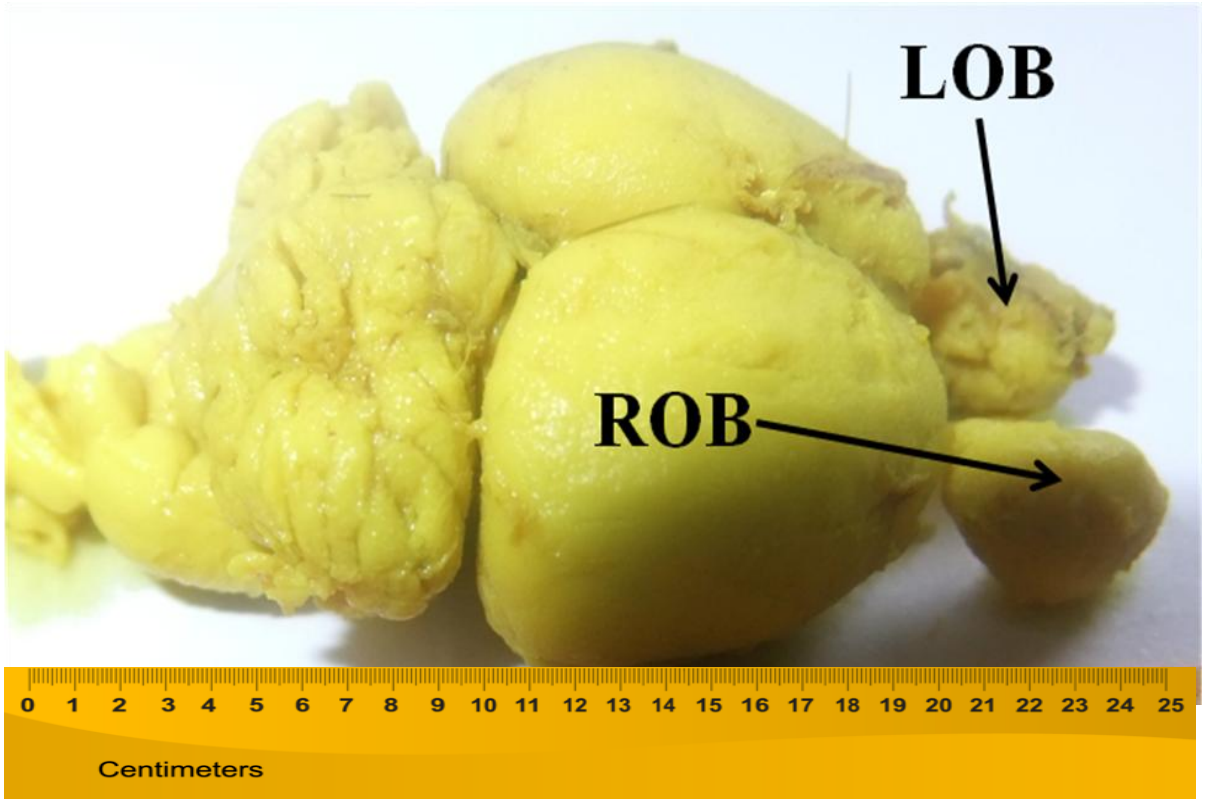


Plate II: The dorsal view of the brain of adult African Giant rat showing the left olfactory bulb, LOB and right olfactory bulb, ROB.

4.5. Morphological features of the cerebrum of adult African Giant Rats

The intact brain of the adult AGR was milky in colour and snail-shaped. The brain of the adult AGR showed two major depressions, a median longitudinal depression called the median longitudinal fissure which contained a sickle-shaped process of dura mater called the *falx cerebri* (Plate III), the longitudinal fissure separated the cerebrum into two hemispheres and a horizontal depression that separates the cerebrum from the cerebellum (Plate IV). The adult AGR had smooth-surfaced or nonconvoluted cerebrum which is lissencephalics. Each cerebral hemisphere had regions, namely frontal, parietal, temporal and occipital regions (Plate V). The cerebral hemisphere of the adult AGR had a smooth dorsal surface (Plat VI), a flat medial surface (Plat VII) and a ventral surface that was irregular in shape (Plate VIII).

The cerebral hemisphere of the adult AGR showed a dorsolateral border located between the dorsolateral and medial surfaces. Ventrolateral border occurred between the Ventrolateral and ventral surfaces. It had no gyri and sulci.

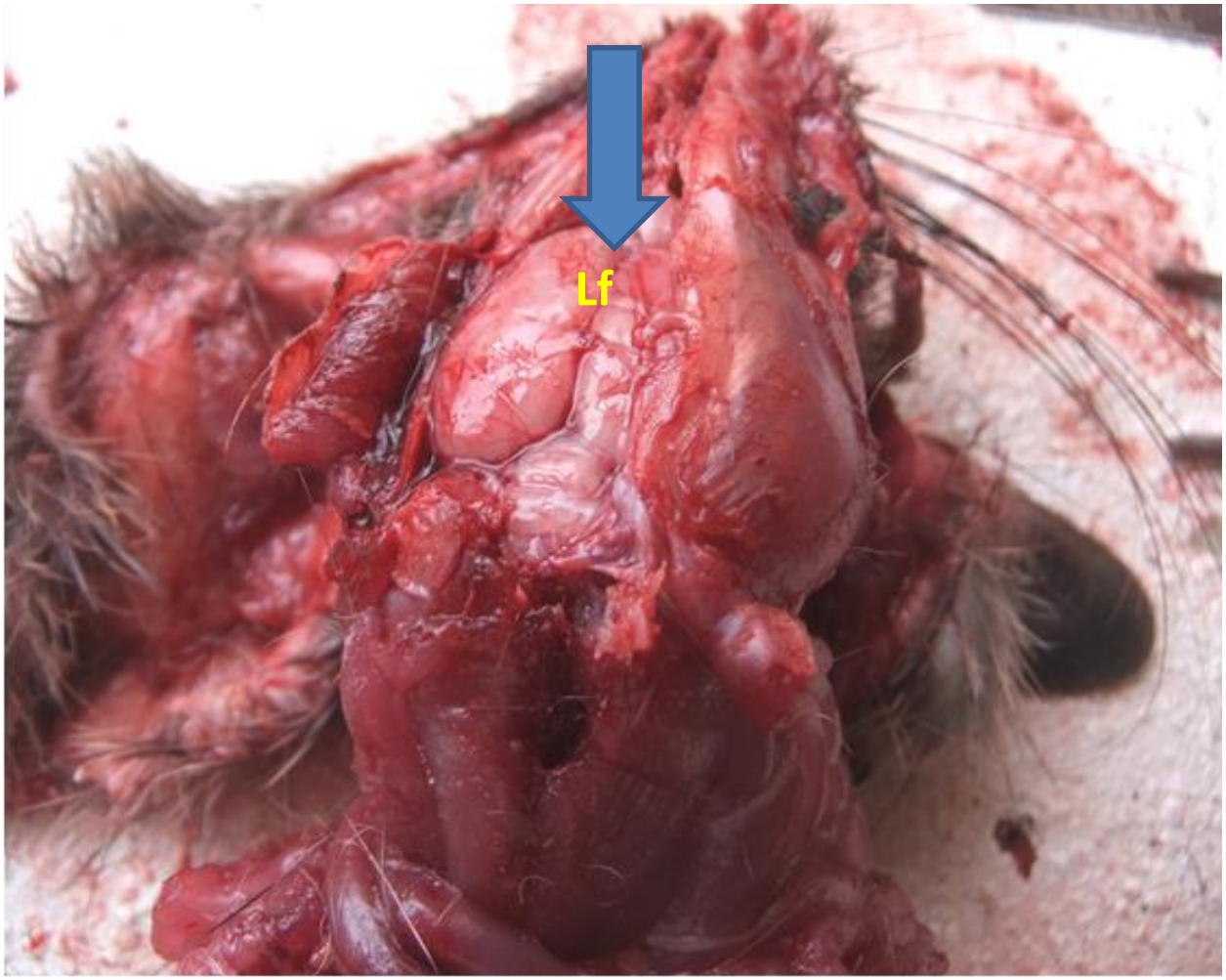


Plate III: Dissected whole brain (in situ) of African giant rat (*Cricetomys gambianus*, Waterhouse-1840), showing longitudinal fissure, Lf.

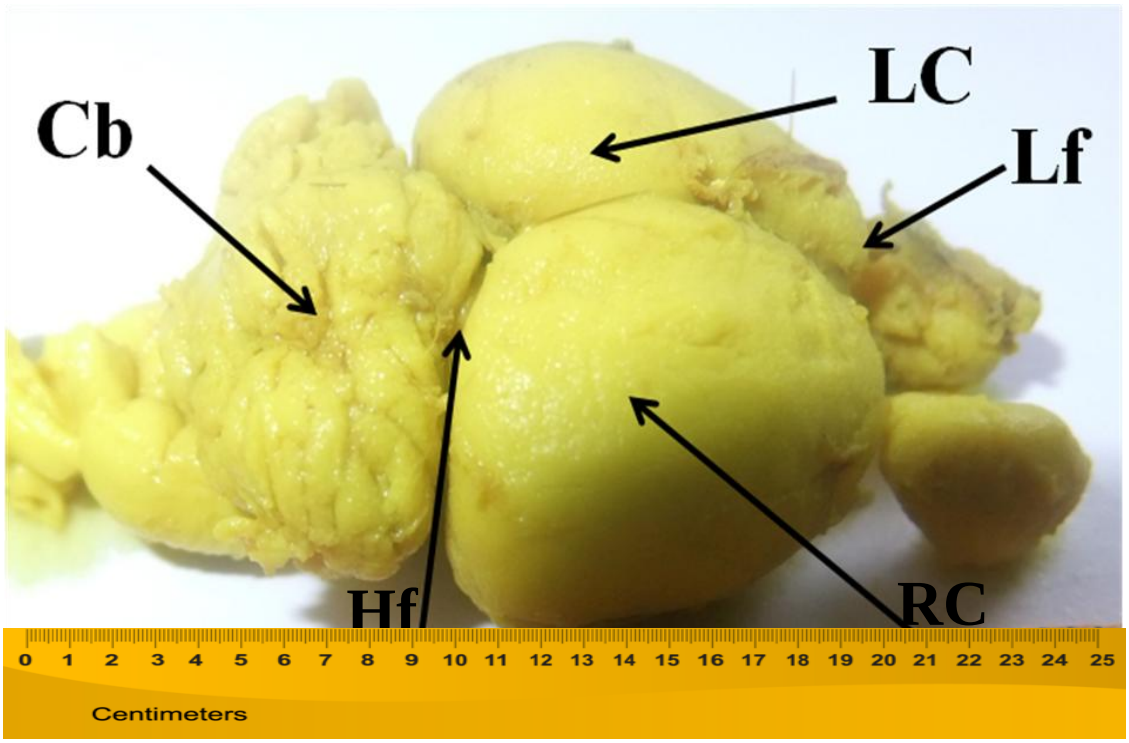


Plate IV: The dorsal view of the cerebrum of adult African Giant rat, showing the left cerebral, LC; and right cerebral, RC, cerebral hemispheres; cerebellum, (Cb); longitudinal fissure, Lf and horizontal fissure, Hf.

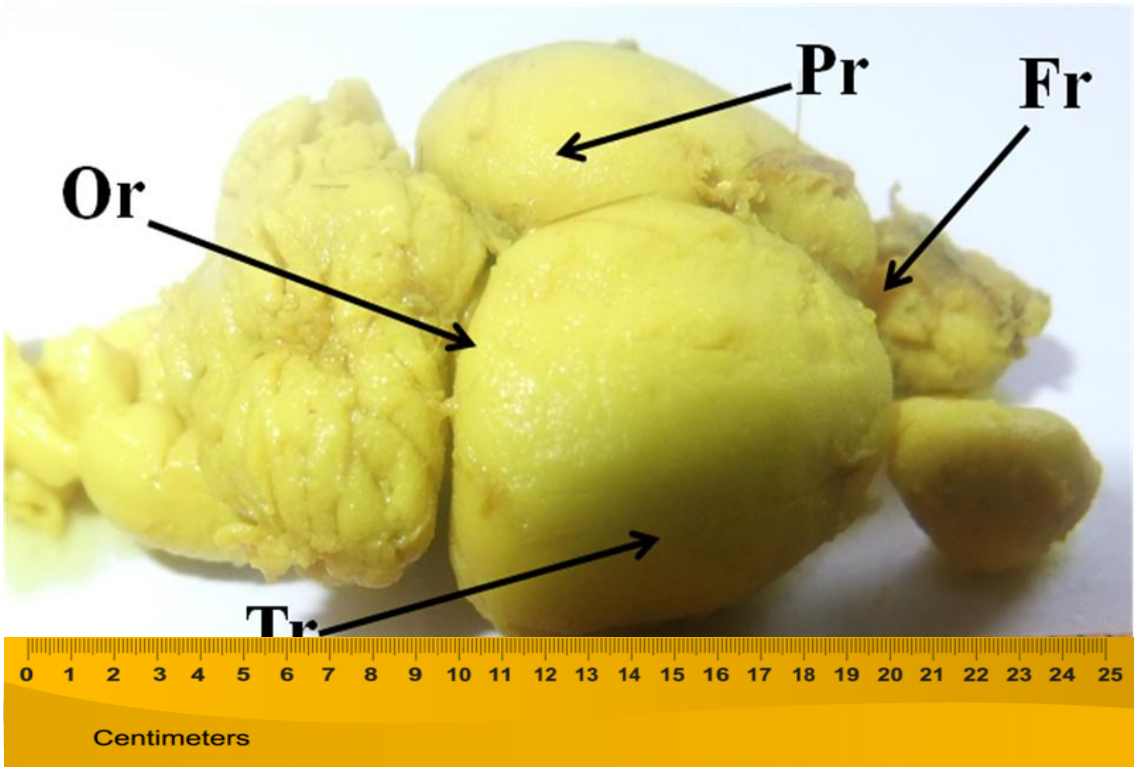


Plate V: The dorsal view of the cerebrum of adult African Giant rat, showing the parietal region, Pr; frontal region, Fr; temporal region, Tr and Occipital region, Or.

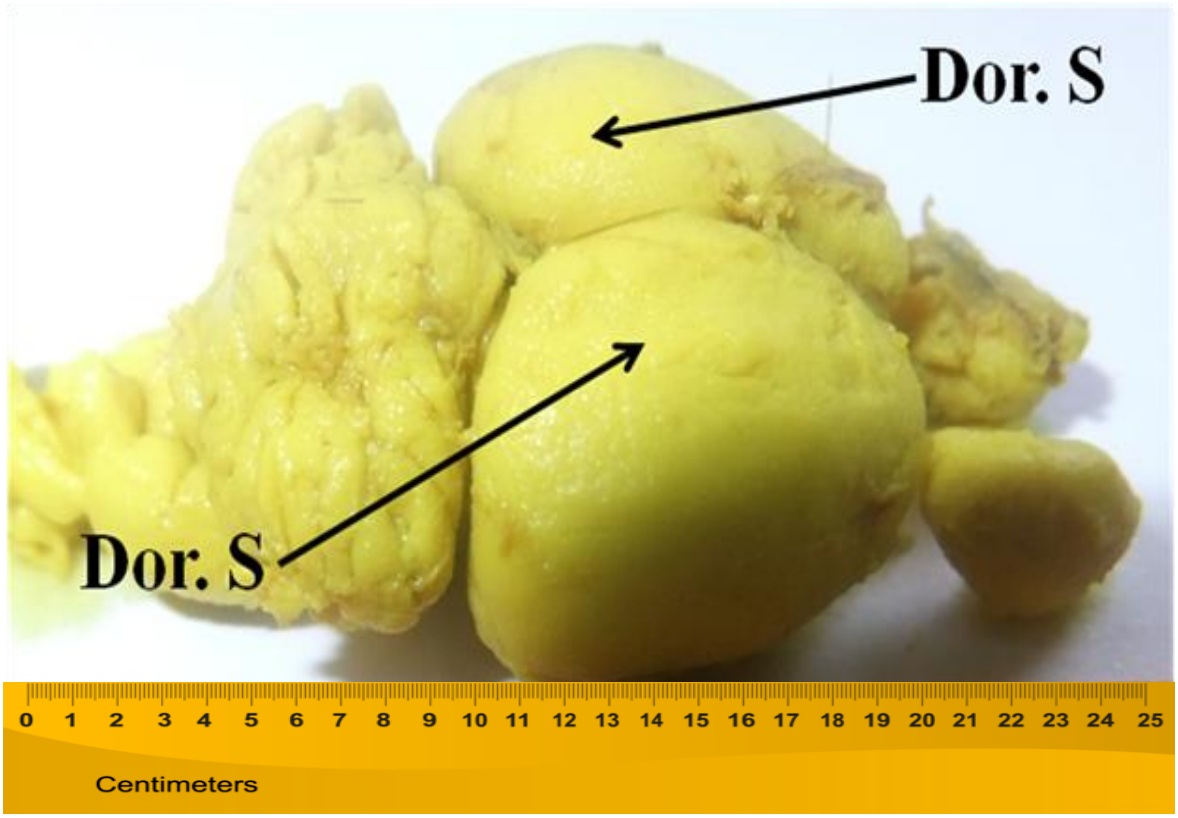


Plate VI: The dorsal view of the cerebrum of adult African Giant Rat, showing the Dorsal surface, Dor. S of the cerebrum.

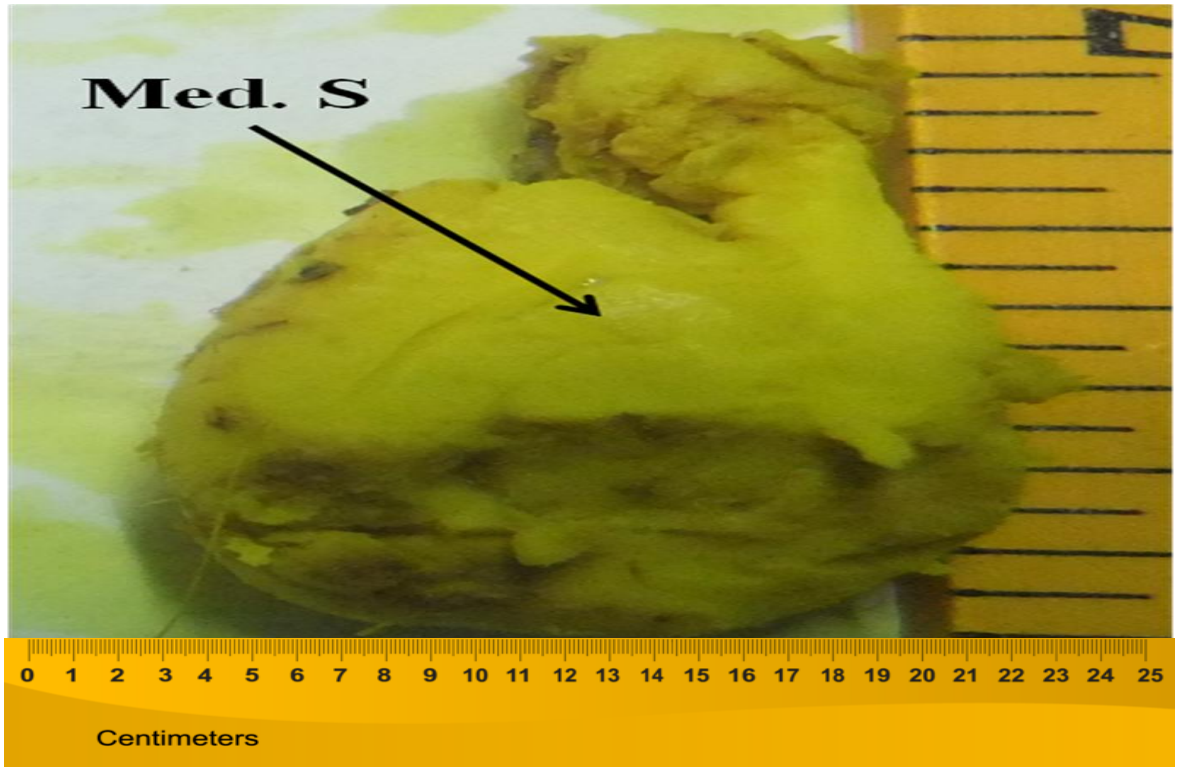


Plate VII: The cerebrum of adult African Giant Rat, showing the medial surface, Med. S of the cerebrum.

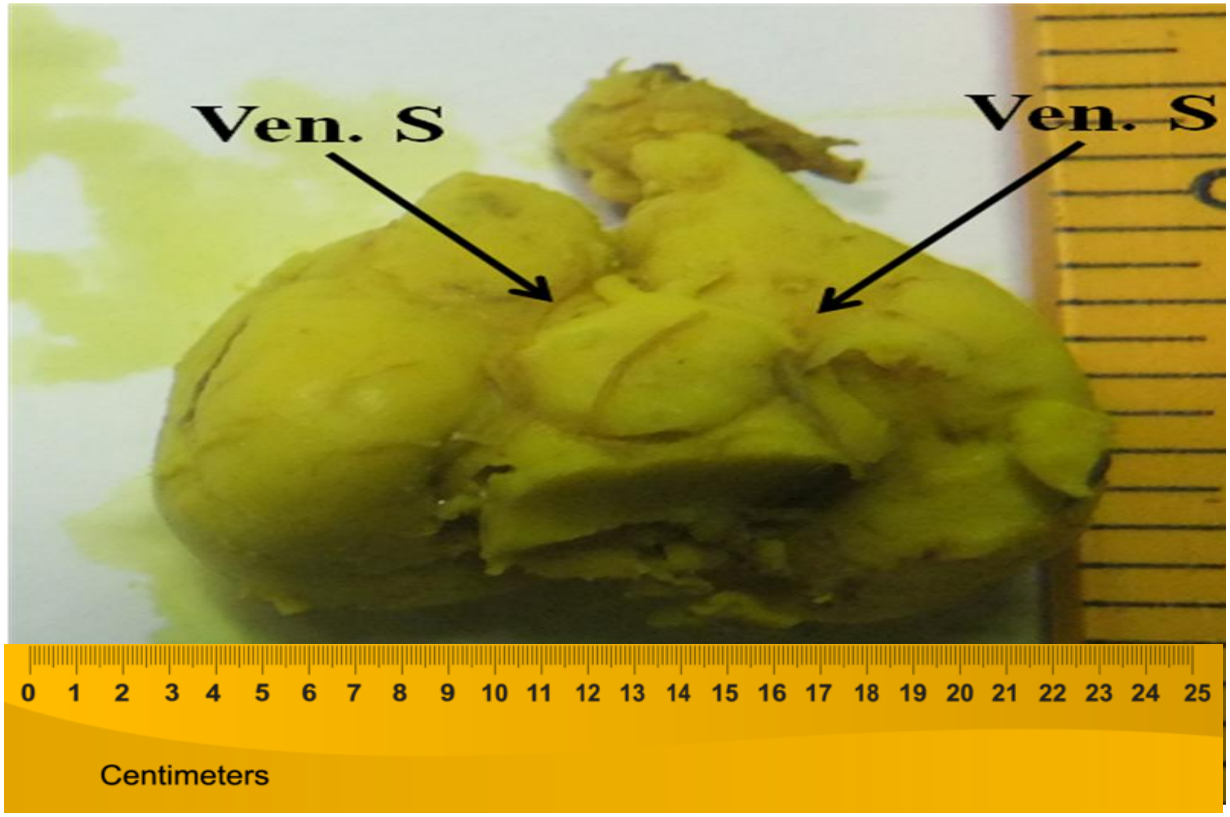


Plate VIII: The ventral view of the cerebrum of adult African Giant Rat, showing the ventral surface, Ven. S of the cerebrum.

4.6. Morphometric Parameters of the Olfactory Bulbs of Adult African Giant Rats

The mean absolute weight, relative olfactory bulb weight, mean width and mean thickness of the olfactory bulb, obtained from all the ten adult AGRs, irrespective of their sex, were 0.95 ± 0.03 g, 0.83 ± 0.16, 4.08 ± 0.27 mm and 2.98 ± 0.10 mm, respectively (Table 4).

Table 4: Body weight, olfactory bulb weight, width and thickness of the African Giant Rat (Mean ± SEM)

Variable	n	Mean ± SEM	SD	Minimum	Maximum
B W (g)	10	1215.0 ± 78.2	247.3	800.0	1500.0
OB W (g)	10	0.95 ± 0.03	0.10	0.80	1.10
ROW	10	0.83 ± 0.16	0.27	0.06	0.14
OB Width (mm)	10	4.08 ± 0.3	0.85	3.01	5.70
OB T (mm)	10	2.98 ± 0.1	0.30	2.61	3.75

Body weight BW; olfactory bulb weight OBW; olfactory bulb width OBT; olfactory bulb thickness OBT; SEM; standard deviation, SD; n=sample size

4.7. Morphometric Parameters of the Olfactory Bulb in Male and Female Adult AGRs

The mean absolute weight, relative olfactory bulb weight, mean width and thickness of the olfactory bulbs in the adult male AGRs were 0.88 ± 0.04 g, 0.06 ± 0.06, 4.55 ± 0.33 mm, and 2.81 ± 0.06 mm, respectively (Table 5). In the adult female AGRs, the mean absolute weight, relative olfactory bulb weight, mean width and thickness of the olfactory bulbs were 1.02 ± 0.04 g, 0.01 ± 0.16, 3.61 ± 0.33 mm and 3.15 ± 0.15 mm, respectively (Table 5).

The olfactory bulb's weight was higher in the adult female AGRs, 1.02 ± 0.04 g than in the adult male AGRs, 0.88 ± 0.04 g, ($P < 0.05$). The width of the olfactory bulb in the adult male and female AGRs, 4.55 ± 0.33 mm and 3.61 ± 0.3 mm respectively were not significantly ($P > 0.05$) different. The thickness of the olfactory bulb in the adult female and male AGRs were higher 3.15 ± 0.15 mm and 2.81 ± 0.06 mm, respectively, and the difference in the values was not significant ($P > 0.05$) (Table 5).

Table 5: Sexual Dimorphism in the Morphometry of the Olfactory bulb of adult African Giant Rats

Variable	Sex	n	Mean ± SEM	SD	Minimum	Maximum	P- value
BW (g)	F	5	1030.0 ± 97.0	22.8	80.0	130.0	
	M	5	1400.0 ± 31.6	70.7	13.0	150.0	
OBW (g)	F	5	1.02 ± 0.04	0.08	0.90	1.10	0.03^{S}
ROW	F	5	0.10 ± 0.16	0.03	0.08	0.14	
	M	5	0.88 ± 0.04	0.08	0.80	1.00	
ROW	M	5	0.06 ± 0.06	0.00	0.06	0.07	
OBWidth (mm)	F	5	3.61 ± 0.33	0.74	3.01	4.80	0.08^{NS}
	M	5	4.55 ± 0.33	0.74	3.95	5.70	
OBT (mm)	F	5	3.15 ± 0.154	0.35	2.90	3.75	0.10^{NS}
	M	5	2.81 ± 0.06	0.14	2.61	3.00	

BW, body weight; OBW, olfactory bulb weight; ROW, relative organ weight; OBT, olfactory bulb width; OBT, olfactory bulb thickness; female, F; male, M; SEM; standard deviation, SD significant difference, S; non-significant difference, NS; n=sample size

4.8. Morphometric Parameters of the Cerebrum of Adult African Giant Rats

The mean absolute cerebral weight, cerebral width and cerebral thickness obtained from all the ten adult AGRs, irrespective of their sex, were 3.44 ± 0.07g, 19.59± 0.42 mm and 12.84 ± 0.15 mm, respectively, (Table 6).

Table 6: Cerebral weight, width and thickness in the African giant rats (Mean ± SEM)

Variable	n	Mean ± SEM	SD	Minimum	Maximum
B W (g)	10	1215.0 ± 78.20	247.3	800.0	1500.0
C W (g)	10	3.4 ± 0.07	0.22	3.00	3.70
ROW	10	0.3 ± 0.23	0.05	0.24	0.41
C Width (mm)	10	19.6 ± 0.42	1.33	17.49	21.30
C T (mm)	10	12.8 ± 0.15	0.46	12.12	13.68

Body weight, BW; cerebral weight, CW; cerebral width; relative organ weight, ROW; C Width; cerebral thickness, CT; standard error of mean, SEM; standard deviation, SD; n=sample size

4.9. Sexual dimorphism in the Morphometric Parameters in the Cerebrum of Adult African Giant Rats

With respect to sex, the mean weight, relative cerebral weight, width and thickness of the cerebrum in the adult male AGRs were 3.62 ± 0.02 g, 0.26 ± 0.06, 20.43 ± 0.33 mm, and 12.91 ± 0.24 mm, respectively, (Table 7). In the adult female, the mean weight, relative cerebral weight, width and thickness of the cerebrum in AGRs were 3.26 ± 0.07 g, 0.32 ± 0.07, 18.77 ± 0.58 mm and 12.77 ± 0.18 mm, respectively, (Table 7). The cerebral weight was higher ($P < 0.01$) in the adult male AGRs, 3.62 ± 0.02 g than in the adult female AGRs (3.26 ± 0.07 g). Similarly, the cerebral width was higher ($P < 0.01$) in the adult male AGRs, (20.43 ± 0.33 mm) than in the adult female AGRs, 18.77 ± 0.58. The cerebral thickness in the adult male and female AGRs were not significantly ($P > 0.05$) different (Table 7).

Table 7: Sexual Dimorphism in the Cerebral Morphometric Parameters in the African Giant Rat (Mean ± SEM)

Variable	Sex	n	Mean ± SEM	SD	Minimum	Maximum	P-value
B W (g)	F	5	1030.0 ± 97.0	216.8	800.0	1300.0	0.02^{S}
	M	5	1400.0 ± 31.6	70.7	1300.0	1500.0	
C W (g)	F	5	3.2600 ± 0.07	0.1673	3.0000	3.4000	0.01^{S}
ROW (F)			0.32 ± 0.07				
	M	5	3.6200 ± 0.02	0.0447	3.6000	3.7000	
ROW (M)			0.26 ± 0.06				
C Width (mm)	F	5	18.768 ± 0.581	1.299	17.490	20.910	0.05^{S}
	M	5	20.428 ± 0.330	0.737	19.700	21.250	
C T (mm)	F	5	12.772 ± 0.181	0.405	12.120	13.180	0.66^{NS}
	M	5	12.910 ± 0.243	0.542	12.380	13.680	

Body weight (BW); cerebral weight (CW); relative organ weight (female) ROW (F); relative organ weight (male) ROW (M), cerebral width (CW); cerebral thickness (CT); female, F; male, M; SEM; standard deviation, SD significant difference, S; non-significant difference, NS; n= sample size

4.10. Cytoarchitecture of the Olfactory Bulb in the Adult African Giant Rats

From the result of this study, it was observed that the olfactory bulb cytoarchitecturally has five layers, namely: the glomerular layer, the external plexiform layer, the mitral cell layer, the internal plexiform layer and the granule cell layer. The central core was the medulla and was composed of white matter, (Plate XI). Cytoarchitecturally, the olfactory bulb of the AGR had the outermost glomerular layer with the periglomerular cells in between the glomerular, (Plate X). The next layer was the external plexiform layer which had the periglomerular cells, (Plate XI). The next layer was the mitral cell layer which had the large mitral-shaped cells in the layer. A tiny internal plexiform layer, with very few periglomerular cells in the layer, (Plate XII). The last layer is the granule cell, which had numerous granule cells in the layer, (Plate XIII). In the centre was the medulla (Plate XIV).

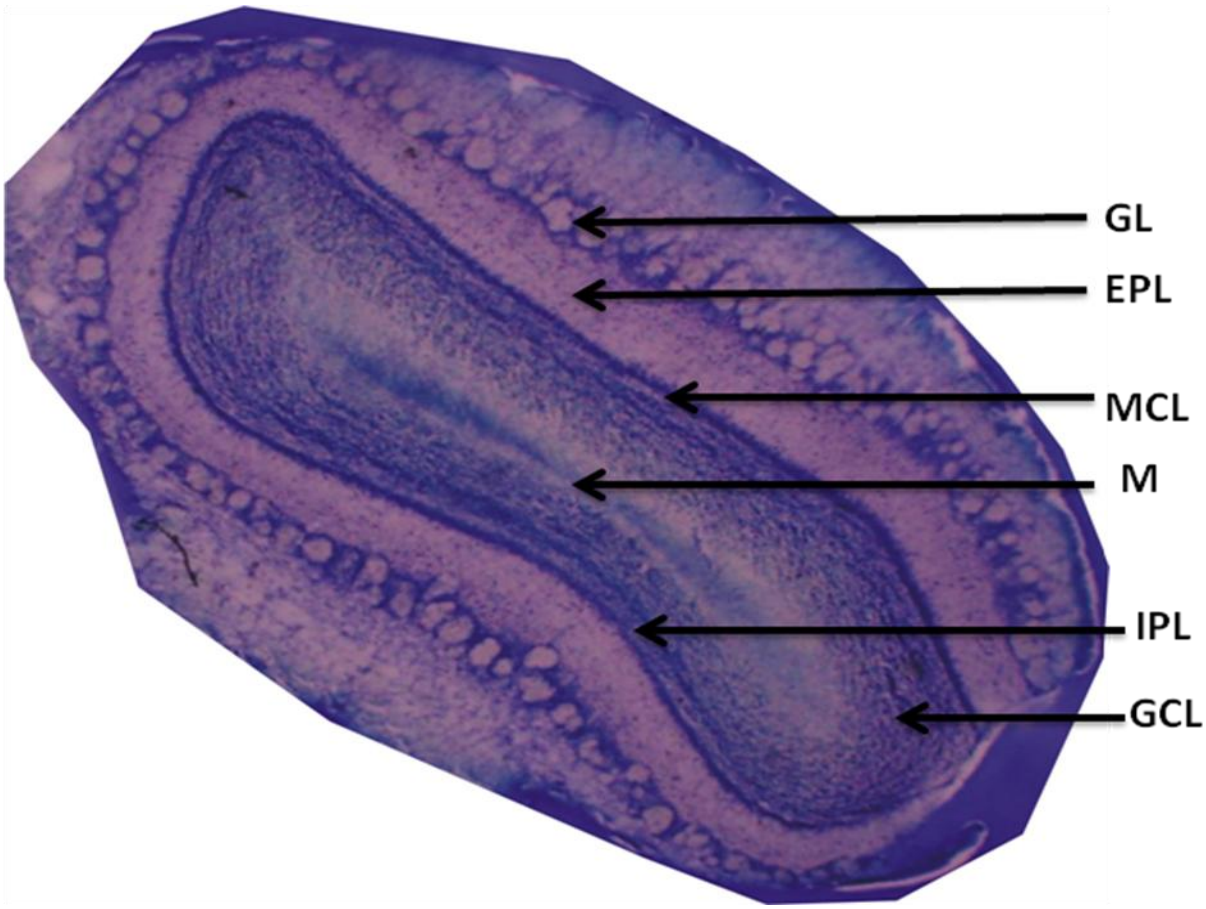


Plate IX: Transverse section of the cytoarchitecture of the olfactory bulb of adult African giant rat. Glomerular layer, GL; external plexiform layer, EPL; mitral cell layer, MCL; internal plexiform layer, IPL; granule cell layer, GCL; medulla, M. Thionin stain. x 12.5.

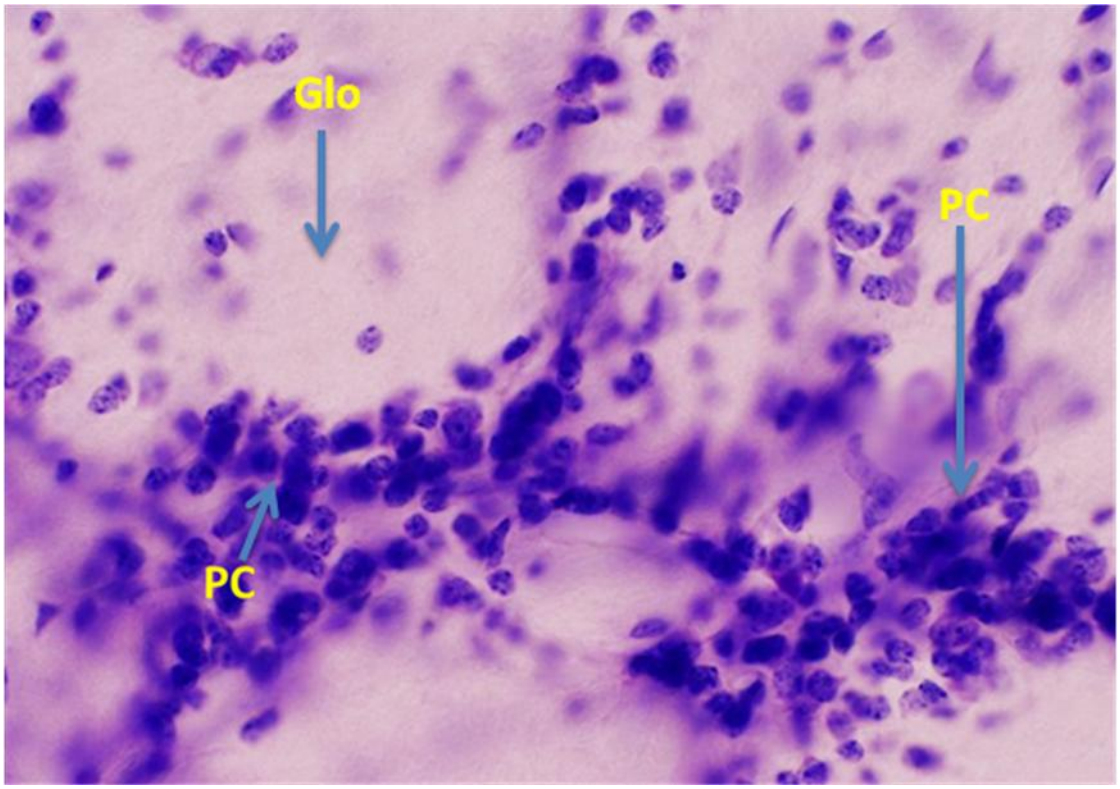


Plate X: Transverse section of the cytoarchitecture of the olfactory bulb of adult African giant rat showing the periglomerular cells, PC and glomerulus, Glo of glomerular layer. Thionin stain. x 600.

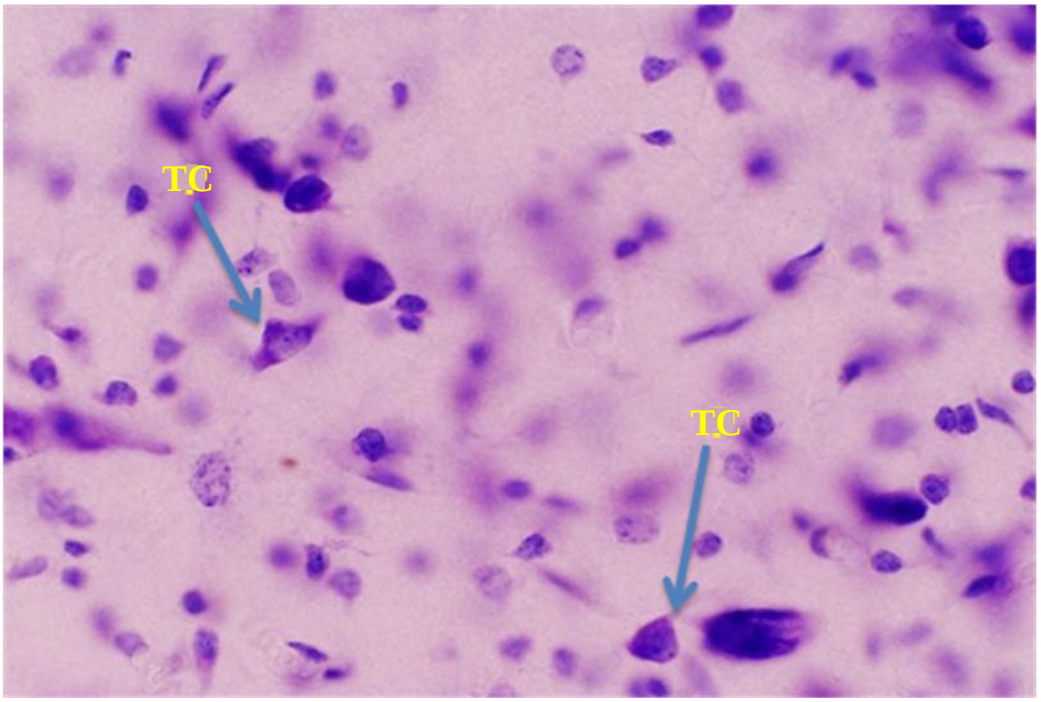


Plate XI**:** Transverse section of the cytoarchitecture of the olfactory bulb of adult African giant rat showing the tufted cells, TC of external plexiform layer. Thionin stain. x 600.

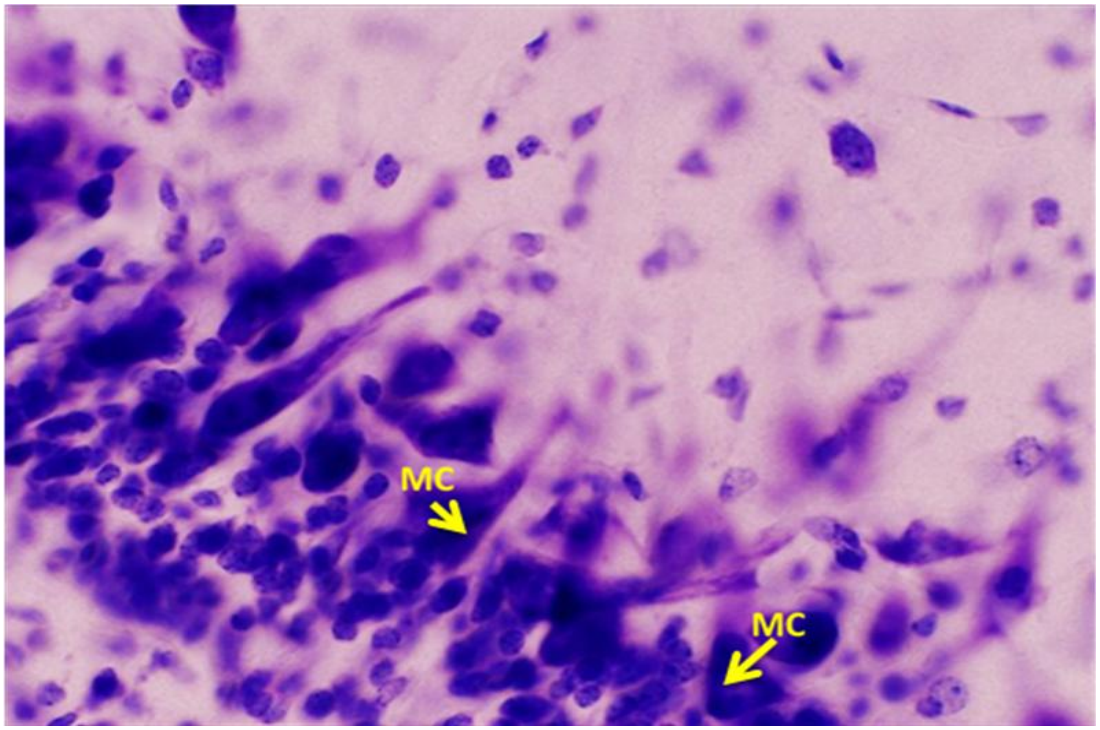


Plate XII: Transverse section of the cytoarchitecture of the olfactory bulb of African giant rat showing the mitral cells, MC of mitral cell layer. Thionin stain. x 600.

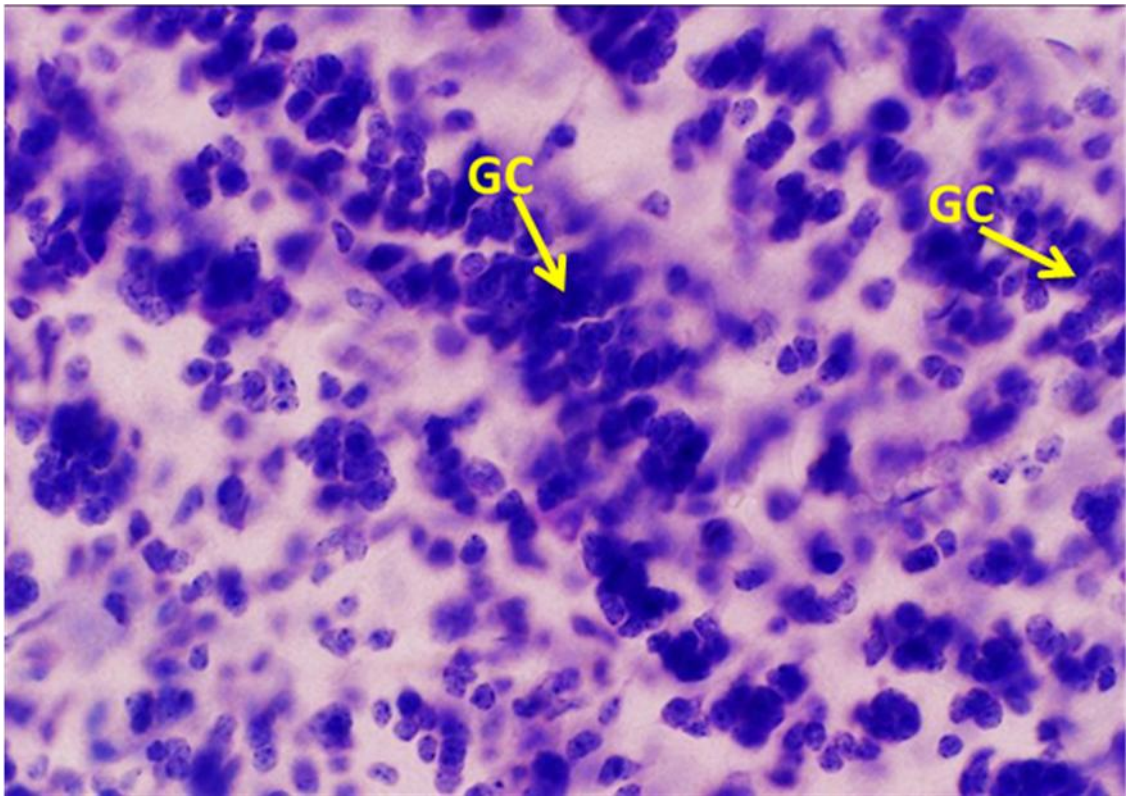


Plate XIII**:** Transverse section of the cytoarchitecture of the olfactory bulb of African Giant rat showing the granule cells, GC of granular layer. Thionin stain. x 600.

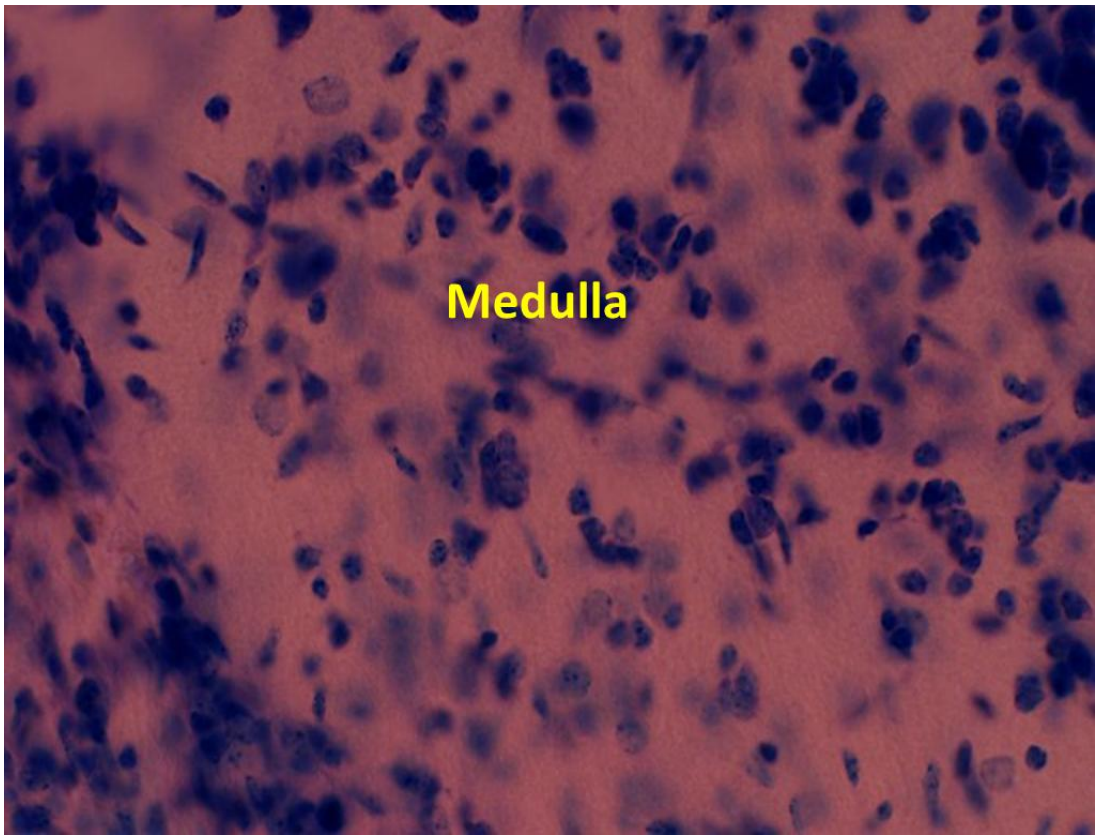


Plate XIV: Transverse section of the cytoarchitecture of the olfactory bulb of adult African Giant rat. Showing the medulla. Thionin stain. x 600.

4.11. Cytoarchitecture of Adult African Giant Rat Cerebral Cortex

The cerebral cortex of the adult AGR was characterized by five to six distinguishable layers of cell types. Between these layers, there are no definite boundaries separating them, but the layers were distinguished on the basis of predominance of different cell types in the individual layers. There was no sharp boundary between layers II and III, so in this study they are referred to as layer II/III, (Plate XV).

Plate XVI shows layer I, also called the molecular or plexiform layer. This layer was the most superficial layer and composed of many apical tuft dendrites of pyramidal neurones and afferent axons. Sparse nuclei are seen belonging to neuroglia.

Plate XVII shows layer II/III, called the external granular/pyramidal layer which had a granular appearance; it was densely populated by the cell bodies of small pyramidal neurones, and stellate cells. This layer also had medium and large pyramidal neurones especially at the deeper layer.

Plate XVIII shows layer IV, the internal granular layer, having small, round bodies of stellate (granule) projection neurons and pyramidal neurons.

Plate XIX shows layer V, the internal pyramidal layer and had stellate (granule) cells and few large pyramidal neurones.

Plate XX shows layer VI, the deepest layer having all morphological forms of cells (granule, pyramidal, fusiform etc) and therefore referred to as the multiform or polymorphic layer.

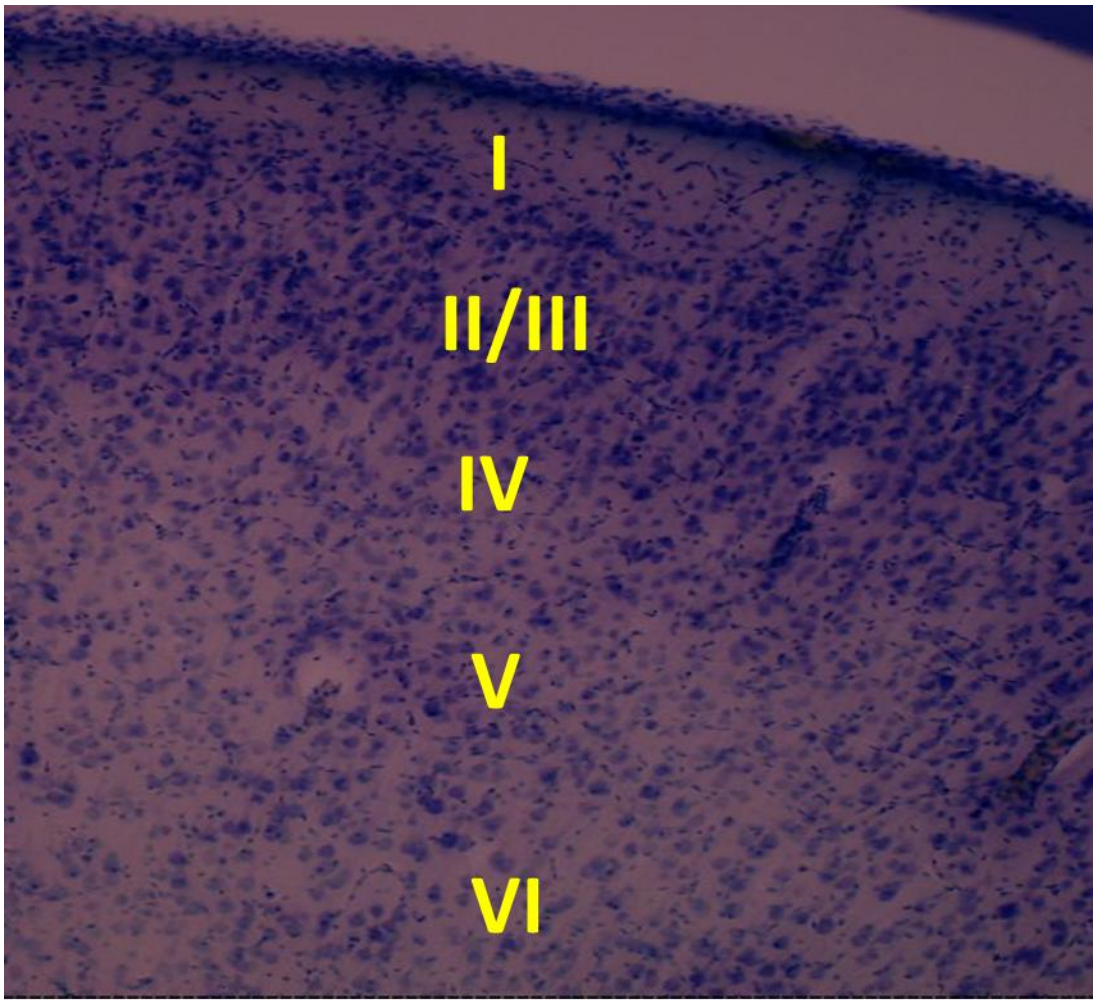


Plate XV: Transverse section of the cytoarchitecture of cerebral cortex of adult Africa Giant Rat. Layer I, molecular layer; layer II/III, external granular/pyramidal layer; layer IV, internal granular layer; layer V, internal pyramidal layer and layer VI, multiform or polymorphic layer. Thionin stain. x 100.

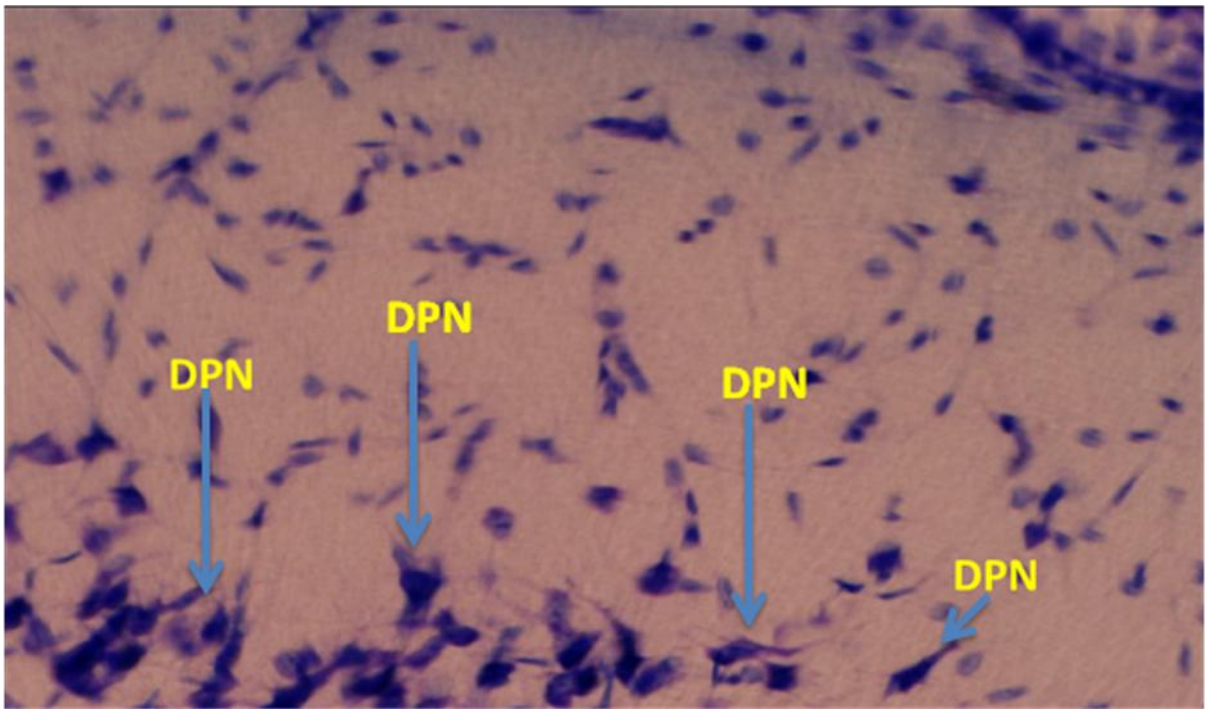


Plate XVI: Transverse section of the cytoarchitecture of cerebral cortex layer I (molecular layer) of adult African Giant rat. Dendrites of pyramidal neurone (DPN). Thionin stain. x 400.

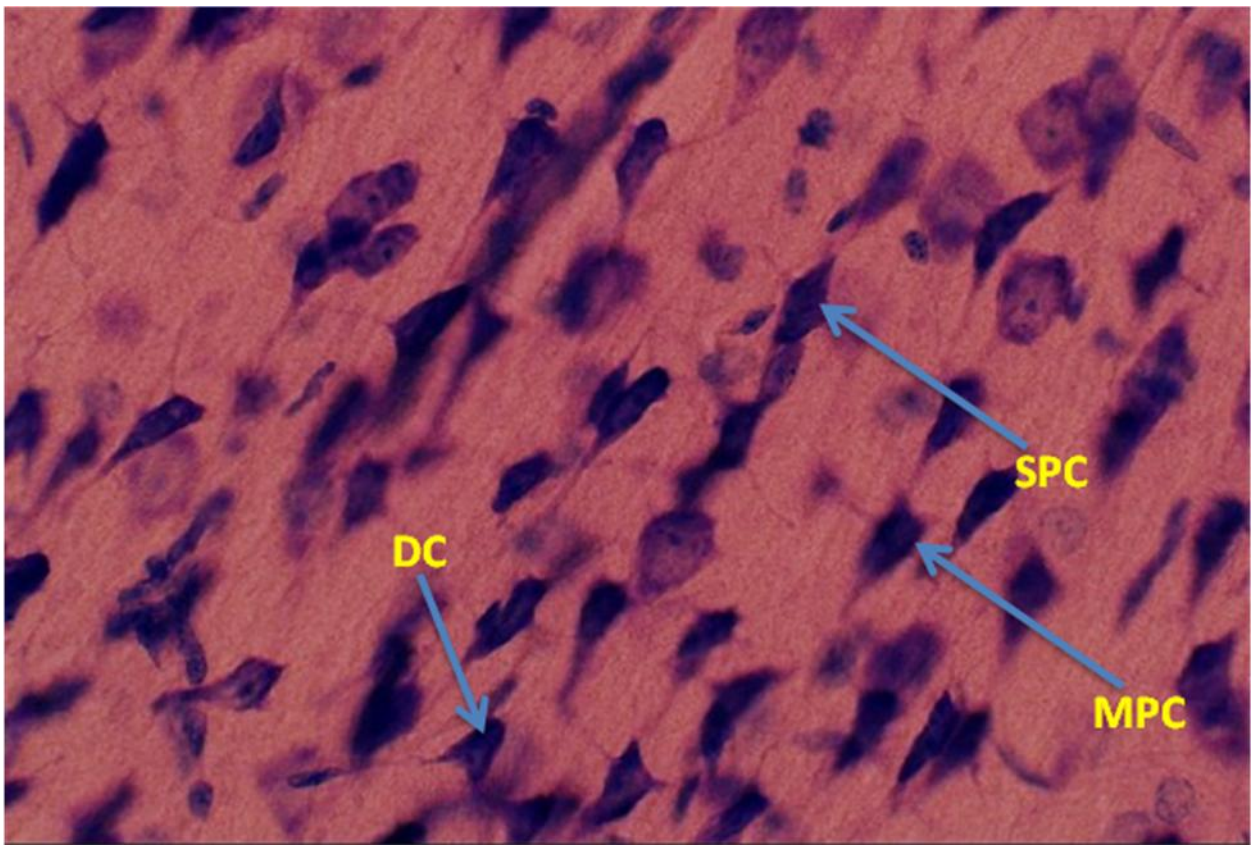


Plate XVII: Transverse section of the cytoarchitecture of Cerebral Cortex layer II/III, external granular/pyramidal layer of the adult African Giant rat. Stellate (granule) cell (GC), small pyramidal cell (SPC) and medium pyramidal cell (MPC). Thionin Stain. x 600.

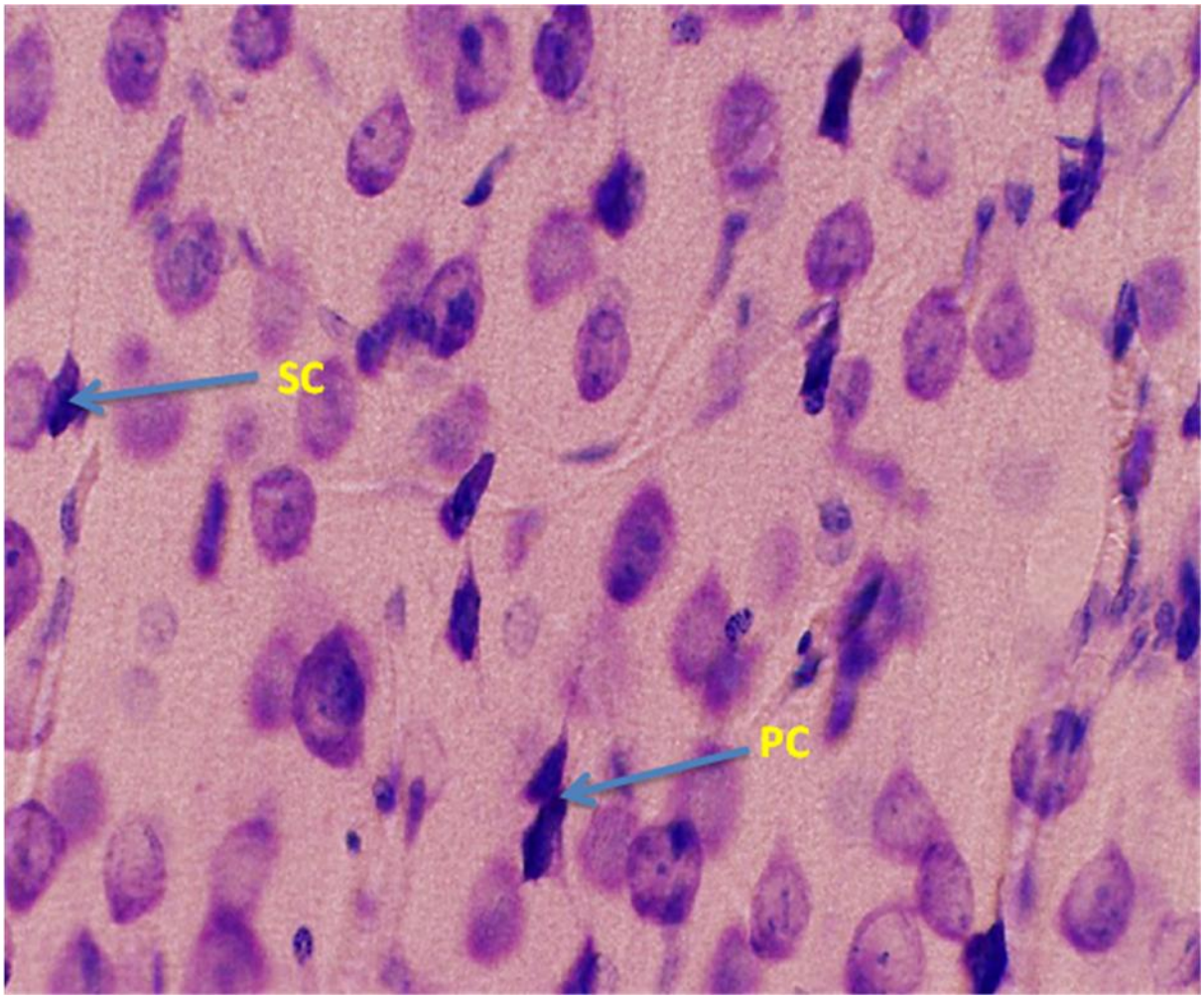


Plate XVIII: Transverse section of the cytoarchitecture of the Cerebral cortex layer IV, internal granular layer of the African Giant rat. Stellate cell (SC), pyramidal neurones (PC). Thionin stain. x 600.

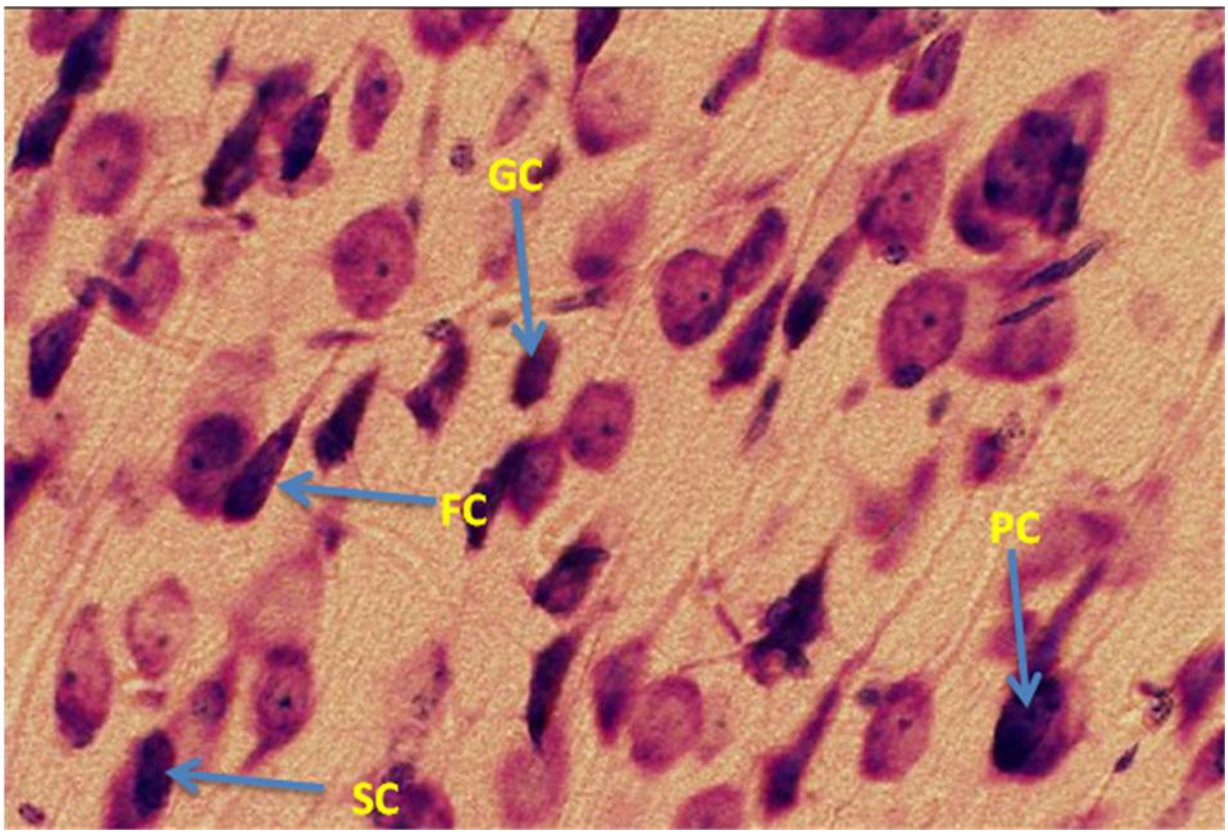


Plate XIX: Transverse section of the cytoarchitecture of the Cerebral Cortex layer V, internal pyramidal layer, of the African Giant rat. Stellate cell (SC); pyramidal cell (PC); granule cell (GC); fusiform cell (FC). Thionin stain. x 600.

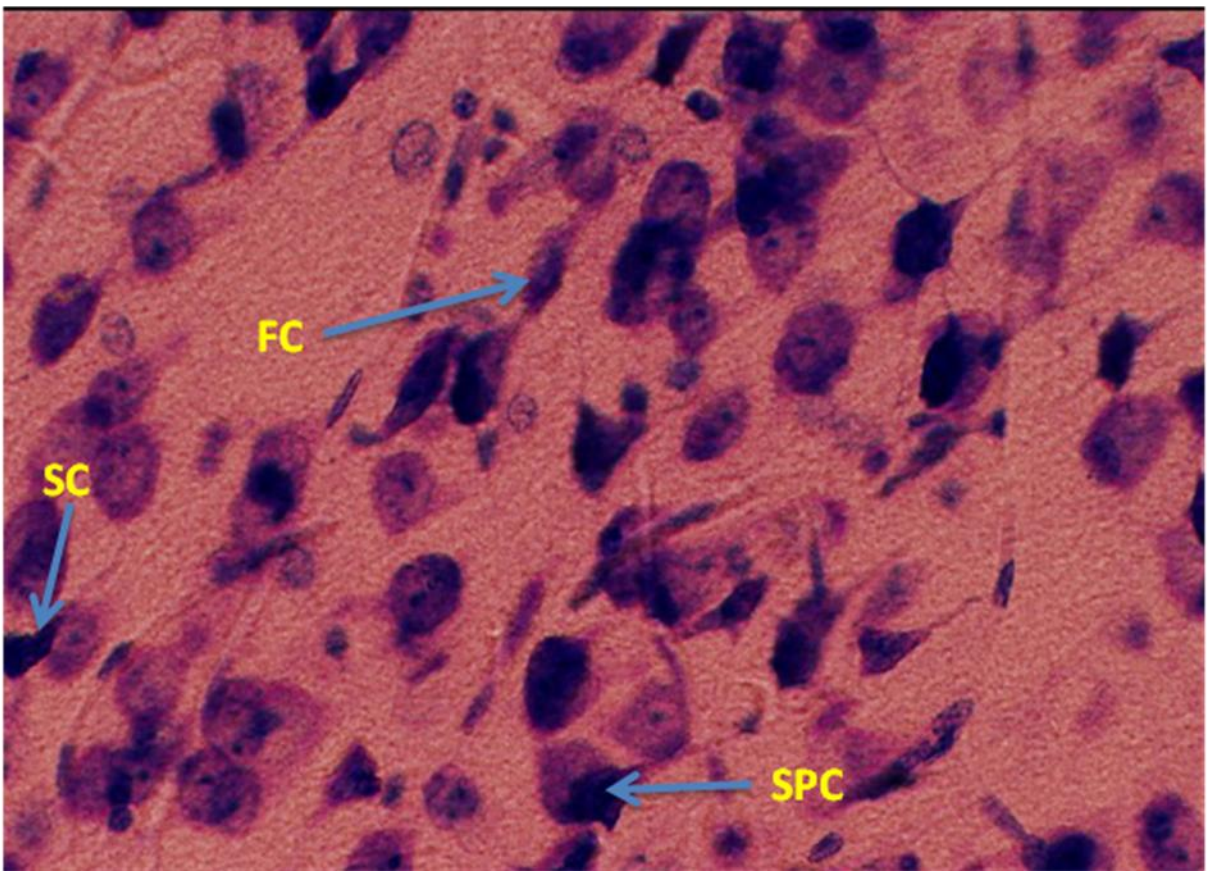


Plate XX: Transverse section of the cytoarchitecture of the Cerebral Cortex layer VI, multiform (polymorphic) layer of the African Giant Rat. Stellate Cell (SC); fusiform cells (FC); Small Pyramidal Cell (SPC). Thionin stain. x 600.

4.12. Designed-based Estimation of Neuronal Number in Olfactory Bulbs of the Adult African Giant Rats

The mean numbers of neurones in the different layers of the olfactory bulbs obtained from all the ten adult AGRs, irrespective of sex, were as follows: the periglomerular cells of the glomerular layer was 736, 060 ± 122, 202, the tufted cells of the external plexiform layer was 228, 531 ± 16, 905, the mitral cells of the mitral cell layer was 163,502 ± 83,518, the periglomerular cells of the internal plexiform layer was 166, 105 ± 22, 889 and the granule cells of the granular cell layer was 225, 8175 ± 97, 325, and a coefficient of error (CE) and coefficient of variation (CV) of 0.05 (0.59) (Table 8).

Table 8: Designed-based estimation of neuronal numbers in Olfactory Bulbs of the Adult African Giant Rat

Variable	n	Mean ± SEM	CE (CV)	SD	Minimum	Maximum
PC	10	$7.4 \times 10^5 \pm 1.2 \times 10^5$	0.05 (0.53)	386436	1.0×10^5	11.2×10^5
TC	10	$2.3 \times 10^5 \pm 1.7 \times 10^4$	0.06 (0.23)	53458	1.5×10^5	3.2×10^5
PC	10	$1.7 \times 10^5 \pm 2.3 \times 10^4$	0.05 (0.44)	72381	9.0×10^4	3.2×10^5
MC	10	$1.6 \times 10^5 \pm 8.4 \times 10^4$	0.06 (1.62)	264107	5.3×10^4	9.1×10^5
GC	10	$22.6 \times 10^5 \pm 9.7 \times 10^5$	0.05 (0.14)	307770	20.1×10^5	30.4×10^5
Mean CE (CV):			0.05 (0.59)			

Periglomerular cells, PC; tufted cells, TC; mitral cells, MC; granule cells, GC; coefficient of error, CE; coefficient of variation, CV; standard error of mean, SEM; standard deviation, SD; n= sample size

4.13. Descriptive Statistics (Optical fractionator) Olfactory Bulbs of the Male and Female Adult AGR: PC, TC, PC, MC, GC

The mean neuronal number in olfactory bulbs of the layers of the adult male AGR were as follows: periglomerular cells of the glomerular layer was $8.1 \times 10^5 \pm 1.1 \times 10^5$ the tufted cells of the external plexiform layer $2.2 \times 10^5 \pm 2.9 \times 10^5$ the mitral cells of the mitral cell layer $7.6 \times 10^5 \pm 9.5 \times 10^4$; the periglomerular cells of the internal plexiform layer $1.5 \times 10^5 \pm 3.1 \times 10^5$ and the granule cells of the granule cell layer was $2.1 \times 10^6 \pm 8.1 \times 10^5$ (Table 9).

In the adult female AGR, the neuronal numbers in the layers of olfactory bulbs layers were as follows: periglomerular cells of the glomerular layer, 661,557 ± 228,114; the tufted cells of the external plexiform layer 240,190 ± 19,006; the mitral cells of the mitral cell layer was 251474 ± 165616, the periglomerular cells of the internal plexiform layer, 182,968 ± 35,762; and the granule cells of the granule cell layer, 2381,234 ± 168,956, (Table 8). The results obtained showed that there was no significant difference in the mean values between the adult male and female AGRs ($P > 0.05$) (Table 9).

Table 9: Design-based estimation of neuronal numbers in the olfactory bulbs of adult male and female African Giant Rats

Variable	Sex	n	Mean ± SEM ($x10^5$)	CE (CV)	SD	Minimum	Maximum	P-value
PC	Female	5	6.6 ± 2.3	0.05(0.77)	510079	102111	1120305	P >0.05
	Male	5	8.1 ± 1.1	0.05(0.31)	248880	425367	1109017	
TC	Female	5	2.4 ± 0.2	0.25(0.18)	42499	172138	287837	P >0.05
	Male	5	2.2 ± 0.3	0.10(0.30)	65451	149777	324522	
PC	Female	5	1.8 ± 0.4	0.12(0.44)	79967	107233	318878	P >0.05
	Male	5	1.5 ± 0.3	0.13(0.45)	68428	90308	262439	
MC	Female	5	2.5 ± 1.7	0.06(1.50)	370328	63493	913516	P >0.05
	Male	5	1.0 ± 0.1	0.06(0.32)	21288	52779	103970	
GC	Female	5	23.8 ±1.7	0.05(0.16)	377798	2067705	3039060	P >0.05
	Male	5	21.4 ± 0.8	0.04(0.08)	180375	2006341	2438021	

Periglomerular cell, PC; tufted cell, TC; periglomerular cell, PC; mitral cell, MC; granule cell, GC; coefficient of error, CE; coefficient of variation, CV; standard error of mean, SEM and standard deviation, SD; n= sample size

4.14. Descriptive Statistics (Cavalieri Principle) Olfactory Bulbs of adult African Giant Rat

The mean volumes of the different layers of olfactory bulb of ten adult AGRs, were 12.6 x 10^9 ± 3.0 x 10^9 mm^3, 18.9 x 10^9 ± 5.2 x 10^9 mm^3, 4.4 x 10^9 ± 1.3 x 10^9 mm^3, 2.3 x 10^9 ± 0.8 x 10^9 mm^3, 12.3 x 10^9 ± 2.7 x 10^9 mm^3 and 12.3 x 10^9 ± 4.2 x 10^9 mm^3 for the glomerular cell layers, external plexiform layer, mitral cell layer, internal plexiform layer, granule cell layer and the medulla, respectively. While the mean olfactory bulb volume and coefficient of error and variation were 62.8 x 10^9 ± 18.5 x 10^9 mm^3, 0.03 and 1.12 respectively (Table 10).

Table 10: Volume (mm^3) of the different layers of the Olfactory Bulbs of adult African Giant Rats according to Cavalieri Principle

Variable	**n**	**Mean ± SEM (10^9)**	**CE (CV)**	**SD (10^9)**	**Minimum (10^9)**	**Maximum (10^9)**
GloCL (mm^3)	10	12.6 ± 3.0	0.03(0.75)	9.5	2.6	32.2
EPL (mm^3)	10	18.9 ± 5.2	0.02(0.88)	16.7	3.5	51.5
MCL (mm^3)	10	4.4 ± 1.3	0.03(0.92)	4.1	0.8	13.8
IPL (mm^3)	10	2.3 ± 0.8	0.05(1.19)	2.8	0.5	8.2
GCL (mm^3)	10	12.3 ± 2.7	0.02(0.71)	8.7	3.8	29.2
Medulla (mm^3)	10	12.3 ± 4.2	0.03(1.07)	13.2	2.8	44.5
Mean CE (CV)			0.03(1.12)			

Glomerular cell layer, GloCL; external plexiform layer, EPL; mitral cell layer, MCL; internal plexiform layer, IPL; granule cell layer, GCL; standard error of mean, SEM; standard deviation, SD; coefficient of error, CE; coefficient of variation, CV and n= sample size

4.15. Descriptive Statistics of Designed-Based (Cavalieri Principle) Estimation of Volume of the Layers of the Olfactory Bulb in Adult African Giant Rat: GloCL, EPL, MCL, IPL, GCL, Medulla

The mean volume of olfactory bulb layers in the adult male AGRs were as follows: glomerular cell layer (GloCL), $18.3 \times 10^9 \pm 4.9 \times 10^9$ mm^3; the external plexiform layer (EPL), $29.0 \times 10^9 \pm 8.0 \times 10^9$ mm^3; the mitral cell layer (MCL), $6.8 \times 10^9 \pm 2.1 \times 10^9$ mm^3; the internal plexiform layer (IPL), $3.9 \times 10^9 \pm 1.4 \times 10^9$ mm^3; the granule cell layer (GCL), $1.5 \times 10^9 \pm 5.4 \times 10^9$ mm^3; and the medulla, $7.4 \times 10^9 \pm 0.3 \times 10^9$ mm^3 (Table11).

In of the adult female AGR, the volume of the olfactory bulb layers were as follows: glomerular cell layer $7.0 \times 10^9 \pm 0.3 \times 10^9$ mm^3; the external plexiform layer $7.9 \times 10^9 \pm 0.2 \times 10^9$ mm^3; the mitral cell layer $2.0 \times 10^9 \pm 0.3 \times 10^9$ mm^3; the internal plexiform layer $7.0 \times 10^9 \pm 0.3 \times 10^9$ mm^3; the granule cell layer $9.1 \times 10^9 \pm 0.3 \times 10^9$ mm^3; and the medulla was $7.4 \times 10^9 \pm 0.3 \times 10^9$ mm^3 (Table 10). There was no significant ($P > 0.05$) difference in the mean values in the adult male and female AGRs (Table 11).

Table 11: Descriptive Statistics (Cavalieri Principle) of the Olfactory Bulb's layer in adult male and female African Giant Rats: GloCL, EPL, MCL, IPL, GCL, Medulla

Variable	**Sex**	**n**	**Mean ± SEM**	**CE (CV)**	**SD**	**Minimum**	**Maximum**
			(10^9)		**(10^9)**	**(10^9)**	**(10^9)**
GloCL	F	5	7.0 ± 0.3	0.02 (0.11)	0.7	6.7	8.3
	M	5	18.3 ± 4.9	0.03 (0.60)	11.0	2.0	3.2
EPL	F	5	7.9 ± 0.2	0.02 (0.08)	0.6	7.6	9.1
	M	5	29.0 ± 8.0	0.03 (0.61)	18.1	3.0	5.2
MCL	F	5	2.0 ± 0.3	0.03 (0.01)	0.8	2.0	2.0
	M	5	6.8 ± 2.1	0.03 (0.70)	4.8	0.8	13.8
IPL	F	5	7.0 ± 0.3	0.05 (0.11)	0.8	0.7	0.9
	M	5	3.9 ± 1.4	0.04 (0.86)	3.3	0.5	8.2
GCL	F	5	9.1 ± 0.3	0.02 (0.08)	0.7	8.8	10.4
	M	5	1.5 ± 5.4	0.03 (0.08)	1.2	3.8	29.2
Medulla	F	5	17.2 ± 7.6	0.03 (0.99)	17.0	4.9	44.4
	M	5	7.4 ± 0.3	0.03 (0.86)	6.4	2.7	18.2

GloCl, glomerular cell layer; EPL, external plexiform layer; MCL, mitral cell layer; IPL, internal plexiform layer; GCL, granule cell layer; standard error of mean, SEM; standard deviation, SD; coefficient of error, CE; coefficient of variation, CV and n= sample size

.

4.16. Volume (mm^3) of the cerebral cortex layers of adult African Giant Rat, according to Cavalieri Principle

Table 12 shows the volumes of the different layers of the olfactory bulbs of adult AGRs, using the Cavalieri Principle, a designed-based stereological method. The mean volumes of the cerebral cortex layers (I, II/111, IV, V and VI) of adult AGRs obtained, irrespective of sex, were $57.9 \times 10^9 \pm 5.8 \times 10^9$ mm^3, $54.3 \times 10^9 \pm 5.1 \times 10^9$ mm^3, $54.7 \times 10^9 \pm 6.2 \times 10^9$ mm^3, $61.7 \times 10^9 \pm 6.5 \times 10^9$ mm^3 and $69.8 \times 10^9 \pm 7.3 \times 10^9$ mm^3 for layers I, II/III, IV, V, and VI, respectively.

Table 12: Volume (mm^3) of the Cerebral Cortex Layers of adult African Giant Rats

Variable	**n**	**Mean ± SEM** (10^9)	**CE (CV)**	**SD** (10^9)	**Minimum** (10^9)	**Maximum** (10^9)	**Range** (10^9)
Layer I	10	57.9 ± 5.8	0.03 (0.31)	18.2	18.3	78.0	59.7
Layer II/III	10	54.3 ± 5.1	0.02 (0.29)	16.2	24.7	74.5	49.8
Layer IV	10	54.7 ± 6.2	0.03 (0.36)	19.6	23.4	81.2	57.8
Layer V	10	61.7 ± 6.5	0.02 (0.34)	20.7	24.9	83.5	58.7
Layer VI	10	69.8 ± 7.3	0.02 (0.33)	23.3	27.1	98.7	71.6
Mean CE(CV)			0.02 (0.33)				

Standard error of mean, SEM; standard deviation, SD; coefficient of error, CE; coefficient of variation, CV and n= sample size

4.17. Descriptive Statistics of Designed-Based Stereological Estimation of Volume of Layers of Cerebral Cortex of Adult African Giant Rats by Cavalieri Principle

The mean volume of cerebral cortex layers of the adult male AGRs were as follows: layer I, 48.0 x 10^9 ± 10.0 x 10^9 mm^3; layer II/III, 45.7 x 10^9 ± 8.2 x 10^9 mm^3; layer IV, 45.2 x 10^9 ± 10.2 x 10^9 mm^3; layer V, 48.1 x 10^9 ± 9.8 x 10^9 mm^3; layer VI, 55.7 x 10^9 ± 11.8 x 10^9 mm^3 (Table 13).

The cerebral cortical layers of adult female AGRs were as follows; layer I, 67.8 x 10^9 ± 0.3 x 10^9 mm^3; layer II/III, 63.1 x 10^9 ± 3.5 x 10^9 mm^3; layer IV, 64.4 x 10^9 ± 4.5 x 10^9 mm^3; layer V, 75.5 x 10^9 ± 1.4 x 10^9 mm^3; layer VI, 84.0 x 10^9 ± 1.9 x 10^9 mm^3 (Table 13) . The differences in mean values of the volumes of the layers in the adult male and female AGRs were insignificant ($P > 0.05$) (Table 13).

Table 13: Volume (mm^3) of the Cerebral Cortex Layers of adult male and female African Giant Rats

Layers	Sex	n	Mean ± SEM (10^9)	CE(CV)	SD (10^9)	Min (10^9)	Max (10^9)	Range (10^9)	P- value
I	F	5	67.8 ± 0.3	0.03(0.1)	0.6	66.9	68.4	1.5	P >0.05
	M	5	48.0 ±10.0	0.02(0.5)	22.4	18.3	77.9	6.0	
II/III	F	5	63.1 ± 3.5	0.03(0.13)	7.9	54.8	72.6	17.8	P >0.05
	M	5	45.7 ± 8.2	0.02(0.4)	18.4	24.7	74.5	49.8	
IV	F	5	64.4 ± 4.6	0.03(0.16)	10.3	53.9	74.5	20.6	P >0.05
	M	5	45.2 ± 10.3	0.02(0.51)	23.0	23.4	81.2	57.8	
V	F	5	75.5 ± 1.4	0.02(0.04)	3.2	71.1	80.1	8.9	P >0.05
	M	5	48.1 ± 9.8	0.02(0.46)	21.9	24.9	83.6	58.7	
VI	F	5	84.0 ± 1.9	0.02(0.50)	4.2	81.1	90.5	9.4	P >0.05
	M	5	55.7 ± 11.8	0.02(0.48)	26.5	27.1	98.7	71.6	

Female, F; male, M; standard error of mean, SEM; standard deviation, SD; coefficient of error, CE; coefficient of variation, CV and n= sample size

CHAPTER FIVE

5.0 DISCUSSION

The olfactory system is relevant for species survival during breeding and reproduction (Shipley *et al*., 2004). Morphologically, the olfactory bulb was large. Nzalak *et al*. (2008) also observed large olfactory bulb in the AGR. Morphological developments of the olfactory bulb are needed for the precocious olfactory environmental interactions (Salas *et al*., 1970, Coopersmith and Leon 1988, Malun and Brunjes 1996, Bailey *et al*., 1999, Guthrie and Gall 2003). This largeness in size may facilitate experimental procedures involving neurobiology of olfaction.

The shape of the cerebrum of the AGR observed in this study was similar to those reported for Wistar rats (Webster *et al*., 1947; Heber and Stromberg, 1976) and rodents like the rabbit (Kozma *et al*., 1976). The intact brain of the AGR was milky in colour and snail-shaped. The cerebrum of the adult AGR showed two major depressions, a longitudinal depression called the longitudinal fissure which contains sickle-shaped processes of *dura mater*, called the *falx cerebri*, the longitudinal fissure separated the cerebrum into two hemispheres. A horizontal depression separated the cerebrum from the cerebellum. The AGRs have smooth-surfaced or non-convoluted cerebrum, which is called lissencephalics. Each cerebral hemisphere has frontal, parietal, temporal and occipital regions. The cerebral hemisphere of the AGR has a smooth superolateral surface, a flat medial surface and an inferior surface that is irregular in shape. The cerebral hemisphere of the adult AGR showed a superolateral border, located between the superolateral and medial surfaces, and an inferolateral border between the superolateral and inferior surfaces. It has no gyri and sulci, hence it is lissencephalics.

In mammals, cerebral cortex presents significant variations across species, ranging from the small and smooth (lissencephalics) cortex of mice, to the large and profoundly folded (gyrencephalic) cortex of humans (Hofman, 1989; Rakic, 1995). As the surface area of the brain increases more functions are made possible. A smooth-surfaced brain is only able to grow to a certain extent. Sulcus increases the surface area of the cerebrum and allows for continued growth. This in turn allows for the functions of the brain to continue growing (Cusack, 2005). The division between the two groups occurs when cortical surface area is about 10 cm^2 and the brain has a volume of 3–4 cm^3. Large rodents such as beavers (18 kg) and capybaras (68 kg) are gyrencephalic and smaller rodents such as rats and mice are lissencephalics (Martin *et al*., 2005).

The variation in the amount of fissures in the brain (gyrification) between species is related to the size of the animal and the size of the brain. Mammals that have smooth-surfaced or non-convoluted brains are called lissencephalics and those that have folded or convoluted brains gyrencephalics (Nonaka-Kinoshita, 2013).

The descriptive morphometric data obtained from all the ten adult AGRs showed that the mean body weight was 1215.0 ± 78.2 g, while the mean nose-rump length was 72.80 ± 0.85 cm. Ibe *et al.* (2010) reported mean body weight and nose-rump length of 999.65 ± 42.62 g and 345.26 ± 7.29 mm, respectively obtained from 29 rats, irrespective of their sex. Thus, the mean nose-rump length obtained in this study; reflected to a large extent, the length of the central nervous system occupied by the brain in the AGR. The mean body weight in the AGR was significantly greater in the male than the female AGRs, but the nose-rump length was slightly higher in the females than in the males, though the difference was not statistically significant. The sexual dimorphism in the body weight of AGRs reported in this study agrees with the results of other researchers, who reported on

the dimorphism in the same species of rat (Henwood, 1985; Nowak, 1999; Ibe, 2010). This finding is also similar to the report of Becker and Middleton (1979) on the adult African white-tailed rats (*Mystromys albicaudatus*), that the males are significantly heavier than the females. However, Byanet *et al*. (2009) reported a higher body weight in female grasscutters (*Thryonomys swinderianus*). Sexual dimorphism in the body weight of AGRs as reported in this study indicated a higher body weight in the male than female animals.

The result of the mean nose-rump length reported in this study showed that the female AGRs have a slightly higher nose-rump length than the males, but the difference was not statistically significant. Ibe *et al*., 2010, reported that the nose-rump was higher in the male African giant rat than in the female African giant rats but the difference was not significant statistically.

The results of this study showed that the AGR has a mean absolute cerebral weight of 3.44 ± 0.07 g, which disagreed with the report of Olude *et al*. (2014), who reported a mean cerebral weight of 5.48 ± 0.56 g in six adult AGRs. The mean cerebral width and cerebral thickness obtained from all the ten adult AGRs, irrespective of their sex, were 19.59 ± 0.42 mm and 12.84 ± 0.15 mm, respectively. A preliminary study was done on the brain weight of the AGR (Nzalak *et al*., 2008), and the brain weight was known to be 85 to 90% of the weight of the cranial content. The brain density of the AGR can be assessed from the data, since the cerebral weight, width and thickness are parameters that give more insight into the morphometric of the cerebrum of the AGR. With respect to sex, the cerebral weight was higher ($P < 0.01$) in the adult male AGRs, 3.62 ± 0.02 g than in the adult female AGRs 3.26 ± 0.07 g, thus, showing sexual dimorphism. Similarly, the cerebral width was higher ($P < 0.01$) in the adult male AGRs, (20.43 ± 0.33 mm) than in

the adult female AGRs, (18.77 ± 0.58 mm). The sexual dimorphism in the absolute cerebral weight and cerebral thickness of the AGR reported in this study. Byanet *et al*., (2009) made similar observation in grasscutter a rodent of similar species as the AGR, he reported sexual dimorphism in the absolute brain weight and that the female brain weighs more than the male brain in absolute terms. In a similar study, Ibe *et al*. (2010), reported a relatively higher brain weight in the female than in the male AGR, but the difference was not significant. The cerebral thickness recorded in this present study showed no sexual dimorphism, even though the cerebral thickness in the adult male AGRs was slightly higher ($P > 0.05$), than that of the female. This finding may be due to size differences between sexes.

The morphometric parameters of the olfactory bulbs in the AGRs investigated in this study were the mean absolute weight, width and thickness of the olfactory bulb. Irrespective of sex, the mean absolute weight, mean width and mean thickness of the olfactory bulb obtained from this present study, were 0.95 ± 0.03 g, 4.08 ± 0.27 mm and 2.98±0.10 mm, respectively. The results of this study showed that the olfactory bulb accounts for 8% the total body weight in the AGR. With respect to sex, the mean absolute of weight of olfactory bulbs in the female AGR was higher ($P < 0.05$) than that of the male and the difference was significant. This finding agrees with the report of Byanet *et al*., (2009) on grasscutters, which is a rodent of similar species with the AGR, who obtained significant differences ($p < 0.0001$ and 0.0259) in the body and olfactory bulb weights. The olfactory bulb accounted for 6.3% and 1% of the body weight in the male and female AGR body weights respectively. The width of the olfactory bulb was not greater in the male AGR than the female AGR. The thickness of olfactory bulbs was not higher in the female AGR than in male. Byanet *et al*. (2009) reported that the olfactory bulb accounts for 6% of the total brain length in males and 4% in females of grasscutters.

From this study, the olfactory bulb weight showed sex difference; it was larger in females than in males. This finding may be one of the reasons for the difference in smell sensitivity between males and females (Wei *et al*., 2008). The females, in turn had lesser olfactory bulb width than the males, but a thicker olfactory bulb than the males, although the difference was not significant. This may be one of the reasons for the difference in smell sensitivity between females and males.

The olfactory glomerular layer, at which the mitral cell dendrites are in synaptic contact with the periglomerular cells, consisted of glomerulars which were made up of synapses. The periglomerular cells are distributed around the glomerulars with which they were closely connected.

The external plexiform layer was mainly made up of primary dendrites of mitral cells and periglomerular cells and nerve fibres. The periglomerular cells were spherical in shape and distributed unevenly, and the cells increased in size closer to the mitral cell layer (Hamilton *et al*., 2005).

The mitral cell layer contained mainly the mitral cell bodies and their dendrites. They are pyramidal in shape and were the largest cell in the olfactory bulb. Wei., *et al*, 2008, made similar findings in dogs, he reported that the mitral cells are pyramidal in shape and were the largest cell types in the olfactory bulb of dog, and that there are also some cell types like the granule and the tufted cells in the mitral cell layer. The internal plexiform layer was a very thin layer and one cell thick; it has a low cell density. It had few periglomerular cells. The periglomerular and granular cells are interneurons in the olfactory bulb.

The granule cell layer takes up the largest part of the olfactory bulb, and is mainly made up of granule cells. The granule cells were round in shape and lied in the deepest part of

the olfactory bulb, and there were more of them than mitral cells. Wei, *et al*. 2008, also reported that there were more granule cells in the olfactory bulb of dog than mitral cells. These features of the structure of the olfactory bulb make it easier for information processing, and they also provide a structural foundation for the spatial encoding of olfactory information (Hamilton *et al*., 2005; Mori *et al*., 2006).

The cerebral cortex of the adult AGR used in this study differed in neuronal morphology, size and population density. There were five to six distinguishable layers with no sharp boundaries separating them. The layers were, however, distinguishable on the basis of predominance of cell types. The cortical layers were also not equally prominent everywhere. Layer I, the molecular or plexiform layer, was the most superficial layer composed of many apical tuft dendrites of pyramidal neurones and afferent axons. Sparse nuclei were observed belonging to neuroglia. It was devoid of neuronal cell bodies; this finding was in agreement with the report of Conn (1995), who reported that the molecular layer of the cerebral cortex was composed of dendrites of pyramidal cells. Layer II/III, had a granular appearance; it was densely populated by the cell bodies of small, medium and large, pyramidal neurones, and stellate cells. The pyramidal cells are the principal output neurons and as their names suggested they are pyramidal in shape, and a have long apical dendrite leaves the top of each pyramidal cell to ascend vertically to the cortical surface (Conn, 1995). The stellate (granule) cells in this present study are small and showed short axons. They are reported to be the principal interneurones of the neocortex (Conn, 1995). Layer IV, had a granular appearance, and it was composed of small, round bodies of stellate projection neurones and pyramidal neurons. Layer V, had few large pyramidal neurons. The cell packing density in this layer is the lowest of all the cortical layers (Conn, 1995). Layer VI, had all morphological forms of cells, ranging from stellate (granule) cells, granule cells, fusiform cells. This layer is called multiform or

polymorphic layer because of the varying cell type with their different sizes. It was observed that the main structure of the olfactory bulb in adult AGR includes olfactory glomerular layer, external plexiform layer, mitral cell layer, internal plexiform layer, granule cell layer and the medulla. This cytoarchitectural arrangement was similar to that of the olfactory bulb of dog, and other rodents (Wei, *et al*., 2008). All were arranged very clearly and regularly in the olfactory bulb.

The mean neuronal number in the different layers of the olfactory bulbs, irrespective of sex, showed that the periglomerular cells, tufted cells, mitral cells, periglomerular cells and the granule cells accounted for 20.72%, 6.44%, 4.61%, 3.27% and 63.68% of the neurones in the five layers of the olfactory bulb in AGR's respectively. The granule cells in the granule cell layer of the bulb have the highest number of neurones followed by periglomerular cells in the glomerular cell layer of the olfactory bulb of AGR. The granule cell layer takes up a large part of the olfactory bulb and is mainly made up of granule cells and their prominency (Wei *et al*., 2008). With respect to sex, the mean neuronal number of the different neuronal types in the cellular five layers of the olfactory bulbs of adult AGRs showed a slightly higher value in the females, except the periglomerular cells in the glomerular cell layer in the males. However, there was no significant difference in the numbers of neurones of the olfactory bulb between male and female AGR. This result implies that there is no sexual variation in neuronal numbers in the olfactory bulb of adult AGRs. In dogs, Wei *et al*. (2008) found that the quantity of mitral cells decreased, but it increased in size, suggesting that the olfactory bulbs developed with the growth in dog (Wei *et al*., 2008). It has been shown that interneurons are the most numerous among olfactory bulb cells, and that they display an important characteristic: most of them are anaxonal cells that establish reciprocal synapses with projection neurons and among themselves (Crespo *et al*., 2013). This microstructural

organization provides a distributive profile to the network, conveying to the neural hubs downstream a non-topographic, diffuse flow of olfactory information (Giessel *et al*., 2014). Given this diffuse nature of the information processed by the olfactory bulb, it is conceivable that the larger the number of these neurons in the olfactory bulb, the more capable it becomes for processing more information to be analyzed by the piriform cortex, cortical amygdala, and other olfactory bulb targets. Several authours have suggested that human neonates are able to identify the smell of their mothers but this ability seems to be lost as one grows (Roy and Roy, 2012). The number of cells in olfactory bulb, and especially the number of neurons, may represent a more accurate indicator of the neural machinery and hence the degree of the olfactory ability.

The Cavalieri Principle is a designed-based stereological unbiased method for estimating the volume of any object. Irrespective of sex, the results showed similarity in the mean volumes of the glomerular cell layers and the granule cell layer of the AGR. The external plexiform layer had the highest volume, while the internal plexiform layer had the smallest volume in the olfactory bulbs of AGR. The volume of mitral cell layer was more than that of the internal plexiform layer in AGR. With respect to sex, the result showed that the volumes of the glomerular cell layer, external plexiform and internal plexiform layers higher were in the male AGR, while the mitral cell layer, granule cell layer and the medulla were higher in the female AGR. However, there were no significant differences in the volume of the layers of the olfactory bulbs between male and female adult AGR. The olfactory glomerular layer, at which the mitral cell dendrites are in synaptic contact with the olfactory nerves and also with the periglomerular cells, consisted of glomerulars which were made up synapses. Oval olfactory glomerulars were arranged regularly in the olfactory bulb, and are surrounded by glial cells. Periglomerular cells which are distributed around the glomerulars were interspaced neurones and they were connected

closely with the glomerulars (Wei *et al*., 2008). Olfaction plays a major role in our interaction with the environment. The olfactory system not only acts for the detection of potential dangers in the environment, such as smoke, gas or dusts, but also it influences our nutrition, social behavior, and well-being. The olfactory bulb plays the central role in the processing of olfactory information. It is the only relay between periphery and the central nervous system; it also processes olfactory information. The olfactory bulb volume varies as a function of olfactory sensitivity and is decreased in patients with olfactory disorders (Yousem *et al*., 1999). In humans, changes in olfactory bulb volume are related to odour identification and/or odour threshold (Mueller *et al*., 2005; Rombaux *et al*., 2006). The olfactory bulb volume is intimately correlated to olfactory function, independently of age. Using the Sniffin' Sticks test, Buschhüter *et al.* (2008) demonstrated that olfactory bulb volume correlated significantly with overall olfactory function, measured by the TDI score; specifically, olfactory bulb volume was found to correlate to specific olfactory functions namely odor thresholds and odor identification (Buschhüter *et al.*, 2008).

Cortical layers are not simply stacked one over the other; there exist characteristic connections between different layers and neuronal types, which span all the thickness of the cortex. Localized difference in the cortex is one of the most useful morphometric traits in human and animal brain studies (Joohwi, 2011). The result of the present study showed that the mean cortical volume of the cerebral cortex in the AGR was 298.4 x 10^9 mm^3. The mean volume for each layer the cerebral cortex of the ten adult AGRs, irrespective of sex, were 57.9 x 10^9 ± 5.8 x 10^9 mm^3, 54.3 x 10^9 ± 5.1 x 10^9 mm^3, 54.7 x 10^9 ± 6.2 x 10^9 mm^3, 61.7 x 10^9 ± 6.5 x10^9 mm^3 and 69.8 x 10^9 ± 7.3 x10^9 mm^3 for layer I, II/111, IV, V and VI respectively. Layer I, II/111, IV, V and VI accounted for 19.7%, 18.5%, 18.6%, 21% and 23.7% of the volume of the cerebral cortex of the AGR,

respectively. For mammals, species with larger brains (in absolute terms, not just in relation to body size) tend to have thicker cortices (Nieuwenhuys *et al*., 1998). The relative thickness of cortical layers seems to be a better predictor for the type of cortical organization than their lateral extent (Kaschube, 2014). With respect to sex, the mean volume in the adult male AGR cerebral cortical layers was 242.7 x 10^9 mm^3. Layer I was 48.0 x 10^9 ± 10.0 x 10^9 mm^3, layer II/III was 45.7 x 10^9 ± 8.2 x 10^9 mm^3, layer IV was 45.2 x 10^9 ± 10.2 x 10^9 mm^3, layer V was 48.1 x 10^9 ± 9.8 x 10^9 mm^3, layer was VI 55.7 x 10^9 ± 11.8 x 10^9 mm^3. The volumes accounted for 19.8%, 18.8%, 18.6%, 19.8% and 23% for layers I, II/III, IV, V and VI respectively. The volume of cerebral cortical layers in adult female AGR was 354.8 x 10^9 mm^3. Layer I was 67.8 x 10^9 ± 2.7 x 10^9 mm^3, layer II/III was 63.1 x 10^9 ± 17.1 x 10^9 mm^3, layer IV was 64.4 x 10^9 ± 4.5 x 10^9 mm^3, layer V was 75.5 x 10^9 ± 1.4 x 10^9 mm^3 and layer VI was 84.0 x 10^9 ± 1.9 x 10^9 mm^3, and these accounted for 19.1%, 17.8%, 12.2%, 21.3%, and 23.6%, for layers I, II/III, IV, V and VI respectively. The results showed that the female adult AGR has higher volume in all the layers of the cerebral cortex in AGR but the difference was not statistically significant ($P > 0.05$). The study conducted by Shepherd (2003) and Hutsler *et al*. (2005) on comparative analysis of cortical layering and supragranular layer enlargement in rodent carnivore and primate species found that layers II/III occupied on average 44% and 35% of the cortical thickness in primates and carnivores, respectively, but in rodents only 26% were devoted on average to these layers. In contrast, layers V and VI together occupied only 34% of the cortical thickness in primates and 39% in carnivores, but a total of 54% in rodents. These differences in percentages may have functional implications and species differences. To the best of our knowledge this study is the first of its kind to report the volume of the different layers of the cerebral cortex in the AGR (*Cricetomys gambianus*).

CHAPTER SIX

6.0 SUMMARY, CONCLUSION AND RECOMMENDATIONS

6.1 Summary

Anatomical studies of the olfactory bulb and the cerebrum of ten adult AGRs were investigated. Their morphologic and histologic features, morphometric and stereological parameters were observed, recorded and evaluated. The mean body weight of the male AGR was higher than that of the female AGR. Morphologically, the cerebrum of the adult AGR consisted of two cerebral hemispheres which were separated along the midline by a longitudinal fissure. The cerebrum in adult AGR was lissencephalics; that is, no sulci and gyri. The cerebral weights were higher in the male AGR than in the female AGR. The olfactory bulbs of the adult AGR were relatively large and located at the frontal lobe of the brain posterior to the nasal cavity. It was globular in shape and the weights were higher in the female AGR. The cerebral cytoarchitecture presented six layers, with layers II and III indistinguishable; but the layers presented the normal cytoarchitectural features as in other similar rodents. Adult female AGRs have higher volume in all the layers of the cerebral cortex, but the difference was not significant. The olfactory bulb cytoarchitecture showed five layer structures with a central core medulla, and each of the layers presented different cell types. The total olfactory neuronal number in AGR was 35.6×10^9; with the granule cells in the granule cell layer of the bulb having the highest number of neurones followed by periglomerular cells in the glomerular cell layer of the olfactory bulb. There was no significant difference in the volume of the layers of the olfactory bulbs between male and female adult AGRs.

6.2 Conclusions

The adult male African Giant rat (AGR) had a higher mean body weight than the female AGR, showing sexual dimorphism. The olfactory bulb in adult AGR was globular in shape and was relatively large and located in the frontal lobe of the adult AGR brain. The cerebrum of the adult AGR was smooth surface and non-convoluted. The cerebrum was lissencephalics, that is, the AGR cerebrum was smooth and lack gyri and sulci. The cerebral weight was higher in adult male AGRs than in females. There was sexual dimorphism in the body weight, olfactory bulb and cerebral weights of adult AGR, The olfactory bulb had five layers; and a central core of medulla, composed of white matter. The cerebral cortex of adult AGR was characterized by five to six distinguishable layers of cell types. Between these layers, there was no distinct boundaries separating them, but the layers were distinguishable based on predominance of difference cell types in the individual layers.

Using the designed-based stereological method, adult AGR had an estimated neuronal number of $35.6 \times 10^5 \pm 23.1 \times 10^5$ in the olfactory bulbs of adult AGR. The different neuronal number between the adult male and female AGRs was not different. Using Cavalieri Principle, the established mean volume of layers olfactory bulb was $68.8 \times 10^9 \pm 18.5 \times 10^9$ mm^3, thus displayed no sexual dimorphism. The established mean volume of cerebral cortical layer was $298.4 \times 10^9 \pm 30.90 \times 10^9$ mm^3, and there was no sexual dimorphism displayed.

This present study revealed the morphologic, morphometric and histological features of the olfactory bulbs and cerebral cortex in African giant rats. And also for the first time reported neuronal numbers in the olfactory bulbs and volumes of the different layers of the olfactory bulbs and cerebral cortex in the African Giant rats (*Cricetomys gambianus*,

Waterhouse-1840). These results have been able to increase our understanding of the olfactory ability in detecting explosive in mines, tuberculosis bacteria in sputum and other brain function in AGR, These results will form a basis for future studies of the olfactory bulbs and cerebrum of the AGR and also may be useful in comparative neuroanatomy with other similar mammals.

6.3 Recommendations

1. The results obtained from this study may be used in comparative neuroanatomy of rodents of similar species.
2. The observations are of value in comparative neuroanatomy of olfaction in rodents and mammals.
3. The findings may be of value in elucidating the mechanism of olfaction in this macrosomatic rodent.
4. The result of this study may be used in understanding the neurobiology of the African Giant Rat.
5. Further studies should be carried out to:
    a. Estimate neuronal number in the cerebral cortex of African Giant rats.
    b. Estimate the volume of individual neurones in the olfactory bulbs and cerebral cortex of African Giant Rat.
    c. Identify neuroglia cells in order to obtain an unbiased estimate of the number and volume of the cells in the cerebrum of African Giant rat.

References

Ache, B. W. (2010). Odorant-specific modes of signaling in mammalian olfaction. *Chemical Senses*, 35(7): 533–539.

Ache, B. W. and Young, J. M. (2005). Olfaction: Diverse species, conserved principles. *Neuron*, 48(3): 417–430.

Adeyemo, O. and Oke, B. O. (1990). Comparison of the testicular and epididymal proteins of the African giant rat (*Cricetomys gambianus*, Waterhouse) and the laboratory rat. *Tropical Veterinarian*, 8: 19-27.

Ajayi, S., Tewe, O. and Faturoti, E. (1978). Behavioral changes in African giant rat (Cricetomys gambianus Waterhouse) under domestication. *East African Wildlife Journal*, 16(2): 137-143.

Ali, M. N., Byanet, O., Salami, S. O., Imam, J., Maidawa, S. M., Umosen, A. D., Alphonsus, C. and Nzalak, J. O. (2008). Gross anatomical aspects of the gastro-intestinal tract of the wild African Giant pouched rat (*Cricetomys gambianus*). *Scientific Research and Essays*, 3(10): 518-520.

Alexandre, F. M., DaSilva, C. G., Josh, S., and Nouchine, H. (2007). Thickening in the somatosensory cortex of patients with migraine. *Neurology*, 69(21): 1990–1995.

Amandor, A. (2003). ISAS (On-line). http:// www.il-st-acad-sci.org/mammals/mami 1002.html. Accessed February, 2012.

Anderson, J. C., Douglas, R. J., Martin, K. A. and Nelson, J. C. (1994). Map of the synapses formed with the dendrites of spiny stellate neurons of cat visual cortex. *Journal of Comparative Neurology*, 341: 25–38.

Andres, K. H. (1965). The fine structure of the olfactory bulb of the rat special consideration of the synaptic connections synaptic connections. (Z cell researchers Microscopic Anatomy) *Z Zellforsch Mikrosk Anat*, 65: 530-560.

Aydi, A., Yilmaz, S., Ozkan, Z. E. O. and Hgun, R. (2008). Morphological investigations on the Circulars arteriosus cepehri inmole-rats (Spalax fencodon, anatomic). *Histological Embyrologia*, 37: 219-221.

Bailey, M., Puche, A. and Shipley, M. (1999). Development of the olfactory bulb evidence for glia-neuron interactions in glomerular formation. *Journal of Comparative Neurology*, 270: 559–568.

Baptist R. and Mensah G. A. (1986). Benin and West Africa: the cane rat - farm animal of the future? *World Animal Review*, 60: 2-6.

Bancroft, J.D. and Gamble, M. (2008). *Theory and Practice of Histological Techniques*. Sixth Churchill Livingstone Elsevier, Philadelphia, PA, USA, Pp. 52-74.

Basile, N.L., Ilona, C. and Antje, H. (2012): Long lasting phantosmia treated with venlafaxine, Neurocase. *The Neural Basis of Cognition*, 18(2): 112-114.

Bastir, M., Rosas, A., Gunz, P., Peña-Melian, A., Manzi, G., Harvati, K., Kruszynski, R., Stringer, C. and Hublin, J. J. (2011). Evolution of the base of the brain in highly encephalized human species. *Nature Communication,* 2: 588.

Becker, S.V. and Middleton, C.C. (1979). Body weight ratios of the African white-tailed rat (*Mystromys albicaudatus*). *Laboratory Animal Science*, 29: 44–47.

Boyce, R.W., Dorph-Petersen, K-A., Lyck, L. and Gundersen, H. J.G. (2010). Design-based stereology: Introduction to basic concept and practical approaches for estimation of cell number. *Toxicology Pathology*, 38: 1011-1025.

Braitenberg, V. and Schüz, A. (1991). *Anatomy of the Cortex: Statistics and Geometry*. Springer-Verlag, NY. Pp. 45.

Brodmann, K. (1909). Contributions to the histological localization of the cerebral cortex . VII. Announcement: cytoarchitectonic cortical outline of the *Prosimians* (*Lemuridae*) . *Journal of Psychology and Neurology* 10287-334.

Buck L., Axel R. (1991). A novel multigene family may encode odorant receptors: a molecular basis for odor recognition. *Cell*, 65: 175-87.

Buschhuter, D., Smitka, M., Puschmann, S., Gerber, J.C., Witt, M., Abolmaali, N.D. and Hummel, T. (2008). Correlation between olfactory bulb volume and olfactory function. *NeuroImage*, *42*, 498–502.

Butler, A.B. and Hodos, W. (2005) Evolution and Variation, *In*: Comparative Vertebrate Neuroanatomy: Evolution and Adaptation, Second Edition, John Wiley & Sons, Inc., Hoboken, NJ, USA, doi: 10.1002/0471733849.

Byanet, O., Onyeanusi, B.I. and Ibrahim, N.D.G. (2009) Sexual dimorphism with respect to the macro-morphometric investigations of the forebrain and cerebellum of the grasscutter (*Thryonomys swinderianus*). *International Journal of Morphology*, 27: 361–365.

Calegari, F., Haubensack, W., Haffner, C. and Huttner, W.B. (2005). Selective lengthening of the cell cycle in the neurogenic subpopulation of neural progenitor cells during mouse brain development. *Journal of Neuroscience*, 25(28): 6533–6538.

Catharine, P. (2007). Migraine Sufferers Have Thicker Brain Cortex. *Neuron*, 14:899-912.

Cauller, L. (1995). Layer I of primary sensory neocortex: where top-down converges upon bottom-up. *Behavioural Brain Res*earch, 71 (1–2): 163–70.

Conn, P.M. (1995). Neuroscience in Medicine. J.B. Lippincott Company, Philadelphia, USA, Pp. 302-317.

Cooper, R.G. (2008). Care, husbandry and diseases of the African Giant rat (*Cricetomys gambianus*). *Journal of South African Veterinary Association*, 79(2): 62- 66.

Coopersmith, R. and Leon, L. (1988). The neurobiology of early olfactory learning. *In*: Blass EM, editor. *Developmental Psychobiology Behavioral Ecology.* New York, USA: Plenum Press. Pp. 283–308.

Crespo, C., Blasco-Ibenez, J.M., Marques-mar, A.I. and Martinez-Guijarro, F.J. (2001). Parvalbumin-containing interneurons do not innervate granule cells in the olfactory bulb. *Journal of Neuro report*, 12(11): 2553-2556.

Crespo, C., Liberia, T., Blasco-Ibáñez, J. M,, Nacher, J. and Varea, E. (2013). The circuits of the olfactory bulb. The exception as a rule. *Anatomocal Record*, 296: 1401–1412.

Creutzfeldt, O.D. (1995). *Cortex Cerebri*: Performance, Structural and Funtional Organization of the Cortex .Springer-Verlag, Berlin, Germany.

Cruz-Orive, L. M. (2005). A new stereological principle for test lines in three-dimensional space. *Journal of Microscopy*, 219(1): 18–28.

Cusack, R. (2005). The intraparietal sulcus and perceptual organization. *Journal of Cognitive Neuroscience*, 17(4): 641-651.

Dale, P., George, J. A., David, F., Lawrence, C. Katz, Anthony-Samuel L-M, James, O. M., and S. Mark Williams. (2001). *Neuroscience*. 2nd Edition. Sinauer Associates, Sunderland (MA), Pp. 345-378.

Denk, W. and Horstmann, H. (2004) Serial block-face scanning electron microscopy to reconstruct three-dimensional tissue nanostructure. *PLoS Biology*, 2(11): e329.

Dombrowski, S. M., Hilgetag, C. C. and Barbas, H. (2001). Quantitative architecture distinguishes prefrontal cortical systems in the Rhesus monkey : they either lack (agranular) or have only a rudimentary granular layer IV (dysgranular). *Cerebral Cortex*, 11: 975-988.

Dorph-Petersen, K., Rosenberg, R. and Nyengaard, J. R. (2004). Estimation of number and volume of immunohistochemically stained neurons in complex brain regions. *In*: Evans, S.M., Janson, A.M. and Nyengaard, J.R. eds. *Quantitative Methods in Neuroscience: A Neuroanatomical Approach*. Oxford University Press, Oxford, U.K. Pp. 216-238.

Drake, R. L., Vogl, W. and Mitchell, A.W.M. (2012). *Gray's Basic Anatomy*. Churchill Livingstone, Elsevier, Philadelphia, PA. USA, pp. 507-520.

Drury, R. A. B. (1967). Carlton's histological technique. *Annals of Internal Medicine*, 67(1): 233-235.

Endo, H., Hayashi, Y., Yamazaki, K., Motokawa, M., Pei, J., Lin, L., Chou, C. and Oshida, T. (2002). Geographical variation of the mandible size and shape in the wild pig (*Suis scrofa*) from Taiwan and Japan. *Zoological Studies*, 41: 452-460.

Eriksen, N. and Pakkenberg, B. (2007). Total neocortical cell number in the *Mysticet*e brain. *The Anatomical Record*, 290: 83-95.

Fiala, J. C. and Harris, K. M. (2001). Cylindrical diameters method for calibrating section thickness in serial electron microscopy. *Journal of Microscopy*, 202: 468–472.

Garcia-Finana, M., Cruz-Orive, L.M., Mackay, C.E., Pakkenberg, B. and Roberts, N. (2003). Comparison of MR imaging against physical sectioning to estimate the volume of human cerebral compartments. *Neuroimage*, 18(2): 505-16.

Gardella, D., Hatton, W.J., Rinda, H.B., Rosen, G.D. and Bartheld, C.S. (2003). Differential tissue shrinkage and compression in the z- axis: implication for optical dissector counting in vibratome, plastic and cryosections. *Journal of Neuroscience Methods*, 124: 45-59.

Geneva International Centre for Humanitarian Demining. (2007). A guide to mine action and explosive remnants of war. Geneva, Switzerland.

Giessel, A. J. and Datta, S.R. (2014). Olfactory maps, circuits and computations. *Current Opinion in Neurobiology*, 24: 120–132.

Gilbert, C. D. and Sigman, M. (2007). "Brain states: top-down influences in sensory processing". *Neurons*, 54(5): 677–696.

Glaser, E. M., and Wilson, P. D. (1999). A comparison of three estimators of the coefficient of error of optical fractionator cell count estimate. *Acta Stereology*, 18: 15-25.

Glaser, J., Green, G. and Hendrick, S. (2007). Stereology for biological research with a focus on Neuroscience (2nd ed.). MBF Press. Williston, VT.

Glauert, A. M., and Glauert, R. H. (1958). Araldite as an embedding medium for electron microscopy, *Journal of Biophysic and Biochemical Cytolology*, 4: 191-194.

Glees, P. (1955).Neuroglia morphology and function. Blackwell, Oxford.

Grady, M. S., Charleston, J. S., Maris, D., Witgen, B. M. and Lifshitx, J. (2003). Neuronal and glial cell number in the hippocampus after experimental traumatic brain injury: analysis by stereological estimation. *Journal of Neurotrauma*, 20(10): 929-941.

Gray, E. G. (1959). Axo-somatic and axo-dendritic synapses of the cerebral cortex: an electron microscope study. *Journal of Anatomy*, 93: 420–433.

Guelle, D., Smith, A., Lewis, A. and Bloodworth, T. (2003). Metal detectors for humanitarian demining. Luxembourg: Office for Official Publications of the European Communities.

Gundersen, H. J. G. (1977). Notes on the estimation of the numerical density of arbitrary profiles: The edge effect. *Journal of Microscopy,* 111: 219–223.

Gundersen, H. J. G. (1978). Estimators of the number of objects per area unbiased by edge effects. *Microscopy Acta*, 81: 107–117.

Gundersen, H. J. G. (1986a).Stereology of arbitrary particles.A review of unbiased number and size estimator and the presentation of some new ones, in memory of William R. Thompson. *Journal of Microsc*opy, 143: 3-45.

Gundersen, H. J. G. (1986b). Stereology of arbitrary particles: a review of unbiased number and size estimators and the presentation of some new ones, in memory of William R. Thompson. *Journal of Microscopy,* 143: 3–45.

Gundersen, H. J. G. and Jensen, E. B. (1987). The efficiency of systematic sampling in stereology and its prediction. *Journal of Microscopy,* 147: 229–263.

Gundersen, H. J., Jensen, E. B., Kieu, K. and Nielsen, J. (1999). The efficiency of systematic sampling in stereology—reconsidered. *Journal of Microscopy,* 193(3): 199–211.

Guthrie, K. and Gall, C. (2003). Anatomic mapping of neuronal odor responses in the developing rat olfactory bulb. *Journal of Comparative Neurology*, 455: 56–71.

Halpern, M. and Martínez-Marcos, A. (2003). Structure and function of the vomeronasal system: An update. *Progress in Neurobiology*, 70(3): 245–318.

Hamilton, K. A., Heinbockel, T., Ennis, M., Szabó, G., Erdélyi, F. and Hayar, A. (2005). Properties of external plexiform layer interneurons in mouse olfactory bulb slices. *Neuroscience,* 133(3): 819–829.

Harris, K. M., Perry, E., Bourne, J., Feinberg, M., Ostroff, L. and Hurlburt, J. (2006) Uniform serial sectioning for transmission electron microscopy. *Journal of Neuroscience, 26*: 12101–12103.

Hebel, R. and Stromberg, M. W. (1976). Anatomy of the laboratory rat: The Williams & Wilkins Company, Baltimore, MD. pp. 169-172.

Henwood, C. (1985). The Handbook of Rodents in Captivity. Unusual Types. Ian Henry Publications, Hornchurch, Essex, England.

Heymann, J. A., Hayles, M., Gestmann, I., Giannuzzi, L. A., Lich, B. and Subramaniam, S. (2006) Site specific 3D imaging of cells and tissues with a dual beam microscope. *Journal of Structural Biology*, 155:63–73.

Hirata, Y. (1964). Some observation on the fine structure of the synapses in the olfactory bulb of mouse, with particular reference to the atypical synaptic configuration. *Journal of Japanese Archive of Histology,* 24: 303-317.

Hofman, M. A. (1989).On the evolution and geometry of the brain in mammals. *Progress on Neurobiology*, 32(2): 137-58.

Hongtu, Z., Joseph, G. I., Niansheng, T., Daniel, B. R., Xuejun, H, Ravi, B. and Bradley, S. P. (2007). A Statistical Analysis of Brain Morphology Using Wild Boot strapping. *IEEE Translational Medical Imaging,* 26(7): 954–966.

Hosseini-Sherifabad, M. and Nyengaard, J. R. (2007). Design-based estimation of neuronal number and individual neuronal volume in the rat hippocampus. *Journal of Neuroscience Methods,* 163: 206-214.

Hubel, D. H. and Wiesel, T. N. (1959). Receptive fields of single neurones in the cat's striate cortex. *Journal of Physiology,* 148(3): 574–591.

Humason, G. L. (1972). *Animal Tissue techniques*.3rd Ed. W. H. Freeman and Company, San Francisco, USA, pp. 212-223.

Ibe, C. S., Onyeanusi, B.I., Hambolu, J.O. and Ayo, J.O. (2010). Sexual dimorphism in the whole brain and brainstem morphometry in the African Giant pouched rat (*Cricetomys gambianus*, Waterhouse- 1840). *Folia Morphological*, 69(2): 69-74.

Ikede, B. O. and Ajayi, S. (1976). Pathological condition of the Giant rat (*Cricetomys gambianus*, Waterhouse) in captivity. *Journal of Nigeria Veterinary Medical Association,* 5(1): 63-65.

International Mine Action Standards (IMAS) (2008). Operational testing of mine detection dogs and handlers. New York: United Nations Mine Action Service. pp. 1-17.

Isaken, M. A. (1997). African Giant pouched rats as Pets. In: Rat & Mouse Gazette of the Rat and Mouse Club of America. In: http://www.rmca.org/Articlesgiant.htm. Accessed 13-05-2009, 03:40: GMT.

Iversen, I. H., and Lattal, K. A. (1991a). The experimental analysis of behavior: Part 1. Amsterdam:.

Iversen, I. H., and Lattal, K. A. (1991b). The experimental analysis of behavior: Part 2. Elsevier, Amsterdam.

Jackowski, A., Paarnavelas, J. G. and Lieberman, A. R. (1978). The reciprocal synapse in the external plexiform layer of the mammalian olfactory bulb. *Journal of Brain Research,* 159: 17-28.

Jones, E.G. (1998). Viewpoint: the core and matrix of thalamic organization. *Neuroscience,* 85(2): 331–345.

Joohwi, L., Cindy, E., Fulton, C., Marc, N., Francois, B., Beatriz, P., Kathy, S., Josephine, J., Martin, S. and Ipek, O. (2011)."Automatic cortical thickness analysis on rodent brain", *Proceeding SPIE* 7962, Medical Imaging 2011: Image Processing, 796248.

Kandel, E. R., Schwartz, J. H. and Jessell, T. M. (2000). *Principles of Neural Science Fourth Edition*. McGraw-Hill United State of America, p. 324.

Kaschube, M. (2014). Neural maps versus salt-and-pepper organization in visual cortex. *Current Opinion in Neurobiology*, 24: 95-102.

Katherine, L., Narr, R. P., Woods, P. M., Thompson, P., Szeszko, D. R., Teodora, D., Mala, G., Arthur, W. T. and Robert, M. B. (2007). Relationships between IQ and Regional Cortical Grey Matter Thickness in Healthy Adults. *Cerebral Cortex*, 17(9): 2163–2171.

Kingdon, J. (1989). *East African Mammals*. Academic Press, London,

Knight, M. (1988). Thermoregulation in the largest African cricetid, the giant rat Cricetomys gambianus. *Comparative Biochemistry and Physiology A-Physiology*, 89(4): 705-708.

Knott, G. W., Quairiaux, C., Genoud, C. and Welker, E. (2002) .Formation of dendritic spines with GABAergic synapses induced by whisker stimulation in adult mice. *Neuron*, 34: 265–273.

Koelega, H. S. and Koster, E. P. (1974). Some experiments on sex differences in odour perception. *Annals of the New York Academy of Sciences*, 237: 234-246.

Korbo, L., Pakkenberg, B., Ladefoged, O., Gundersen, H. J. G., Arlien-Soborg, P. and Pakkenberg, H. (1990). An efficient method for estimating the total number of neurones in rat brain cortex. *Journal of Neuroscience Methods*, 30: 93-100.

Kozma, C., Macklin, W., Cummins, L.M. and Mauer, R. (1974). In: Weisbroth , S.H., Flatt, R.E. and Kraus, A.L. editors. The biology of the laboratory rabbit. Academic Press, New York, p. 5072.

Kruggel, F., Brückner, M.K., Arendt, T., Christopher, J.W. and von Cramon, D.Y. (2003). Analyzing the neocortical fine-structure. *Medical Image Analysis*, 7(3): 251–264.

Lam, Y. W., Sherman, S. M. (2010). Functional Organization of the Somatosensory Cortical Layer VI Feedback to the Thalamus. *Cerebral Cortex* 20(1): 13–24.

Landmine Monitor Report (2009). Retrieved from www.*lm.icbl.org/lm/2009*.

Leopold, D. A., Loehrl, T. A. and Schwob, J. E. (2002). Long-term follow-up of surgically treated phantosmia. *Archive of Otolaryngology Head Neck Surg*ery, 128(6): 642-647.

Levy, L. and Henkin, R. (2000). Physiologically initiated and inhibited phantosmia: cyclic unirhinal, episodic, recurrent phantosmia revealed by brain fmri. *Journal of Computer Assisted Tomography*, 24(4): 501-520.

Magi, M. (2003). Giant rats to sniff out Tuberculosis. In: http/:www.NewScientist.com. Accessed: 16/12/2008. 17:33:32 GMT.

Mahoney, A., Weetjens, B. J., Cox, C., Beyene, N., Mgode, G., Jubitana, M., Kuipers, D., Kazwala, R., Mfinanga, G. S., Durgin, A. and Poling, A. (2012). Pouched rats' detection of tuberculosis in human sputum sample: Comparison to culturing and polymerase chain reaction. *Tuberculosis Research and Treatment*, 2012: 1-5.

Malekani, M., Westlin, L., Paulus, J. and Potgieter, H. (2002). Oestrus occurrence in captive female *Cricetomys gambianus* (*Rodentia*: *Cricetidae*). *Journal of Zoology*, 257(3): 295-301.

Malun, D. and Brunjes, P. C. (1996). Development of olfactory glomeruli: Temporal and spatial interactions between olfactory receptor axons and mitral cells in opossums and rats. *Journal of Comparative Neurology*, 368: 1–16.

Marcus, L. F. (1990). Chapter 4. Traditional morphometrics. In Proceedings of the Michigan Morphometric Workshop.Special Publication No. 2. F. J. Rohlf and F. L. Bookstein. Ann Arbor MI, The University of Michigan Museum of Zoology: 77–122.

Mase, S. R., Ramsay, A., Ng, V., Henry, M., Hopewell, P. C. and Cunningham, J. (2007). Yield of serial sputum specimen examinations in the diagnosis of pulmonary tuberculosis: a systematic review. *International Journal of Tuberculosis Lung Disease*, 11(5): 485-495.

Mashiko, H., Yoshida, A. C., Kikuchi, S. S., Niimi, K., Takahashi, E., Aruga, J., Okano ,H. and Shimogori, T. (2012). Comparative anatomy of marmoset and mouse cortex from genomic expression. *Journal of Neuroscience*, 32(15): 5039-5053.

Malekani, M., Westlin, L., Paulus, J. and Potgieter, H. (2002). Oestrus occurrence in captive female *Cricetomys gambianus* (*Rodentia*: *Cricetidae*). *Journal of Zoology*, 257(3): 295-301.

Mensah G. A. (1991). Wildlife farming: grasscutter rearing Thryonomys swinderianus In, Proceedings of the 10th World Forestry Congress, pp 301-309.

Michael, H. R. and Wojciech, P. (2006). Histology: A text and Atlas. Lippincott Williams and Wilkins, 5th Edition. Toronto, Canada, Pp. 787-799.

Molnár, Z. and Clowry, G. (2012). Cerebral cortical development in rodents and primates. *Progress in Brain Research.*195: 45-70.

Moore, K. L. and Persaud, T.V.N. (2003). The Developing Human (Clinically Oriented Embryology), 8th Edition. Saunders Elsevier, Philadelphis, PA. USA, Pp. 380-392.

Moore, K.L., Dalley II, A.F. and Anne M. R. Agur, A.M.R. (2014). Clinically Oriented Anatomy, 7th Edition, Lippincott Williams & Wilkins, Baltimore, MD. Pp. 1134.

Mori, K., Takahashi, Y.K., Igarashi, K.M. and Yamaguchi, M. (2006). Maps of odorant molecular features in the Mammalian olfactory bulb. *Physiology Review*, 86(2): 409–433.

Mountcastle, V. (1997). The columnar organization of the neocortex. *Brain*, 120(4): 701–722.

Mueller, A., Rodewald, A., Reden, J., Gerber, J., von Kummer, R. and Hummel, T. (2005). Reduced olfactory bulb volume in post-traumatic and post-infectious olfactory dysfunction. *Neuroreport, 16*: 475–478.

Mühlfeld, C. and Och, M. (2014). Measuring structure – What's the point in counting? *Annals of Anatomy*, 196:1-2

National Research Council, NRC (1991). Microlivestock: Little known small animals with promising economic future. *In Veit Meyer Noel* (Ed.). National Academy Press, Washington, D.C., Pp. 183-185.

Naushad, A., Dilkash, Syed, .M. H and Aijaz, A. K. (2010). Effects of lead on the olfactory bulb the adult albino rats. *Current Neurobiology*, 1: 55-57.

Nielsen, B. S., Lund, L. R., Christensen, I. J., Johnsen, M., Usher, P. A., Linda Wulf-Andersen, L. .W., Frandsen, T. L., Danø, K. and Gundersen, H. J. G. (2001). A precise and efficient stereological method for determining murine lung metastasis volumes. *American Journal of Pathology*, 158(6): 1997–2003.

Nieuwenhuys, R., Donkelaar, H. J. and Nicholson, C. (1998). *The central nervous system of vertebrates, Volume 1*. Springer. Berlin, Germany, Pp. 2011–2012.

Nolte, J. (2007). *Elsevier's Intergrated Neuroscience*. Mosby, an affiliate of Elsevier Inc. Philadelphia, USA, Pp. 47-60.

Nonaka-Kinoshita, M., Reillo, I., Artegiani, B., Martı´nez-Martı´nez, M.A., Nelson, M., Borrell, V. and Calegari1, F. (2013). Regulation of cerebral cortex size and folding by expansion of basal progenitors. *The European Molecular Biology Organization Journal*, 1–12.

Nowak, R. (1999). Walker's mammals of the world. Vol. 2. The John Hopkins University Press, Baltimore and London.

Nyengaard, J.R. (1999). Stereologic methods and their applications in kidney research. *Journal of American Society of Nephrology*, 10(5): 1100 -1123.

Nyengaard, J.R. and Gundersen, H.J. (2006). Sampling for stereology in lungs. *European Respiration Review,* 15: 101, 107 -114.

Nzalak, J.O., Byanet, O., Salami, S.O., Umosen, A.D., Maidawa, S.M., Ali, M.N. and Imam, J. (2008). Comparative Morphometric studies of the cerebellum and forebrain of the African Giant rat (AGR) (*Cricetomys gambianus*, Waterhouse) and that of Grasscutter (*Thryonomys swinderianus). Journal of Animal and Veterinary Advances,* 7(9): 1090-1092.

Ogwuegbu, S.O., Oke, B.O. and Aire, T.A. (1983). Histomorphometric, histochemical and microstereological studies of the accessory glands of the male African Giant rat (*Cricetomys gambianus*, Waterhouse) in Ibadan, Nigeria. *African Journal of Ecology*, 21: 329-333.

Oke, B.O. and Aire, T.A. (1989).The bulbourethral gland of African giant the Giant rat (*Cricetomys gambianus,* Waterhouse). *Veterinary Archive*, 59: 267-274.

Oke, B.O. and Aire, T.A. (1990). Ultrastructural evidence of secretion in different zones of the caput epididymis of the African Giant rat (*Cricetomys gambianus*, Waterhouse). *Veterinary Archive*, 60: 207-212.

Oke, B.O. and Aire, T.A. (1996). The coagulating gland of the African Giant rat. *Tropical Veterinarian*, 14: 23-29.

Oke, B.O., Aire, T.A., Adeyemo, O. and Heath, E. (1988). The Structure of the epididymis of the African Giant rat (*Cricetomys gambianus*, Waterhouse). Histological, histochemical and microstereological studies. *Journal of Anatomy*, 160: 9-19.

Olopade, J.O. and Onwuka, S.K. (2003). A preliminary investigation into some aspects of the craniofacial indices of the Red Sokoto (Maradi) goat in Nigeria. *Folia Veterinaria*, 47: 57-59.

Olopade, J.O. and Onwuka, S.K. (2005). Some aspects of the clinical anatomy of the mandibular and maxillofacial regions of the West African Dwarf goat in Nigeria. *International Journal of Morphology*, 23: 33-36.

Olayemi, F. and Adesina, E. (2002). Plasma biochemical values in the African Giant rat (Cricetomys gambianus, Waterhouse) and the West African hinge backed tortoise (*Kinixys erosa*). *Veterinarski Arhiv*, 72(6): 335-342.

Olude, M.A., Olapade, J.O. and Ihunwo, A.O. (2014). Adult neurogenesis in the African Giant rat (*Cricetomys gambianus*, Waterhouse). *Metabolic Brain Disease*, Mar 1. [Epub ahead of print]

Olude, M.A., Olapade, J.O., Fatola, I.O. and Onwuka, S.K. (2009). Some aspects of the neurocraniometry of the AGR (*Cricetomys gambianus*, Waterhouse). *Folia Morphological*, 68(4): 224-227,

Onyeanusi, B.I., Adeniyi, A.A., Ayo, J.O. and Nzalak, J.O. (2007). Morphometric studies of the kidneys of the African Giant rat (*Cricectomys gambianus,* Waterhouse). *Journal of Animal and Veterinary Advances,* 6(11): 1273-1276.

Onyeanusi, B.I., Ibe, C S., Sonfada, M.L., Umar, A.A., Abdulrahman, B. and Salihu, M.D. (2009). A study of the kidney in the African Giant rat (Criceomys gambianus, Waterhouse) and the Wistar rat (*Rattus norvegious*).*Proceedings of 4th Annual Conference of International Research and Development Institute,* 4 (2): 7-13.

Orona, E., Rainer, E.C. and Scott, J.W. (1984). Dendritic and axonal organisation of mitral and tufted cells in the rat olfactory bulb. *Journal of Comparative Neurology*, 226(3): 346-356.

Pakkenberg, B. and Gundersen, H.J. (1997). Neocortical neuron number in humans: effect of sex and age. *Journal of Comparative Neurology*, 384: 312-320.

Perry, N.D., Hanson, B., Hobgood, W., Lopez, R.L., Okraska, C.R., Karem, K., Damon, I.K. and Carroll, D.S. (2006). New invasive species in Southern Florida: Gambian rat (*Cricetomys gambianus*). *Journal of Mammology*, 87(2): 262-264.

Peter, A. and Jones, E.G. (1994). Cerebral cortex (ed), vol 1-10. Plenum, New York, USA.

Peter, A.B., Frank, Z. (2006). Pheromonal communication in vertebrates. *Nature*, 444: 308–315.

Poling, A., Weetjens, B., Cox, C., Mgode, G., Jubitana, M. and Kazwala, R. (2010). Using giant African rats to detect tuberculosis. *American Journal of Tropical Medicine and Hygiene*, 83: 1308-1310.

Poling, A., Weetjens, B.J., Cox, C., Beyene, N.W., and Sully, A. (2010). Using giant African pouched rats (*Cricetomys gambianus*) to detect landmines. *The Psychological Record,* 60: 715–727.

Poling, A., Weetjens, B.J., Cox, C., Beyene, N.W., Bach, H. and Sully, A. (2011). Using pouched rats to detect land mines: another victory for operant conditioning. *Journal of Applied Behaviour Analysis*, 44: 315–355.

Rakic, P. (1995). Radial versus tangential migration of neuronal clones in the developing cerebral cortex. *Proceedings of National Academy of Sciences of the United State of America,* 92(25): 11323–11327.

Rall, W., Shepherd, G.M., Resse, T.S. and Brightman, M.W. (1966). Dendro-dendritic synaptic pathway for inhibition in the olfactory bulb. *Journal of Experimental Neurology*, 14: 44-56.

Rogely, W.B., Dorph-Petersen, K-A., Lise, L. and Gundersen, H.J.G. (2010). Design-based Stereology: Introduction to Basic Concepts and Practical Approaches for Estimation of Cell Number. *Toxicologic Pathology*, 38: 1011-1025.

Rogers, M. (1982). "A description of the generating curve of bivalves with straight hingess". *Palaeontology,* 25: 109–117.

Roy, S. and Roy, N. (2012). Histogenesis of the olfactory bulbs in human foetus. *International Journal of Biological and Medical Research*, 3(1): 1561-1564.

Rombaux, P., Mouraux, A., Bertrand, B., Nicolas, G., Duprez, T. and Hummel, T. (2006). Retronasal and orthonasal olfactory function in relation to olfactory bulb volume in patients with posttraumatic loss of smell. *Laryngoscope*, *116*: 901–905.

Royet, J.P. and Plailly, J. (2004). Lateralization of olfactory processes. *Chemical Senses*, 29(8): 731–45.

Rubio-Garrido, P. Pérez-de-Manzo, F., Porrero, C., Galazo, M.J. and Clascá, F. (2009). Thalamic input to distal apical dendrites in neocortical layer 1 is massive and highly convergent. *Cerebral Cortex*, 19(10): 2380–2395.

Ryan, J. (1989). Evolution of cheek pouches in African pouched rats (*Rodentia: Cricetomyinae*). *Journal of Mammology,* 70(2): 267-271.

Sadler, T.W. (2005). Langman's Essential Medical Embryology. Lippincott Williams & Wilkins. Philadelpia, USA, Pp. 460-462.

Salas, M., Schapiro, S. and Guzman-Flores, C. (1970). Development of olfactory bulb discrimination between maternal and food odors. *Physiology of Behaviour*, 5: 1261–1264.

Schmitz, C. and Hof, P.R. (2005). Design-based stereology in neuroscience. *Neuroscience*, 130: 813–831.

Segev, I. (1999). Taming time in the olfactory bulb. *Journal of Nature Neuroscience*, 2(12): 1041-1043.

Serag, A., Aljabar, P., Ball, G., Counsell, S.J., Boardman, J.P., Rutherford, M.A., Edwards, A.D., Hajnal, J.V. and Rueckert, D. (2012). Construction of a consistent high-definition spatio-temporal atlas of the developing brain using adaptive kernel regression. *NeuroImage*, 59(3): 2255–2265.

Sereno, M.I. and Tootell, R.B.H. (2005) "From Monkeys to humans: what do we now know about brain homologies," *Current Opinion in Neurobiology*, 15: 135-144.

Shepherd, G. (2003). *The Synaptic Organization of the Brain*. 5th edition. Oxford University, Oxford, England, Pp. 576-598.

Shepherd, G.M., Harris, K.M. (1998). Three dimensional structure and composition of CA3–CA1 axons in rat hippocampal slices: implications for presynaptic connectivity and compartmentalization. *Journal of Neuroscience*, 18: 8300–8310.

Shipley, M., Ennis, M. and Puche, A. (2004). Olfactory system. In: Paxinos G, editor. The rat nervous system. 3rd ed. CA: Elsevier Academic Press, USA, Pp 923–964.

Shipp, S. (2007). Structure and function of the cerebral cortex. *Current Biology*, 17(12): 443–449.

Singh, I. (2014). Textbook of Human Neuroanatomy. Jaypee Brothers Medical Publishers (P)LTD. New Delhi, India. Pp. 79-93.

Singleton, M., Rosenberger, A.L., Robinson, C. and O'Neill, R. (2011). "Allometric and metameric shape variation in *Pan* mandibular molars: A digital morphometric analysis". *Anatomical Record-Advances in Integrative Anatomy and Evolutionary Biology*, 294(2): 322–334.

Sinnatamby, C.S. (2011). *Last's Anatomy: Regional and Applied.* (12 edition). Churchill Livingstone, Toronto, Canada, Pp. 455-464.

Skinner, B.F. (1938). The behavior of organisms: An experimental analysis. Appleton-Century Crofts. New York, USA.

Skinner, B.F. (1953). Science and human behavior. Free Press, New York, USA.

Solveig, W., Nina, E., Torben, D, and Bente, P. (2010). A neurological Comparative studt of the Harp Seal (Pagophilus groenlandicus) and Harbor Porpoise (*Phacoena phocoena*) brain. *The Anatomical Record*, 293: 2129-2135.

Sorra, K.E. and Harris, K.M. (2000). Overview on the structure, composition, function, development, and plasticity of hippocampal dendritic spines. *Hippocampus*, 10: 501–511.

Spors, H., Albeanu, D.F., Murthy, V.N., Rinberg, D., Uchida, N., Wachowiak, M. and Friedrich, R. W. (2012). Illuminating Vertebrate Olfactory Processing. *Journal of Neuroscience*, 32(41): 14102–14108.

Steingart, K.R., Henry, M., Ng, V., Hopewell, P.C., Ramsay, A. and Cunningham, J. (2006). Fluorescence versus conventional sputum smear microscopy for tuberculosis: a systematic review. *Lancet Infectious Disease*, 6: 570-581.

Stephen, C., Noctor, A.C., Flint, T.A., Weissman, Ryan. S.D. and Arnold, R.K. (2001). Neurons derived from radial glial cells establish radial units in neocortex". *Nature*, 409 (6821): 714–720.

Sterio, D.C. (1984). The unbiased estimation of number and sizes of arbitrary particles using the dissector. *Journal of Microscopy*, 134(2): 127 – 136.

Sun, W. and Dan, Y. (2009). Layer-specific network oscillation and spatiotemporal receptive field in the visual cortex. *Proceeding of National Academy of Science, USA*, 106 (42): 17986- 17991.

Tomer, R., Denes, A.S., Tessmar-Raible, K. and Arendt, D. (2010). Profiling by image registration reveals common origin of annelid mushroom bodies and vertebrate pallium. *Cell,* 142(5): 800–809.

Treloar, H.B., Miller, A.M. and Ray. A. (2010) Development of the Olfactory System. In: Menini A, editor. *The Neurobiology of Olfaction*. CRC Press, Boca Raton (FL), USA.

Tsai, L. and Barnea, G.A. (2014). Critical period defined by axon-targeting mechanisms in the murine olfactory bulb. *Science,* 344: 197–200.

Verhagen, R., Cox, C., Mauchango, M., Weetjens, B.J. and Billet, M. (2003). Preliminary results on the use of rats as indicators of buried explosives in field conditions. In GICHD (Ed.), Mine detection dogs: Training, operations, and odor detection (pp. 175–199). Geneva: GICHD.

Verhagen, R., Weetjens, M., Cox, C., Weetjens, B.J., and Billet, M. (2006). Rats to the rescue: Results of the first tests on real minefield. *Journal of Mine Action*, 9: 2-7.

Wachinger, C., Golland, P. and Reuter, M., (2014). Brainprint: Identifying subjects by their brain. In: Medical Image Computing and Computer-Assisted Intervention–MICCAI 2014. Springer, pp. 41– 22 48.

Walløe, S., Eriksen, N., Dabelsteen, T. and Pakkenberg, B. (2010). A Neurological Comparative Study of the Harp Seal (*Pagophilus groenlandicus*) and Harbor Porpoise (*Phocoena phocoena*) Brain. *The Anatomical Record,* 293:2129–2135.

Wang, J.W. (2012). Presynaptic modulation of early olfactory processing in Drosophila. *Developmental Neurobiology,* 72(1): 87–99.

Webster, S.H., Liljegreen, E.T. and Zimicen, D.J. (1947). Body weight ratios for liver, kidney and spleen of laboratory animals. 1 Albino rat. *American Journal of Anatomy*, 81: 471-514.

Weetjens, B.J., Mgode, G.F., Machang'u, R.S., Kazwala, R., Mfinanga, G. and Lwilla, F. (2009). African pouched rats for the detection of pulmonary tuberculosis in sputum samples. *International Journal of Tuberculosis Lung Disease* 13: 737-743.

Wei, Q., Zhang, H. and Guo, B. (2008). Histological structure difference of dog's olfactory bulb between different age and sex. *Zoological Research*, 29(5): 537-545.

West, M.J. (1993). New stereological methods for counting neurons. *Neurobiology of Aging*, 14 (4): 275-85.

West, M.J. (2002). Design-based stereological methods for counting neurons. *Progress in Brain Research*, 135: 43-51.

White, E.L. and Rock, M.P. (1980). Three-dimensional aspects and synaptic relationships of a Golgi impregnated spiny stellate cell reconstructed from serial thin sections. *Journal of Neurocytology,* 9: 615– 636.

White, J.G., Southgate, E., Thomson, J.N. and Brenner, S. (1986). The structure of the nervous system of the nematode *Caenorhabditis elegans*. *Philosophical Transactions of the Royal Society of London B,* 314: 1-340.

World Health Organization (2010). Global Tuberculosis Control: Epidemiology, Strategy, Financing. Geneva: World Health Organization Press.

Yilmaz, S., Ozkan, Z.E. and Ozdemir, D. (1998). Macro-anatomical investigations on the skeletons of porcupine (*Hystrix cristata*). I. Ossa membri thoracici. *Tropical Journal of Veterinary Animal Science.* 22: 389-392.

Yousem, D.M., Geckle, R.J., Bilker, W.B., Kroger, H. and Doty, R.L. (1999). Posttraumatic smell loss: Relationship of psychophysical tests and volumes of the olfactory bulbs and tracts and the temporal lobes. *Academic Radiology*, *6*, 264–272.

Zecevic, N. and Rakic, P. (2001). Development of layer I neurons in the primate cerebral cortex. *Journal of Neuroscience.* 21 (15): 5607–5619.

Zhu, C.G. (2002). The anatomy of the nervous system. People's Sanitation Press, Beijing, Pp. 705-709.

APPENDICES

Appendix I

PREPARATION OF 1% GLUTARALDEHYDE AND 4% FORMALDELHYDE FIXATIVES

A lower concentraction of Glutaraldehyde and formaldehyde especially used for vascular profusion.

16% Formaldehyde Solution:	13ml
50% Glutaraldehyde EM Grade:	5ml
0.2M Sodium Phosphate Buffer:	50ml
Distilled Water:	32ml

Final mixture is 4% formaldehyde, 1% Glutaraldehyde and 0.12 M Buffer, pH 7.2.

The osmolarity can be adjusted by adding sucrose to NaCl. The pH may also need to be adjusted to your desirable point.

Appendix II

COMPOSITION AND PREPARATION OF THIONIN STAIN FOR FIXED TISSUES (RAT)

A. Stock Solutions

1. M Sodium Acetate Solution: 16.4 g Sodium Acetate (anhydrous) dissolve in 200 ml distilled water.

2. 1.0 M Glacial Acetic Acid: add 12.2 ml Glacial Acetic Acid to 200 ml distilled water

3. 0.25% Thionin Solution: 0.25 g Thionin in 100 ml distilled water.

Thionin is hard to dissolve. Use a glass rod or a stir bar to stir. Do not use a metal rod to stir the Thionin. Filter through # 4 Whatman paper using the ground glass filter for Thionin.

B. Thionin Staining Solution:

1. 180 ml distilled water

2. 9 ml Sodium Acetate Solution

3. 21 ml Acetic Acid Solution

This is the buffer solution. Adjust pH to 4.3

4. Add 18 ml 0.25% Thionin Solution

C. Staining Procedure:

1. Float sections in phosphate buffered solution

2. Mount sections at chrome-gelatine coated slides. Absorb water around the sections with towel, lay slides vertical and air dry at room temperature for 20 minutes

3. Re-hydrate in demineralised water for 15 minutes

4. Stain in Thionin for 1 minute

5. Differentiate colour fixation in demineralised water for 3 minutes in 3 changes

6. Dehydration:

50% Ethanol 1 x 1 minute

70% Ethanol 1 x 1 minute

96% Ethanol 2 x 1 minute

99% Ethanol 3 x 1 minute

Xylene 5 x 5 minute

g. Cover slip with XAM

Appendix III

PREPARATION OF AGAROSE GEL FOR EMBEDDING

To prepare 5 % low-melting point agarose in 1xPhospahte buffer solution (PBS), keep at 42°C.

1. Dissolve 5g agarose in 100 ml of distilled water or 0.1 M PB and heat to make 5 % agarose gel solution.

2. To embed the brains, fill agarose into a tissue embedding mold, transfer the brain with as little buffer as possible, gently stir the lot with a glass rod, so that the agarose can properly contact the tissue.

3. Keep on ice until the agarose has solidified, then trim away the edges so that a small block suitable for sectioning is obtained.

4. The block should not be too high, as this may lead to less precise cutting. Glue the block(s) onto a mount, adjust the vibratome and cut sections of 60 microns in ice cold Krebs buffer. The slices are best handled with a pair of spatulas, which provide good support to the tissue when it is transferred between dishes.

Appendix IV

FORMULAS

1. Calculating number of cell using designed-based unbiased stereological method (Optical fractionator): $N_{total} = (1/ssf. 1/asf .1/hsf \sum Q\square)2$

Where ssf is section sampling fraction, asf is area sampling fraction, hsf is height sampling fraction, $\sum Q\square$ is the sum of count.

2. Calculating volumes using designed-based unbiased stereological method (Cavalieri principle): The estimated volume *V* of the layers of the cerebral cortex was:

$$V = t\,(a/p)\sum Pi$$

where *t* is the slab thickness, or intersectional distance

P_i is the number of points that hit the different layers of the OB on the slab *i*,

(a/p) is the area associated with each point

3. Calculating coefficient of error (CE):

$$CE = \frac{\sqrt{Var_{SURS} + Var_{Noise}}}{\sum_{1=1}^{N} P1}$$

Where CE is the coefficient of error, Var_{SURS} is the variance of systematic uniform random sampling, Var_{Noise} is the variance of noise, N is the number of points, P is the point, and $\sum P$ is the sum of points.

4. Calculating coefficient of variation (CV):

CV=Standard deviation/mean

4. Calculation of Area sample fraction (Asf) :

Asf = a (frame)／a(x, y-step)

Where a (frame) is the area of frame

X, y-step is the step length

Appendix V

GLOSSARY

a. Systemic uniform random sampling (SURS): To ensure that all parts of the olfactory bulb were uniformly sampled.

b. Section sampling fraction *(ssf):* Depending on the size of the brain, *ssf* was chosen to be between 1/260th to 1/290th to obtain 12-13 sections per brain

c. Area sampling fraction *(asf)*: in each sample section, neuronal count was made with optical disector at regular predetermined x, y position in the olfactory bulb. The disector was positioned randomly over olfactory bulb within the x, y step pattern by the newCAST^{TM}-GRID software (Visiopharm, Denmark)

d. Height sample fraction ***(hsf)***: this is the height of the disector relative to the section thickness.

e. NewCAST software: new computer assisted stereological tool software.